INTERNATIONAL ATOMIC ENERGY AGENCY
UNITED NATIONS EDUCATIONAL, SCIENTIFIC AND CULTURAL ORGANIZATION
INTERNATIONAL CENTRE FOR THEORETICAL PHYSICS
I.C.T.P., P.O. BOX 586, 34100 TRIESTE, ITALY. CABLE: CENTRATOM TRIESTE

H4.SMR/449-22

WINTER COLLEGE ON HIGH RESOLUTION SPECTROSCOPY

(8 January - 2 February 1990)

TRAPPED ION FREQUENCY STANDARDS

W.M. Itano
J.C. Bergquist, J.J. Bollinger
F. Elsner, S.L. Gilbert
D.J. Heinzen, M.G. Raizen, D.J. Wineland

Time and Frequency Division
National Institute of Standards & Technology
Boulder, Colorada, 80303
U.S.A.

Trapped Ion Frequency Standards

W. M. Itano
J. C. Bergquist
J. J. Bollinger
F. Elsner
S. L. Gilbert
D. J. Heinzen
M. G. Raizen
D. J. Wineland

Time and Frequency Division
National Institute of Standards and Technology
(formerly the National Bureau of Standards)
Boulder, Colorado USA 80303

Supported in part by the Air Force Office of Scientific Research and the Office of Naval Research

OUTLINE

I. Introduction

Frequency standards and clocks

Advantages of ion traps

II. Penning traps

Penning trap operation

Laser cooling

Sympathetic cooling

Optical pumping

Double resonance

Ramsey method

Frequency servo

III. Paul traps

Paul trap operation

Electron shelving

Dicke narrowing

1-ion frequency servo

Article for the McGraw-Hill Encyclopedia of Science and Technology

ATOMIC CLOCKS

Wayne M. Itano
Time and Frequency Division
National Institute of Standards and Technology
Boulder, CO 80303

An atomic clock is a device which uses an internal resonance frequency of atoms (or molecules) to measure the passage of time. The terms "atomic clock" and "atomic frequency standard" are often used interchangeably. A frequency standard generates pulses at regular intervals. A frequency standard can be made into a clock by the addition of an electronic counter, which records the number of pulses.

Basic principles Most methods of timekeeping rely on counting some periodic event, such as the rotation of the earth, the motion of a pendulum in a grandfather clock, or the vibrations of a quartz crystal in a watch. An atomic clock relies on counting periodic events determined by the difference of two different energy states of an atom. According to quantum mechanics, the internal energy of an atom can take only certain discrete values. A transition between two energy states with energies E_1 and E_2 may be accompanied by the absorption or emission of a photon (particle of electromagnetic radiation). The frequency ν of this radiation is given by the equation $h\nu = |E_2 - E_1|$, where h is Planck's constant. A basic advantage of atomic clocks is that the frequency-determining elements, atoms of a particular isotope, are the same everywhere. Thus, atomic clocks constructed and operated independently will measure the same time interval, that is, the length of time between two events. In order for the two clocks to agree on the time, they must be synchronized at some earlier time.

An atomic frequency standard can be either active or passive. An active standard uses as a reference the electromagnetic radiation emitted by atoms as they decay from a higher energy state to a lower energy state. An example is a self-oscillating maser. A passive standard attempts to match the frequency of an electronic oscillator or laser to the resonant frequency of the atoms by means of a feedback circuit. The cesium atomic beam and the rubidium gas cell are examples of passive standards. Either kind of standard requires some kind of frequency synthesis to produce an output near a convenient frequency, such as 5 MHz, which is proportional to the atomic resonance frequency.

Two different gauges of the quality of a clock are accuracy and stability. The accuracy of a frequency standard is defined in terms of the deviation of its frequency from an ideal standard. In practice, it might be defined in terms of the frequency differences measured between independently constructed and operated standards of the same type. Improving the accuracy depends on understanding and controlling all the parameters that might cause the frequency to shift. The stability of a frequency standard is defined in terms of the constancy of its average frequency from one interval of time to the next. For many frequency standards, the stability initially improves with increasing measurement time but eventually gets worse. That is, a more

precise measurement of the frequency can be made by averaging together successive measurements, until some imperfection in the apparatus causes the frequency to change. The stability increases with increased Q (resonance frequency divided by the width of the resonance) and with increased measurement signal-to-noise ratio.

Commonly used types of atomic clock The three most commonly used types of atomic clock are the cesium atomic beam, the hydrogen maser, and the rubidium gas cell. The cesium clock has high accuracy and good long-term stability. The hydrogen maser has the best stability for periods of up to a few hours. The rubidium cell is the least expensive and most compact and also has good short-term stability.

Cesium The cesium atomic beam clock (see Fig. 1) uses a 9193 MHz transition between two hyperfine energy states of the cesium-133 atom. Both the atomic nucleus and the outermost electron have magnetic moments; that is, they are like small magnets, with a north and a south pole. The two hyperfine energy states differ in the relative orientations of these magnetic moments. The cesium atoms travel in a collimated beam, through an evacuated region. Atoms in the different hyperfine states are deflected into different trajectories by a nonuniform magnetic field. Atoms in one of the two states are made to pass through a microwave cavity, where they are exposed to radiation near their resonance frequency. The resonant radiation may cause the atom to make a transition from one state to the other; if that happens, the atom is deflected by a second, nonuniform magnetic field onto a detector. The Q of the resonance is over 10^8 for some laboratory standards and somewhat less for the smaller standards which are commercially available. The cesium atomic beam is the most accurate of all atomic clocks. The best ones have an error of only about 2 parts in 10^{14}, or about 1 second in a million years. For this reason, cesium has become the basis of the international definition of the second, "the duration of 9 192 631 770 periods of the radiation corresponding to the transition between the two hyperfine states of the ground state of the cesium-133 atom." The cesium clock is especially well suited for applications such as timekeeping, where absolute accuracy without recalibration is necessary. Measurements from many cesium clocks throughout the world are averaged together to define an international time scale which is uniform to parts in 10^{14}, or about 1 microsecond in a year.

Hydrogen The hydrogen maser (see Fig. 2) is based on the hyperfine transition of atomic hydrogen, which has a frequency of 1420 MHz. Atoms in the higher hyperfine energy state are selected by a focusing magnetic field, so that they enter an evacuated storage bulb inside a microwave cavity. The atoms bounce off the Teflon-coated walls for about 1 second before they are induced to make a transition to the lower hyperfine state, by a process called stimulated emission. The stimulated emission from many atoms creates a self-sustaining microwave oscillation. The resonance Q is about 10^9. The best hydrogen masers have a stability of about 1 part in 10^{15} for averaging periods of 10^4 seconds. Over longer periods of time, the frequency drifts, due primarily to changes of the cavity tuning. Collisions with the walls cause the frequency to be shifted by about 1 part in 10^{11} relative to that of a free atom, but the magnitude of the shift varies from one device to another. This shift limits the accuracy of the hydrogen maser to about 1 part in 10^{12}. The hydrogen maser can also be operated as a passive device, with improved long-

term stability, due to the addition of automatic cavity tuning. The short-term stability is worse than for an active maser.

Rubidium The rubidium gas cell (see Fig. 3) is based on the 6835 MHz hyperfine transition of rubidium-87. The rubidium atoms are contained in a glass cell together with a buffer gas, such as argon, which prevents them from migrating to the cell walls. A method called optical pumping is used to prepare the atoms in one hyperfine state. Filtered light from a rubidium resonance lamp is absorbed by atoms in one of the two hyperfine states, causing them to be excited to a higher state, from which they quickly decay to the other hyperfine state. If the atoms are then subjected to microwave radiation at the hyperfine transition frequency, they are induced to make transitions back to the other hyperfine state. They can then absorb light again from the lamp; this results in a detectable decrease in the light transmitted through the cell. The Q is only about 10^7, but the short-term stability is quite good, reaching 1 part in 10^{13} for averaging times of 1 day. After longer periods, changes in the buffer gas pressure and the lamp cause the frequency to drift. The accuracy is not better than a part in 10^{10}. Rubidium standards are used in applications that do not require the accuracy of a cesium standard.

Experimental atomic clocks Many other kinds of atomic clock, such as thallium atomic beams and ammonia and rubidium masers, have been demonstrated in the laboratory. The first atomic clock, constructed at the National Bureau of Standards in 1949, was based on a 24 GHz transition in the ammonia molecule.

Some laboratories are trying to improve the cesium atomic beam clock by replacing the magnetic state selection with laser optical pumping and fluorescence detection. Improved performance is expected because of increased signal-to-noise ratio and a more uniform magnetic field. Other laboratories are studying atomic beam standards using magnesium, calcium, or methane, which have frequencies higher than that of cesium.

Hydrogen masers operated at low temperatures (a few kelvins above absolute zero) may be capable of much better stabilities than conventional hydrogen masers. The improvement is expected to come from the reduced electronic noise and the fact that oscillation can be maintained with a greater number of atoms.

Atomic frequency standards can also be based on optical transitions. One of the best developed optical frequency standards is the 3.39 μm (88 THz) helium-neon laser, stabilized to a transition in the methane molecule. Frequency synthesis chains have been built to link the optical frequency to radiofrequencies.

Ion traps, which confine ions in a vacuum by electric and magnetic fields (see Fig. 4), are under study for use in atomic clocks. They provide a benign environment for the ions while still allowing a long measurement time. Clocks based on optically pumped mercury-199 ions have been built and show good stability. Other trapped ion standards make use of laser cooling to reduce frequency errors due to Doppler shifts. Laser cooling is a method by which resonant light pressure is used to damp the motion of atoms. A Q of 3×10^{11} has been observed on a hyperfine transition of laser cooled beryllium-9 ions. Even higher Q's may be observable on certain optical transitions. Already an optical transition has been observed in a single, trapped mercury ion with a Q of about 3×10^{11}. It should be possible to increase the Q by a factor of

1000 in the near future. An optical frequency standard based on such an ion might be capable of an accuracy of 1 part in 10^{18}.

Applications Atomic clocks are used in applications for which less expensive alternatives, such as quartz oscillators, do not provide adequate performance. The use of atomic clocks in maintaining a uniform international time scale has already been mentioned. The following are some other applications.

Navigation The Global Positioning System (GPS) is a satellite based system which enables a user with a suitable radio receiver to determine his position within about 10 meters (33 feet). The satellites send out accurately timed radio pulses, from which the user's receiver can calculate its location and time. The satellites and the ground stations, but not the users, need atomic clocks (usually cesium clocks).

Communications Various digital communication systems require precise synchronization of transmitters and receivers in a network. Some systems use time division multiplexing (TDM), in which many channels of information are sent over the same line by sequentially allotting a small time slot to each channel. Timing is very critical when there are several sources of information with their own clocks. The primary timing is provided by cesium clocks.

Radio astronomy Very long baseline interferometry (VLBI) is a technique which allows two or more widely separated radio telescopes to achieve very high angular resolution by correlation of their signals. The system has the resolution that a single telescope would have, if its aperture were equal to the distance between the telescopes. This can be thousands of miles. The accurate timing needed to correlate the signals is provided by hydrogen masers.

Space exploration Doppler tracking navigation of space probes requires very stable local oscillators, derived from atomic frequency standards. Doppler tracking relies on determining the velocity of the spacecraft by measuring the frequency shift of a signal after it has been echoed back to the earth by a transponder on the spacecraft. Stable local oscillators are also needed for studies of planetary atmospheres and rings by fluctuations of the radio signals transmitted through them.

Fundamental science According to Einstein's special and general theories of relativity, a moving clock runs slower than a stationary one, and a clock on the surface of the earth runs slower than one far away from the earth. These predictions were verified to high accuracy by an experiment in which a hydrogen maser was launched in a rocket to an altitude of 10 000 kilometers (6000 miles).

Bibliography

H. Hellwig, K.M. Evenson, and D.J. Wineland, "Time, Frequency and Physical Measurement," Physics Today, 31(12):23-30, December 1978.

H. Hellwig, "Atomic Frequency Standards: A Survey," Proceedings of the IEEE, 63(2):212-229, February 1975.

J. Jespersen and J. Fitz-Randolph, From Sundials to Atomic Clocks (Dover Publications, 1982).

N.F. Ramsey, "History of Atomic Clocks," Journal of Research of the National Bureau of Standards, 88(5):301-320, September-October 1983.

N.F. Ramsey, "Precise Measurement of Time," American Scientist, 76(1):42-49, January-February 1988.

D.J. Wineland, "Trapped Ions, Laser Cooling, and Better Clocks," Science, 226:395-400, 26 October 1984.

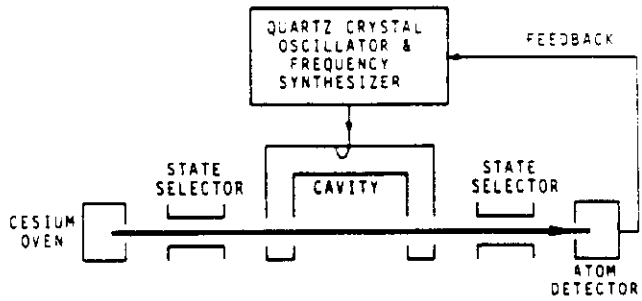

1. The cesium atomic beam

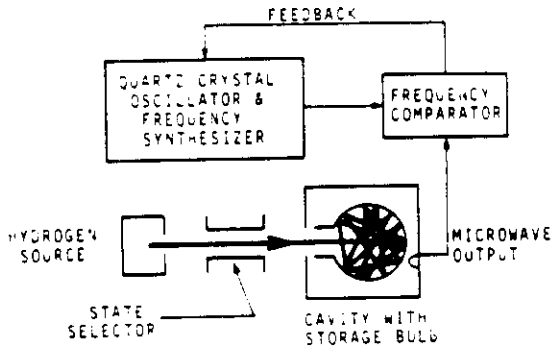

2. The hydrogen maser

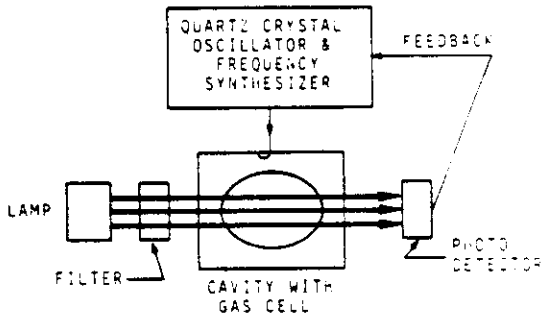

3. The rubidium gas cell

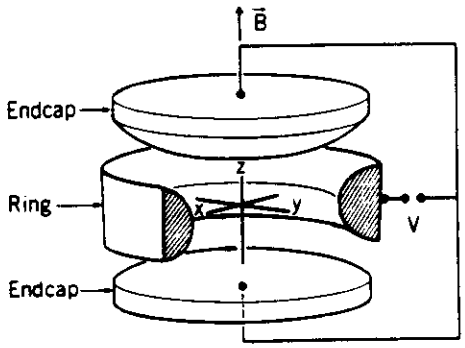

4. Electrodes used to create the confining electric potential for a Penning ion trap or a Paul ion trap. An electric potential V, which is static for a Penning trap and oscillating for a Paul trap, is applied between the ring electrode and the endcap electrodes. The Penning trap requires a uniform magnetic field $\vec{B}$.

Single-Particle Orbit in a Penning Trap

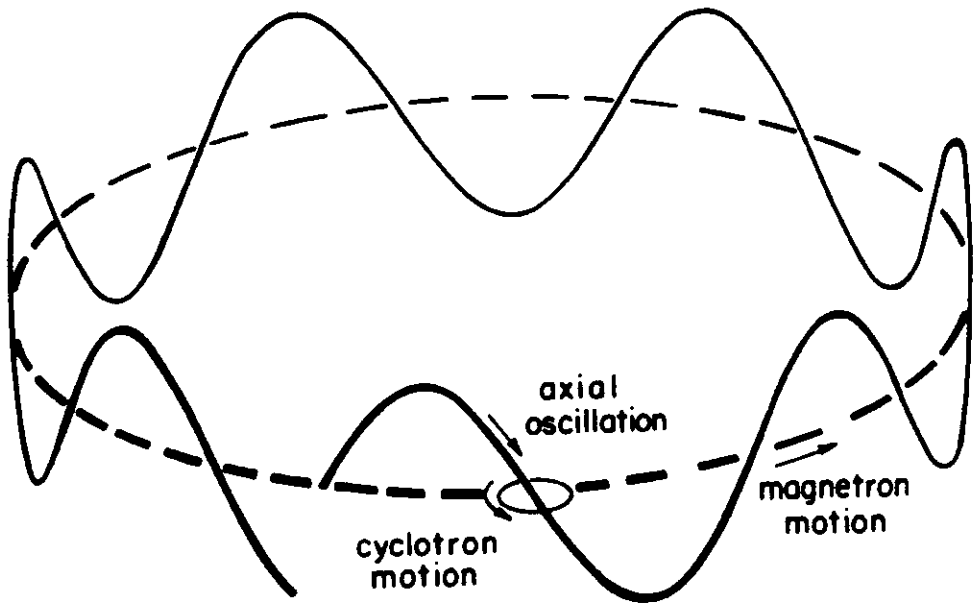

$$\text{Cyclotron frequency}: \ \omega_c = \frac{qB}{mc}$$

3 eigenfrequencies:

$$\text{axial}: \ \omega_z = \sqrt{\frac{4qU}{m(r_o^2 + 2z_o^2)}}$$

$$\text{modified cyclotron}: \ \omega_c' = \tfrac{1}{2}\omega_c + \sqrt{\tfrac{1}{4}\omega_c^2 - \tfrac{1}{2}\omega_z^2}$$

$$\text{magnetron}: \ \omega_m = \tfrac{1}{2}\omega_c - \sqrt{\tfrac{1}{4}\omega_c^2 - \tfrac{1}{2}\omega_z^2}$$

Projection of orbit in a Penning trap on the x-y plane

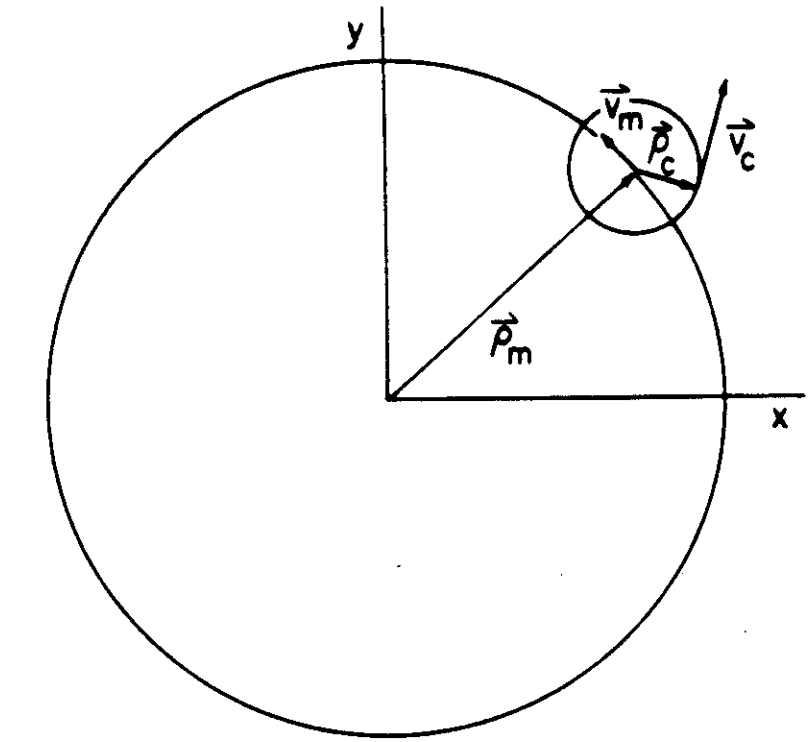

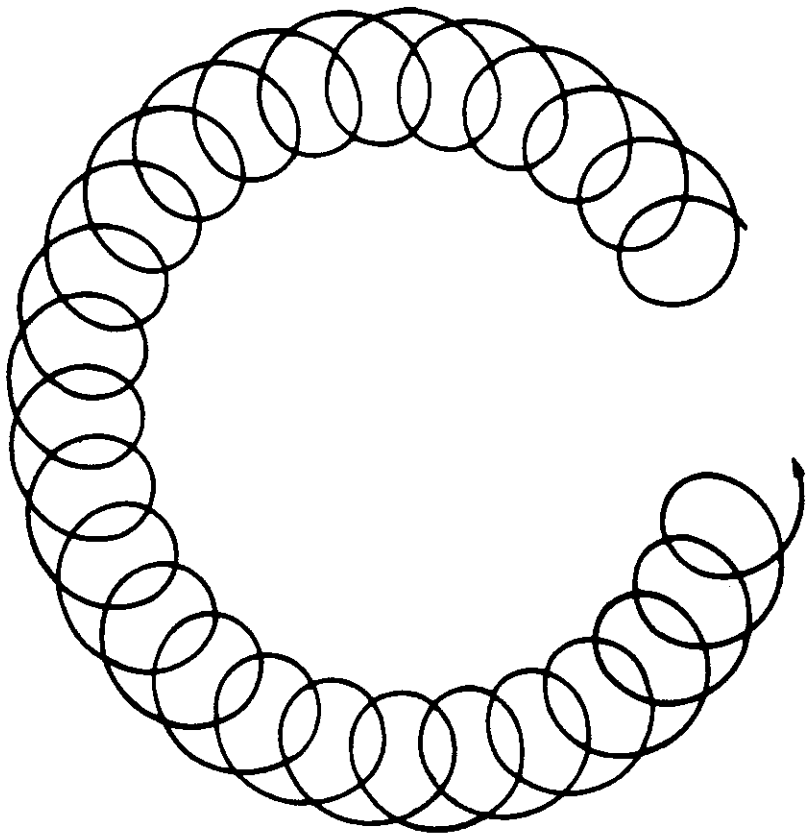

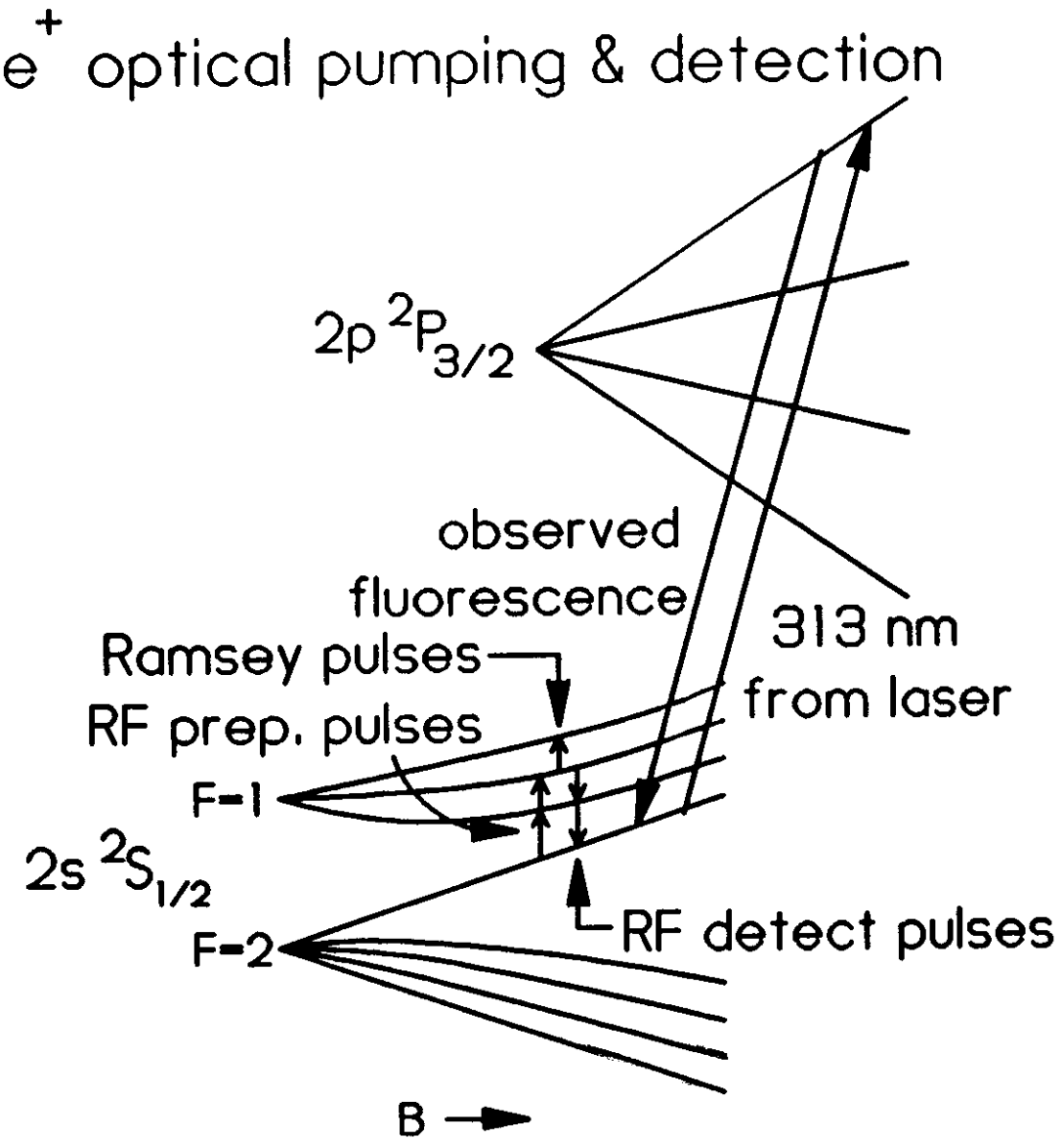
$^9Be^+$ optical pumping & detection
$2p\ ^2P_{3/2}$
observed
fluorescence
313 nm
from laser
Ramsey pulses
RF prep. pulses
F=1
$2s\ ^2S_{1/2}$
F=2
RF detect pulses
B

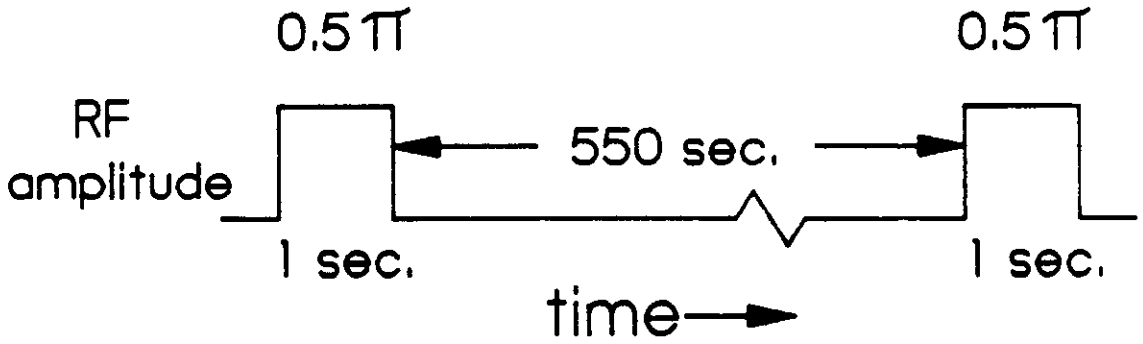
0.5π
0.5π
RF
amplitude
550 sec.
1 sec.
1 sec.
time

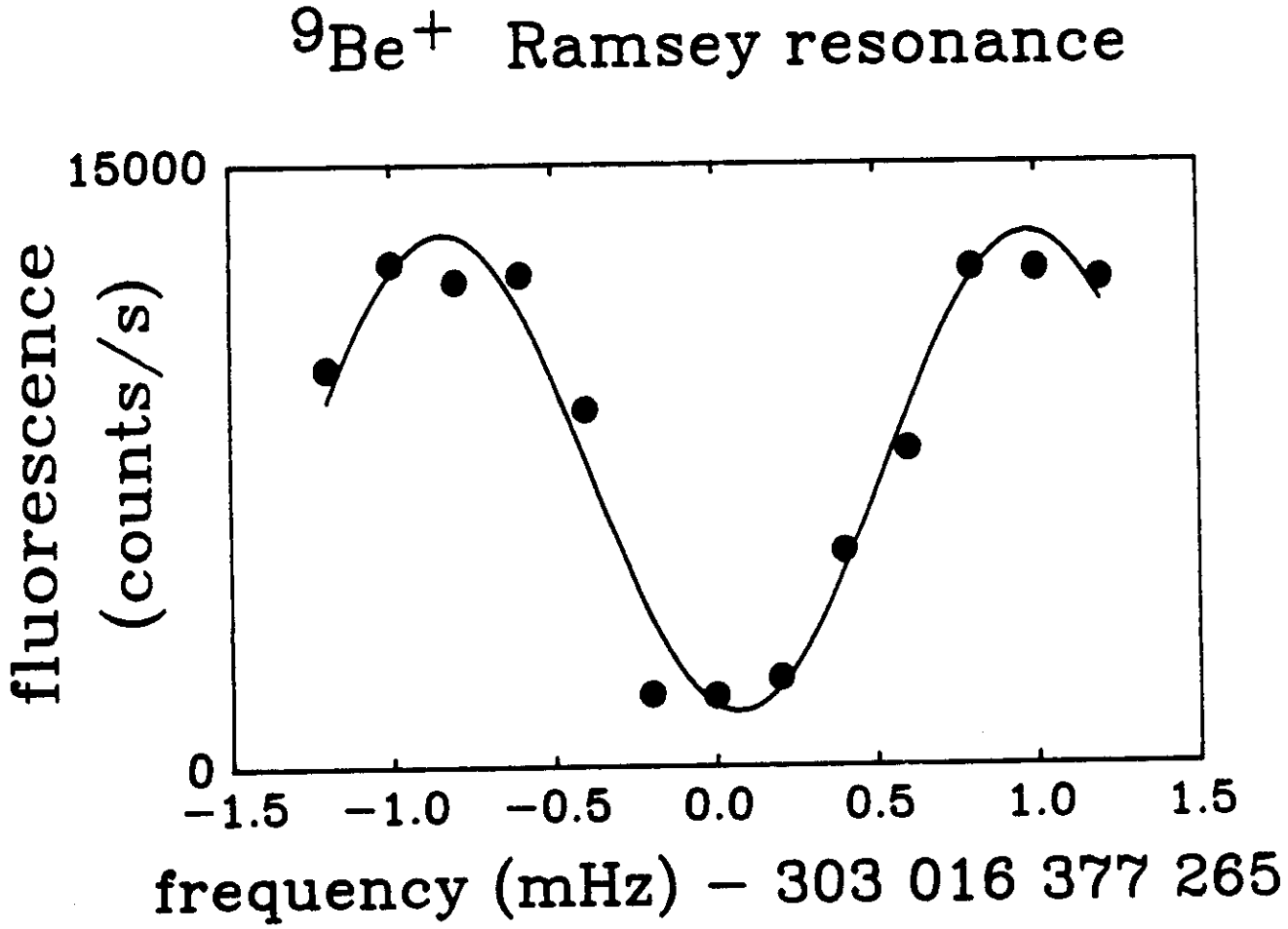
$^9Be^+$ Ramsey resonance
15000
0
fluorescence
(counts/s)
−1.5
−1.0
−0.5
0.0
0.5
1.0
1.5
frequency (mHz) − 303 016 377 265

Effective Potential due to Rapidly Oscillating Force

High-frequency force:

$$\vec{F}(\vec{r},\vec{t}) = \vec{f}(\vec{r})\cos(\Omega t)$$

Effective time-independent potential:

$$V_{\text{eff}}(\vec{r}) = \frac{|\,\vec{f}(\vec{r})\,|^2}{4m\Omega^2}$$

Effective Potential in a Paul Trap

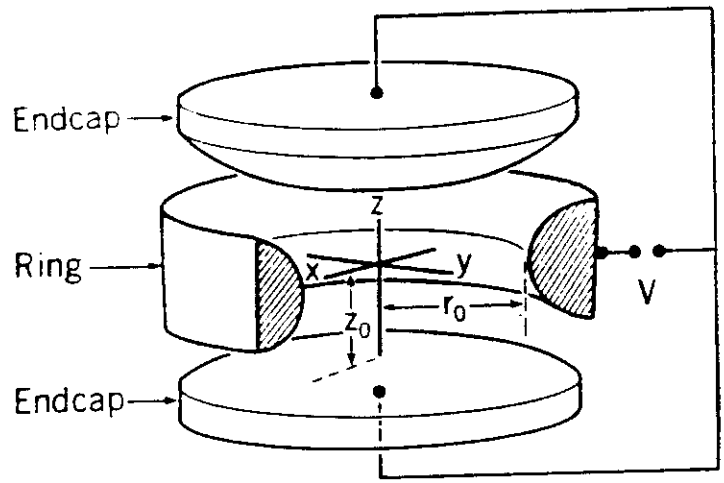

Electric potential inside trap:

$$\phi(x,y,z) = \frac{U_0 + V_0\cos(\Omega t)}{r_0^2 + 2z_0^2}(x^2 + y^2 - 2z^2)$$

$$= \frac{U_0 + V_0\cos(\Omega t)}{A^2}(x^2 + y^2 - 2z^2)$$

Effective potential energy:

$$q\phi_{\text{eff}}(x,y,z) = \left(\frac{q^2V_0^2}{m\Omega^2A^4} + \frac{qU_0}{A^2}\right)(x^2 + y^2)$$

$$+ \left(\frac{4q^2V_0^2}{m\Omega^2A^4} - \frac{2qU_0}{A^2}\right)z^2$$

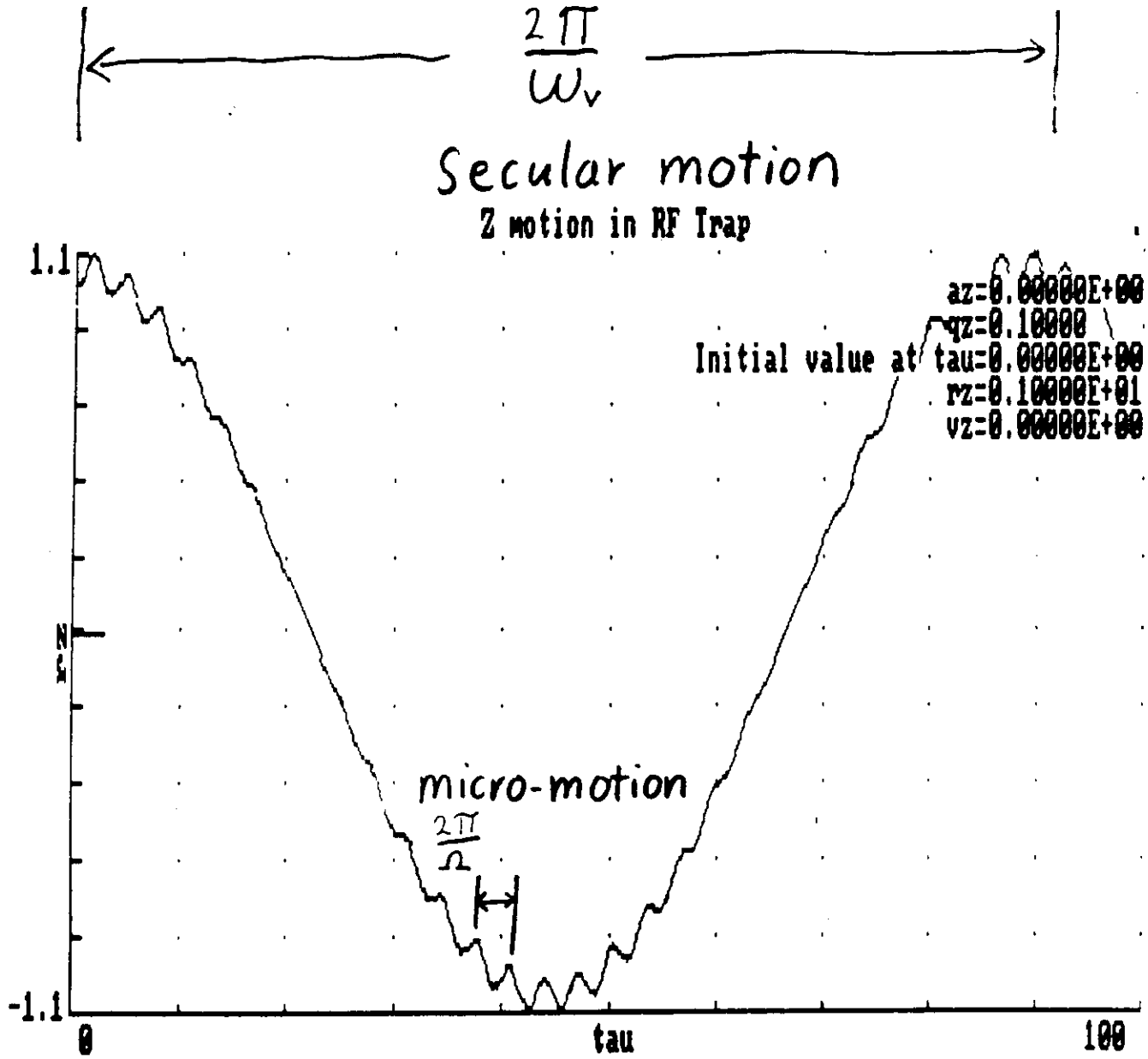
$\frac{2\pi}{\omega_v}$
Secular motion
Z motion in RF Trap
1.1
-1.1
0
tau
100
az=0.00000E+00
qz=0.10000
Initial value at tau=0.00000E+00
rz=0.10000E+01
vz=0.00000E+00
micro-motion
$\frac{2\pi}{\Omega}$

Doppler-Induced Motional Sidebands

Electric field of laser beam:

$$\vec{E} = \mathrm{Re}\ \vec{E}_o e^{i(kx-\omega_o t)}$$

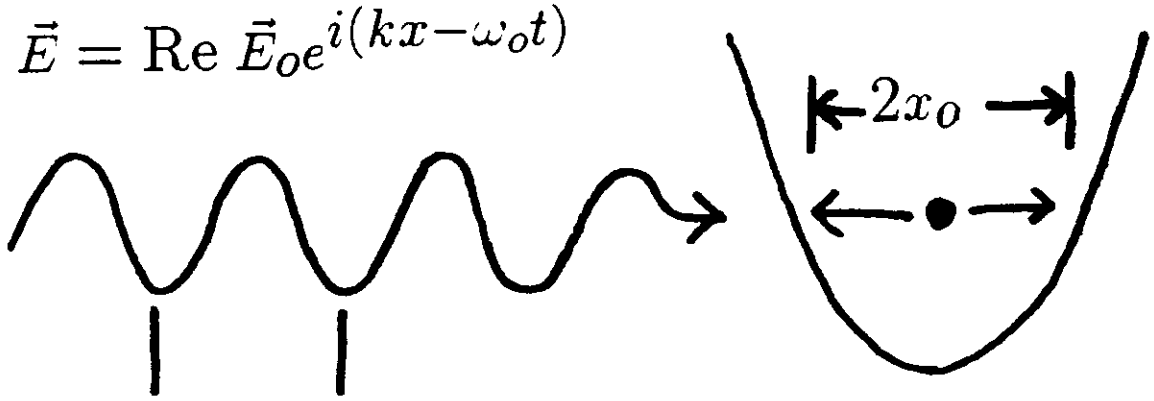

$$\lambda = \frac{2\pi}{k} \qquad x = x_o \cos \Omega t$$

In ion's frame:

$$\vec{E} = \mathrm{Re}\ \vec{E}_o e^{i(kx_o \cos \Omega t - \omega_o t)}$$

$$= \mathrm{Re}\ \vec{E}_o \sum_{n=-\infty}^{+\infty} i^n J_n(kx_o) e^{-i(\omega_o - n\Omega)t}$$

(Frequency modulation spectrum)

Accuracy of 1-ion optical frequency standard

Source of error	**Size** ($\Delta\nu/\nu$)
2nd-order Doppler	$\approx 1 \times 10^{-18}$
Magnetic field	$< 1 \times 10^{-18}$
Electric field (at 300K)	$\approx 1 \times 10^{-16}$ $(\propto T^4)$
Electric quadrupole	$\approx 1 \times 10^{-16}$ (can be calibrated)

Laser Spectroscopy of Trapped Atomic Ions

WAYNE M. ITANO, J. C. BERGQUIST, D. J. WINELAND

Recent developments in laser spectroscopy of atomic ions stored in electromagnetic traps are reviewed with emphasis on techniques that appear to hold the greatest promise of attaining extremely high resolution. Among these techniques are laser cooling and the use of single, isolated ions as experimental samples. Doppler shifts and other perturbing influences can be largely eliminated. Atomic resonances with line widths of a few parts in 10^{11} have been observed at frequencies ranging from the radio frequency to the ultraviolet. Experimental accuracies of one part in 10^{18} appear to be attainable.

ATOMIC SPECTROSCOPY DATES FROM THE 19TH CENTURY, when it was discovered that atomic vapors emitted and absorbed light at discrete resonance wavelengths, characteristic of each chemical element. When the quantum theory of atoms was developed in the 20th century by Niels Bohr and others, it was realized that these characteristic patterns of resonances, called spectra, were due to the quantum nature of the atom. The atom normally exists only in certain states of definite energy. Transitions between these allowed states are accompanied by the absorption or emission of quanta of light, called photons. The frequency ν of the light is related to the energy change ΔE of the atom by the formula $h\nu = |\Delta E|$, where h is Planck's constant. Accurate and detailed information about atomic spectra was crucial to the development of the modern theory of quantum mechanics.

Traditional (that is, nonlaser) optical spectroscopic methods, such as dispersing the light emitted from a gas with a diffraction grating, are limited in resolution by Doppler frequency shifts. Doppler shifts are the result of the motions of the atoms in a gas and cause the resonance absorption or emission lines to be much broader than the natural line widths (the line widths that would be observed if the atoms were motionless and isolated from perturbing influences such as collisions). Under typical laboratory conditions, the Doppler broadening results in a line width of about one millionth of the transition frequency, whereas the natural line widths are typically at least 100 times narrower. For example, the 280-nm first resonance line of Mg^+, which has a frequency of about 1.07×10^{15} Hz, has a Doppler-broadened line width at room temperature of about 3 GHz, whereas the natural line width is only 43 MHz. For a transition with a stable lower level, the natural line width (in hertz) is the inverse of the mean lifetime of the upper level (in seconds), divided by 2π.

The development of tunable lasers in the 1970s led to great advances in the resolution and accuracy with which optical atomic spectra could be observed. Laser light sources have high intensity and narrow line width. These properties make it possible to use various nonlinear spectroscopic techniques, such as saturated absorption or multiphoton absorption, that cancel the effects of first-order Doppler shifts, that is, Doppler shifts that are linear in the velocities of the atoms (*1*). The natural line width and the second-order Doppler shift, which is quadratic in the atomic velocities, still remain, however. The second-order Doppler shift is a result of relativistic time dilation. The atomic resonance is shifted like a clock, which runs at a rate that is slower for a moving atom than for an atom at rest. For typical laboratory conditions, this shift is very small, about one part in 10^{12}. Sometimes, even this shift can be troublesome. A good example is the work of Barger *et al.* on the 657-nm transition of calcium, which has a frequency of 4.57×10^{14}

The authors are with the Time and Frequency Division, National Bureau of Standards, Boulder, CO 80303.

Hz and a natural line width of 410 Hz (*2*). Resonances with line widths as small as 2 kHz were observed, but they were severely shifted and distorted by the second-order Doppler shift.

In order to reduce both the first- and second-order Doppler shifts, some method of reducing the temperature of the atoms under study is required. An atomic vapor placed in a conventional refrigeration device would quickly condense on the walls of the container. But laser cooling, a method by which laser radiation pressure is used to reduce the velocities of atoms, achieves the cooling without contact with material objects (*3–5*). The technique was proposed independently by Hänsch and Schawlow (*6*) for free atoms and by Wineland and Dehmelt (*7*) for trapped ions. Laser cooling to temperatures on the order of 1 mK has been demonstrated with some kinds of atoms and atomic ions. This reduces the second-order Doppler shifts to the level where they are not a problem. An atom or atomic ion of mass 100 u (unified atomic mass units) cooled to 1 mK has a second-order Doppler shift of 1.4 parts in 10^{18}.

Transit-time broadening is another effect that limits the resolution with which spectra can be observed. The observed resonance line width cannot be much less than the inverse of the observation time. This is a consequence of Heisenberg's uncertainty relation applied to time and energy. In the case of the work on calcium, the observation time was limited to about 0.3 msec by the time it took the atoms to pass through the 21-cm-long resonance region (*2*). One way to increase the observation time is by trapping the atoms with electromagnetic fields. In some experiments, atoms are confined with specially coated walls or by buffer gases, but collisions with the wall or buffer gas molecules shift and broaden the observed resonances. Atomic ions can be trapped for long periods by fields that do not disturb their resonance frequencies by significant amounts. Neutral atoms have been trapped by static magnetic fields (*8*) and by optical fields (*9, 10*), but the trapping fields tend to strongly perturb the resonances.

The work described in this article has the goal of achieving greatly improved spectroscopic resolution and accuracy. The experimental methods involve the use of frequency-stabilized lasers to measure the spectra of atomic ions, sometimes single ions, that are laser cooled and electromagnetically trapped. The most obvious applications of such work are frequency standards and clocks of great accuracy; this is the primary goal of the work done in our laboratories at the National Bureau of Standards (NBS). These experiments have applications to other areas of physics, however, such as atomic physics and quantum optics. One example is the recent observation of quantum jumps (sudden changes of quantum state) of an individual atomic ion (*11–13*).

Ion Traps

Ion traps confine ions by means of electric and magnetic fields (*14, 15*). Two types of ion traps are commonly used for spectroscopic experiments, the Penning trap and the Paul or rf (radio frequency) trap.

The Penning trap is based on a combination of static electric and magnetic fields. The electric fields are produced by applying an electric potential between the ring and endcap electrodes, which are shown schematically in Fig. 1. The electric forces repel the ions from the endcaps and provide confinement along the axis of the trap. A strong, uniform magnetic field is applied along the trap axis to provide radial confinement. Full three-dimensional confinement is provided by this combination of electric and magnetic fields. For a trap with inside dimensions of about 1 cm, a typical value of the electric potential difference is 1 volt and of the magnetic field, 1 tesla. The potential energy of an ion is lowered as it moves out

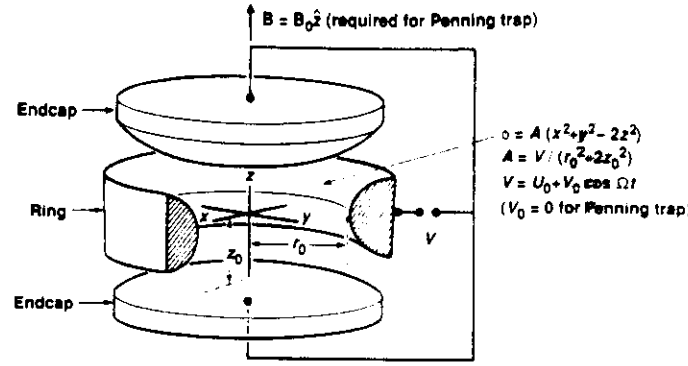

Fig. 1. Electrodes for a Penning or rf ion trap. The electric potential field ϕ is created by applying the voltage V between the endcap electrodes and the ring electrode. The uniform magnetic field **B** is required only for a Penning trap. [Adapted from (*42*) with permission from Plenum Press]

radially from the axis of the trap. Hence, even though an ion would remain trapped forever if undisturbed, collisions with neutral background gas molecules increase the radial extent of the orbit until eventually the ion collides with the ring. In practice, under conditions of high vacuum, it is not uncommon for an ion to remain confined for days.

The rf trap uses oscillating electric fields and does not require a magnetic field. The electrode structure is the same as that of a Penning trap (see Fig. 1), but the applied electric potential varies sinusoidally in time. The electric field forces an ion to oscillate in position with an amplitude proportional to the field strength. The phase of the motion with respect to the applied field is such that the average force on the ion in the spatially nonuniform field is directed toward regions of weaker field (the center of the trap in this case). The trajectory of an ion can be separated into a part that oscillates at the frequency of the applied field, called the micromotion, and a part that varies more slowly, called the secular motion. The oscillating field creates an effective potential-energy well, sometimes called a pseudopotential, for the secular motion of an ion. For a trap with electrodes like those in Fig. 1, the pseudopotential is approximately a three-dimensional harmonic well, so the secular motion is characterized by well-defined frequencies. The electrodes of an rf trap identical to those used in the NBS experiments with Hg^+ ions (*12, 16, 17*) are shown in Fig. 2. The inside radius of the trap is slightly less than 1 mm. Under typical operating conditions, an electric potential of peak amplitude 570 volts and frequency 21 MHz is applied, creating a pseudopotential well about 15 eV deep. The frequency of the secular motion is about 1.5 MHz. In some cases, an ion can be held in the trap for several days before it is lost, possibly through a chemical reaction with a residual gas molecule.

Laser Cooling

It has been known for a long time that light can exert a force on a material body. In 1873, Maxwell showed that his theory of electromagnetic fields predicted that a beam of light would exert a force on a reflecting or absorbing body. This phenomenon is commonly known as radiation pressure. Light has momentum, the momentum density being numerically equal to the energy density divided by c, the speed of light. Radiation pressure is thus a consequence of conservation of momentum. In the early 1900s, radiation pressure was observed experimentally by Nichols and Hull in the United States (*18*) and by Lebedev in Russia (*19*), and shown to be in good agreement with theory. In 1933, Frisch first observed radiation pressure on the atomic scale (*20*). In his experiment, a beam of

[illegible] traveling through an evacuated chamber was deflected by a lamp emitting sodium resonance light of wavelength 589 nm. The average deflection of an atom was that due to a transfer of momentum equal to that of a single photon, $\hbar k$.

The force exerted by light on atoms is often divided into two parts. These are called the light-pressure or scattering force and the gradient or dipole force (*21*). In some simple cases, these two forces can be clearly distinguished, but in the general case, particularly for high light intensities, the simple descriptions of the forces break down, and a quantum-mechanical description is required.

The scattering force is simply radiation pressure at the atomic level, the force observed by Frisch (*20*). The average scattering force is in the direction of propagation of the light and is equal to the product of the momentum per photon and the photon scattering rate. The force reaches a maximum when the light is resonant with an atomic transition. Fluctuations in the scattering force arise because the photon scatterings take place at random times and because the direction of the reemitted photon, and hence the direction of the recoil momentum due to this reemission, is random.

The dipole force can be understood by considering the atom to be a polarizable body. The optical electric field induces an electric dipole moment in the atom; the induced dipole is acted on by the optical electric field. If the light intensity is spatially nonuniform, a force is induced parallel to the gradient of the intensity. The dipole force attracts an atom to a region of high light intensity if the frequency of the light is below the atomic resonance and repels it if it is above. Sodium atoms have been trapped, by means of the dipole force, near the focus of a laser beam tuned below the first resonance transition (*10*).

The laser cooling that has been demonstrated in ion traps is based on the use of the scattering force only. It is also possible to cool by use of the dipole force (*22*), as has recently been demonstrated in an atomic beam experiment (*23*), but this method does not appear to have any advantage for trapped ions. The theoretical description of the cooling depends on whether the natural line width γ of the resonance transition used for cooling is greater than or less than the frequencies of the oscillatory motion ω_z of the ion in the trap. The former case is called the heavy-particle or weak-binding limit; the latter is called the sideband-cooling or strong-binding limit (*3*, *5*, *24*). (Both γ and ω_z are expressed in angular frequency units.)

Consider first the heavy-particle limit, $\gamma \gg \omega_z$, where ω_z is any of the motional frequencies. In this limit, each photon scattering event takes place in a time much less than a motional cycle, so that the scattering force can be considered to be made up of a series of impulses. Assume that a trapped ion is irradiated with a beam of light tuned lower than the resonance frequency. When the velocity of the ion is opposed to the direction of propagation of the laser beam, the frequency of the light in the frame of reference of the ion is Doppler-shifted closer to resonance than if it had zero velocity. Hence, the magnitude of the scattering force is higher when the atom moves against the laser beam, and its velocity is damped. When it moves in the same direction as the light, the light is Doppler-shifted away from resonance, and the magnitudes of the scattering force is reduced. The net effect is to reduce the kinetic energy of the ion, that is, to cool it. The ion is heated if the light is

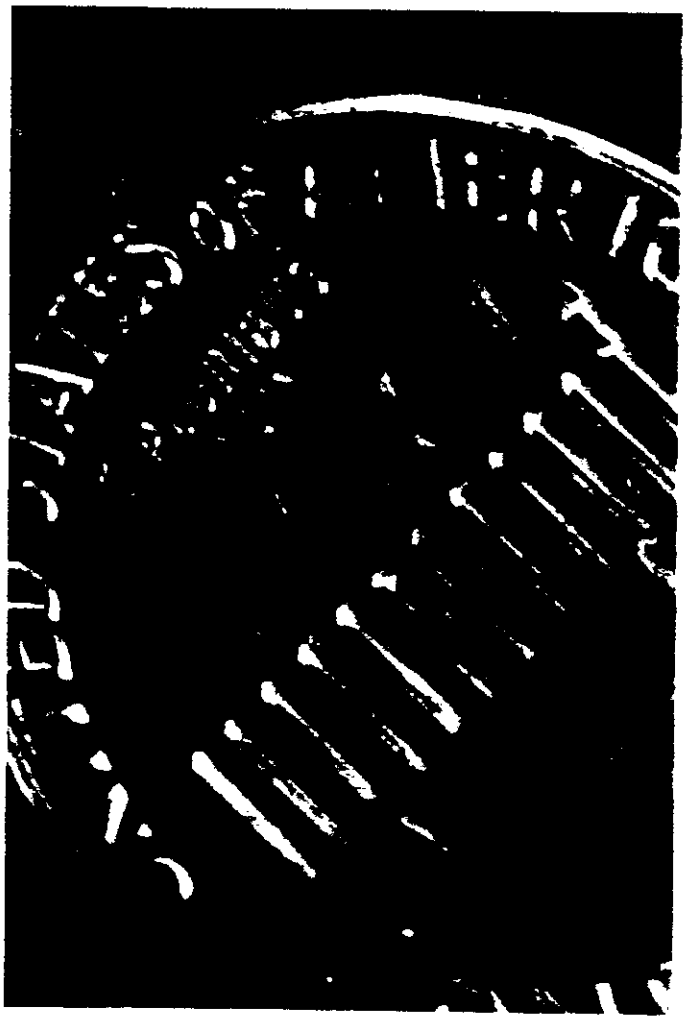

Fig. 2. The electrodes of a small rf trap, shown on a coin for scale.

Fig. 3. False color image of a single Hg^+ ion (small isolated dot slightly below the center) stored in an rf trap. The other smaller dots due to light reflected from the trap electrodes, whose orientation is the same as in Fig. 2. The largest reflection is from the front surface of the ring electrode. The two smaller reflections are from the edges of two of the endcap electrodes. Computerized imaging system developed by C. Manney and J. Bolanger (NBS). [Adapted from (*45*) with permission from the American Institute of Physics.]

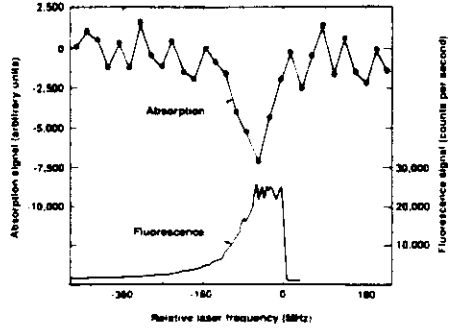

Fig. 4. The absorption signal of a single Hg^+ ion stored in an rf trap (upper trace). Radio-frequency modulation and demodulation techniques were used to reduce noise, resulting in a signal proportional to the derivative of the absorption with respect to laser frequency. The lower trace is the fluorescence signal, observed at the same time. The fluorescence drops off suddenly when the frequency is above resonance, due to laser heating. The flattened top of this curve is due to the frequency modulation. Integration times per point are 50 seconds and 10 seconds in the upper and lower traces, respectively. [Adapted from (*17*) with permission from the Optical Society of America]

higher in frequency than the resonance.) The minimum number of photon scatterings required to cool an ion substantially, starting from 300 K, is on the order of the ratio of the ion's momentum to a photon momentum, or about 10,000. Because of the inherent fluctuations of the scattering force, which cause heating, the kinetic energy is not damped to zero, but eventually reaches a steady value that depends on the degree of frequency detuning below the resonance. The detuning that gives the lowest temperature is equal to one half of the natural line width. This minimum temperature T_{min} is given by the relation $k_B T_{min} \simeq \hbar\gamma/2$, where k_B is Boltzmann's constant and $\hbar$ is Planck's constant divided by 2π. For example, T_{min} for Mg^+ ($\gamma/2\pi$ = 43 MHz) is 1 mK.

Now consider the sideband-cooling ($\gamma << \omega_v$) limit. The absorption spectrum of the ion consists of an unshifted resonance line at angular frequency ω_0, called the carrier, and a series of discrete lines on both sides of the carrier, each having (ideally) the natural line width, and separated by multiples and combinations of the motional frequencies. These extra lines, called motional sidebands, are the result of the periodic frequency modulation of the light frequency, arising from the Doppler effect, as observed by the moving ion. To cool an ion, the frequency of the laser beam is tuned to a sideband on the low-frequency side of the carrier, for example, to $\omega_0 - p\omega_v$, where p is a positive integer. The ion is induced to make transitions to the upper electronic state, with a decrease in the vibrational energy. When the ion makes a transition back to its ground electronic state, it may either increase or decrease its vibrational energy, but the average vibrational energy change is equal to $R = (\hbar\omega_0)^2/(2Mc^2)$, where M is the mass of the ion. The quantity R, sometimes called the recoil energy, is the kinetic energy that an initially motionless-free ion acquires after emitting a photon of energy $\hbar\omega_0$. If $R < p\hbar\omega_v$, the ion is cooled. If $R << \hbar\omega_v$, which is not hard to satisfy in practice, and if the frequency width of the light is much less than γ, then the ion can be cooled until it occupies the lowest quantum state of the trap potential most of the time. In this limit, the fraction of the time that the ion is not in the lowest state is on the order of $(\gamma/\omega_v)^2$ (*3, 5, 24, 25*). The sideband cooling discussion can also be applied to the $\gamma >> \omega_v$ case (*24, 26*). Recently, Lindberg, Javanainen, and Stenholm (*27*) have treated theoretically the general case of laser cooling of an ion trapped in a harmonic well, for an arbitrary ratio of γ to ω_v and also for arbitrary laser intensity. The lowest temperatures are obtained in the low-intensity limit.

The first experimental observations of laser cooling were made in 1978 at NBS by Wineland, Drullinger, and Walls (*28*) and at the University of Heidelberg by Neuhauser, Hohenstatt, Toschek, and Dehmelt (*26*). The NBS experiment used Mg^+ ions in a Penning trap, whereas the Heidelberg experiment used Ba^+ ions in an rf trap. In later experiments at these and other laboratories, cooling of trapped ions has been observed to temperatures in the range of a few millikelvin, close to the theoretical limit. So far, only strongly allowed transitions have been used for cooling, so the theory for the $\gamma >> \omega_v$ case applies.

Only a few kinds of ions have been laser-cooled. Laser cooling requires that the ion be cycled repeatedly between the ground state and an excited state. To be laser-cooled easily, an ion should have a strongly allowed resonance transition, at a wavelength where a tunable, continuous wave radiation source is available, and be free of intermediate metastable levels that would interrupt the cycling. Even Ba^+, one of the first ions to be laser-cooled, is not ideal, since it can decay into a metastable level from the upper level of the resonance transition. A second laser is required to drive the ion out of the metastable level. A way to cool a species of ion that cannot be laser-cooled directly is to store it in a trap together with a species that can be cooled directly. As one species is laser-cooled, the other species is cooled indirectly by Coulomb collisions. This technique, called sympathetic laser cooling, has been demonstrated in an experiment in which Hg^+ ions in a Penning trap were cooled to less than 1 K by Coulomb coupling with laser-cooled Be^+ ions (*29*).

Spectroscopy of Atomic Ions in Traps

A number of spectroscopic measurements have been made of non-laser-cooled ions in traps, particularly at microwave frequencies (*14, 15, 30, 31*). In the more accurate of these experiments, the uncertainty was due mainly to the second-order Doppler shift. For cases in which laser cooling can be applied, Doppler shifts are suppressed, and spectra can be observed with extremely high resolution, nearly free from perturbing influences.

Dicke showed in 1953 that the confinement of an atom to a

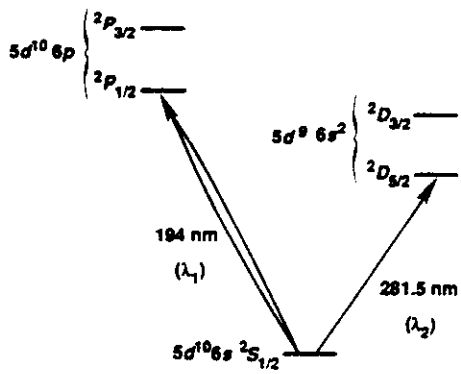

Fig. 5. Lowest energy levels of Hg^+. Absorption of a λ_2 photon is detected by the cessation of laser-induced fluorescence at λ_1. [Adapted from (*12*) with permission from the American Institute of Physics]

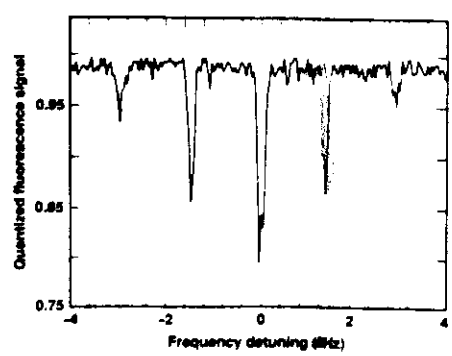

Fig. 6. The 281.5-nm transition observed in a single Hg^+ ion. The frequency detuning of the laser is plotted on the horizontal axis. The intensity ratios of the motional sidebands to the carrier (central line) indicate a temperature of about 6 mK. [Adapted from (*16*) with permission from the American Institute of Physics]

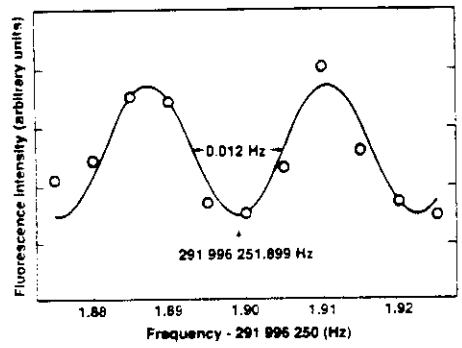

Fig. 7. Graph of a radio frequency hyperfine-structure resonance in $^{25}Mg^+$ ions stored in a Penning trap. Fluorescence intensity is plotted as a function of field frequency minus an offset of 291 996 250 Hz. Arrow indicates center of resonance. The oscillatory line shape results from the use of Ramsey's separated-oscillatory-field method. [Adapted from (*38*) with permission from the American Institute of Physics]

region of space smaller than the resonance-radiation wavelength leads to a suppression of the first-order Doppler shift broadening (*32*). It is easy to satisfy this condition, commonly called the Lamb-Dicke criterion, for a microwave resonance, since the wavelengths can be several centimeters long. Microwave frequency standards such as the atomic hydrogen maser make use of this fact. In the optical region, it can be satisfied for a single, laser-cooled ion confined in a trap. (Coulomb repulsion between ions makes it difficult to satisfy the Lamb-Dicke criterion when more than one ion is in the trap.)

The second-order Doppler shift of an ion that is laser-cooled to T_{min} is around one part in 10^{18} even for a strongly allowed transition (high γ). If more than one ion is present in the trap, then the kinetic energies per ion, and hence the second-order Doppler shifts, are necessarily higher. In the case of the rf trap, the Coulomb repulsion between ions leads to their being trapped away from the center of the trap, so the oscillating electric field, and hence the micromotion, is nonzero. In the case of the Penning trap, the presence of the other ions leads to increased velocities of rotation around the trap axis in the presence of crossed electric and magnetic fields. It appears that, for a single ion, shifts of resonance frequencies owing to electric and magnetic fields could be as small as a part in 10^{18}, since the ion is trapped in a region where the electric field approaches zero (*33*, *34*).

Naturally, the signal-to-noise ratio suffers when the sample under observation consists of only a single ion. However, once an ion has been trapped and cooled, its presence can be detected easily by laser-induced fluorescence, since a strongly allowed transition can scatter as many as 10^8 photons per second. In fact, a single, trapped Ba^+ ion has been observed visually, through a microscope, by laser-induced fluorescence (*35*). Single ions have been observed in both Penning and rf traps (*11*, *13*, *15*, *30*, *35*). Figure 3 shows a false color image of the 194-nm laser-induced fluorescence of a single Hg^+ ion confined in an rf trap. This image was obtained at NBS with a position-sensing photomultiplier tube interfaced to a computer. It has even been possible to detect the resonance absorption due to a single Hg^+ ion by a decrease of the intensity of the 194-nm beam passing through the trap (*17*). The fraction of the light absorbed by the ion was around 10^{-5}. Figure 4 shows the absorption signal and the fluorescence signal, measured simultaneously as the laser was swept through the resonance.

A transition with a narrow natural line width would be difficult to detect directly by fluorescence, since the long lifetime of the upper state limits the rate at which photons are emitted. A way around this problem was suggested by Dehmelt (*36*). Consider an atom that has both a strongly allowed transition (at wavelength λ_1) and a weakly allowed transition (at wavelength λ_2) from the ground state. Figure 5 shows an example of such an atom (Hg^+). The narrow resonance at λ_2 is detected as follows: The atom is assumed to be initially in the ground state. Laser light at a wavelength near λ_2 is pulsed on, possibly driving the atom to the long-lived upper level of this transition. Then light at a wavelength near λ_1 is pulsed on. If the atom had made a transition in the previous step, no fluorescence would be observed; otherwise fluorescence will be observed at an easily detectable level. The detection of presence or absence of the λ_1 fluorescence is much easier than attempting to detect the one λ_2 photon that eventually is emitted when the long-lived state spontaneously decays. The method is called "electron shelving," since the optical electron is temporarily shelved in the long-lived level.

So far, only a few measurements of the optical spectra of trapped laser-cooled ions have been made. Some measurements have been made of strongly allowed transitions in Be^+ and Mg^+, with resolutions near the natural line widths of tens of megahertz. These measurements have yielded some values for energy level splittings, including fine-structure and hyperfine-structure splittings (*15*, *30*). A two-photon transition from the ground $6^2S_{1/2}$ to the $5^2D_{3/2}$ state has been observed in a single Ba^+ ion, with a resolution, limited by the laser line width, of 3 MHz (*37*). Recently, at NBS, the $5d^{10}6s\ ^2S_{1/2}$ to $5d^96s^2\ ^2D_{5/2}$ 281.5-nm transition has been observed in a single, trapped Hg^+ ion (*16*). The ion was laser-cooled, by means of the 194-nm $6s\ ^2S_{1/2}$ to $6p\ ^2P_{1/2}$ transition, to near the theoretical limit of 1.7 mK. Figure 6 shows the spectrum obtained by tuning a laser across the narrow *S*-to-*D* transition. The electron shelving detection method was used. Immediately after the 281.5-nm radiation was shut off, the 194-nm fluorescence intensity was measured. If it was low enough to indicate that the ion had made a transition to the *D*-state, the signal was defined to be 0. Otherwise, it was defined to be 1. The average of these measurements is plotted along the vertical axis. The carrier and the two closest motional sidebands on each side are visible. The line widths were deliberately broadened to reduce the time required to sweep the resonance. On other sweeps, line widths of about 30 kHz were observed, a result mainly of laser frequency instability. The lifetime of the upper level is approximately 0.1 second, so the natural line width is about 1.6 Hz. The size of the sidebands indicates that the ion has been cooled approximately to the Lamb-Dicke regime. The root-mean-square amplitude of motion is estimated to be 50 nm.

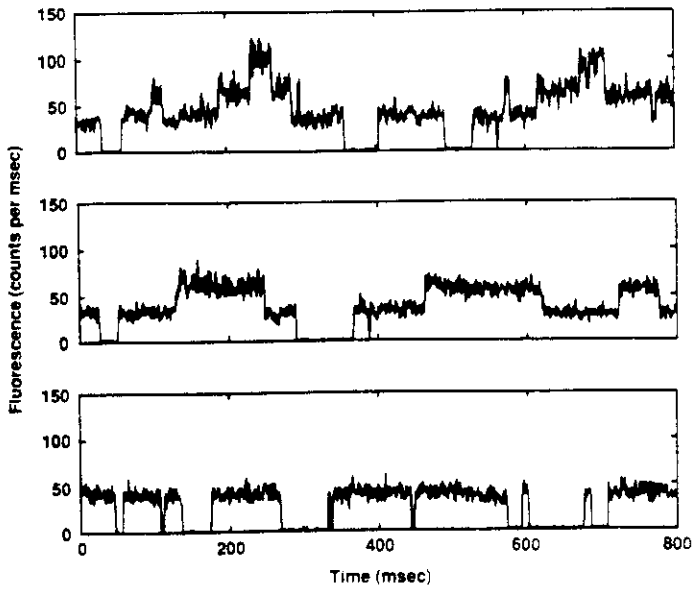

Fig. 8. Fluorescence intensity as a function of time for samples of three ions (top trace), two ions (middle trace), and one ion (bottom trace) in an rf trap. The fluorescence changes suddenly each time an Hg^+ ion either makes a transition to a metastable *D*-state (step down) or back to the ground *S*-state from a *D*-state (step up). The integration time per point is 1 msec.

I-22

Microwave spectra of trapped ions are usually observed by some form of microwave-optical double resonance. Hyperfine splittings and g-factors of the ground states of several atomic ions have been measured (*15, 30, 31*). So far, all of these experiments involve samples of more than one ion. Figure 7 shows an example of the kind of resolution that can be obtained with trapped ions (*38*). The line width of the resonance (a hyperfine transition in $^{25}Mg^+$) is only 12 mHz. The fractional resolution is about the same as for the Hg^+ S-to-D optical transition. In another experiment at NBS, the frequency of a hyperfine transition in $^9Be^+$ has been measured with an accuracy of about one part in 10^{13}, which is comparable to the most accurate frequency standards in existence (*39*). The accuracy was limited to this value by the second-order Doppler shift, because the laser cooling had to be shut off while the microwave transition was being driven, in order not to perturb the resonance frequency, and the ions heated up during this period. Sympathetic laser cooling using Mg^+ might provide a solution to this problem.

Quantum Jumps

Recently, Cook and Kimble (*40*) theoretically investigated a three-level atom like the one considered by Dehmelt in his "shelved electron" proposal. Light at wavelengths λ_1 and λ_2 was assumed to be present at the same time. They predicted that one would observe the λ_1 fluorescence to turn off and on abruptly as the atom made transitions (quantum jumps) to and from the long-lived upper level. This paper generated a great deal of theoretical interest, and the problem was approached from various viewpoints (*41*). The novelty of this problem is that theorists are accustomed to calculating, and experimenters are accustomed to measuring, ensemble averages rather than following the development in time of a single quantum system.

The experiment that is the most similar to the one treated by Cook and Kimble was performed at NBS on a single, trapped Hg^+ ion (*12*). Light at 194 nm (λ_1) and 281.5 nm (λ_2) was present at the same time (see Fig. 5). The 194-nm fluorescence level was observed to be bistable, switching suddenly between a steady level and zero. The rate at which the switches occurred increased as the intensity of the 281.5-nm light was increased. The statistical properties of the quantum jumps were consistent with theory and with previous measurements of the lifetime of the $^2D_{5/2}$ state. If the intensity of the 194-nm light is increased, then quantum jumps are observed even without the 281.5-nm light present. [These events occurred at a low rate in the data of (*12*).] The reason for these events is that the upper level of the 194-nm transition has a small probability (about 1 in 10^7) of decaying to the $^2D_{3/2}$ level rather than back to the ground state. The $^2D_{3/2}$ state has a lifetime of about 10 msec and about an equal probability of decaying either to the $^2D_{5/2}$ level or to the ground state. The bottom trace of Fig. 8 shows the 194-nm fluorescence intensity of a single ion as a function of time, clearly showing the quantum jumps. The middle and top traces in Fig. 8 show the fluorescence when two or three ions are in the trap. When more than one ion is present in the trap, the fluorescence level jumps between several discrete levels, depending upon how many ions are in one of the D-states. Quantum jumps have been observed by other groups, using trapped Ba^+ ions (*11, 13*).

Conclusions

Spectroscopy of trapped atomic ions has already achieved impressive levels of accuracy and resolution. The ultimate limits have certainly not been reached, and no fundamental (as opposed to technical) obstacles preventing the achievement of measurement accuracies (in special cases) of one part in 10^{18} are foreseen (*33, 34*). Interesting spin-offs from the quest for improved spectroscopic methods, such as the observation of quantum jumps, will no doubt continue to appear.

REFERENCES AND NOTES

1. *High-Resolution Laser Spectroscopy*, K. Shimoda, Ed. (Springer-Verlag, Berlin, 1976); M. D. Levenson, *Introduction to Nonlinear Laser Spectroscopy* (Academic Press, New York, 1982).
2. R. L. Barger, J. C. Bergquist, T. C. English, D. J. Glaze, *Appl. Phys. Lett.* **34**, 850 (1979); R. L. Barger, *Opt. Lett.* **6**, 145 (1981).
3. S. Stenholm, *Rev. Mod. Phys.* **58**, 699 (1986).
4. W. D. Phillips and H. J. Metcalf, *Sci. Am.* **256**, 50 (March 1987).
5. D. J. Wineland and W. M. Itano, *Phys. Rev. A* **20**, 1521 (1979); W. M. Itano and D. J. Wineland, *ibid.* **25**, 35 (1982).
6. T. W. Hänsch and A. L. Schawlow, *Opt. Commun.* **13**, 68 (1975).
7. D. J. Wineland and H. Dehmelt, *Bull. Am. Phys. Soc.* **20**, 637 (1975).
8. A. L. Migdall, J. V. Prodan, W. D. Phillips, T. H. Bergeman, H. J. Metcalf, *Phys. Rev. Lett.* **54**, 2596 (1985).
9. S. Chu, L. Hollberg, J. E. Bjorkholm, A. Cable, A. Ashkin, *ibid.* **55**, 48 (1985).
10. S. Chu, J. E. Bjorkholm, A. Ashkin, A. Cable, *ibid.* **57**, 314 (1986).
11. W. Nagourney, J. Sandberg, H. Dehmelt, *ibid.* **56**, 2797 (1986).
12. J. C. Bergquist, R. G. Hulet, W. M. Itano, D. J. Wineland, *ibid.* **57**, 1699 (1986).
13. T. Sauter, W. Neuhauser, R. Blatt, P. E. Toschek, *ibid.*, p. 1696.
14. H. Dehmelt, *Adv. At. Mol. Phys.* **3**, 53 (1967); *ibid.* **5**, 109 (1969).
15. D. J. Wineland, W. M. Itano, R. S. Van Dyck, Jr., *ibid.* **19**, 135 (1983).
16. J. C. Bergquist, W. M. Itano, D. J. Wineland, *Phys. Rev. A* **36**, 428 (1987).
17. D. J. Wineland, W. M. Itano, J. C. Bergquist, *Opt. Lett.*, **12**, 389 (1987).
18. E. F. Nichols and G. F. Hull, *Phys. Rev.* **13**, 307 (1901).
19. P. Lebedev, *Ann. Phys. (Leipzig)* **6**, 433 (1901); *ibid.* **32**, 411 (1910).
20. O. Frisch, *Z. Phys.* **86**, 42 (1933).
21. A. Ashkin, *Science* **210**, 1081 (1980); V. S. Letokhov and V. G. Minogin, *Phys. Rep.* **73**, 1 (1981); A. P. Kazantsev, G. A. Ryabenko, G. I. Surdutovich, V. P. Yakovlev, *ibid.* **129**, 75 (1985).
22. A. P. Kazantsev, V. S. Smirnov, G. I. Surdutovich, D. O. Chudesnikov, V. P. Yakovlev, *J. Opt. Soc. Am. B* **2**, 1731 (1985); J. Dalibard and C. Cohen-Tannoudji, *ibid.*, p. 1707.
23. A. Aspect, J. Dalibard, A. Heidmann, C. Salomon, C. Cohen-Tannoudji, *Phys. Rev. Lett.* **57**, 1688 (1986).
24. H. Dehmelt, in *Advances in Laser Spectroscopy*, F. T. Arecchi, F. Strumia, H. Walther, Eds., vol. 95 of NATO Advanced Science Institutes Series B (Plenum, New York, 1983), pp. 153–187.
25. D. J. Wineland, W. M. Itano, J. C. Bergquist, R. G. Hulet, *Phys. Rev. A*, in press.
26. W. Neuhauser, M. Hohenstatt, P. Toschek, H. Dehmelt, *Phys. Rev. Lett.* **41**, 233 (1978).
27. M. Lindberg, *J. Phys. B* **17**, 2129 (1984); J. Javanainen, M. Lindberg, S. Stenholm, *J. Opt. Soc. Am. B* **1**, 111 (1984).
28. D. J. Wineland, R. E. Drullinger, F. L. Walls, *Phys. Rev. Lett.* **40**, 1639 (1978).
29. D. J. Larson, J. C. Bergquist, J. J. Bollinger, W. M. Itano, D. J. Wineland, *ibid.* **57**, 70 (1986).
30. D. J. Wineland, W. M. Itano, J. C. Bergquist, J. J. Bollinger, J. D. Prestage, in *Atomic Physics Nine: Proceedings of the Ninth International Conference on Atomic Physics, Seattle, Washington, July 1984*, R. S. Van Dyck, Jr., and E. N. Fortson, Eds. (World Scientific, Singapore, 1984), p. 3.
31. G. Werth, in *ibid.*, p. 28.
32. R. H. Dicke, *Phys. Rev.* **89**, 472 (1953).
33. H. G. Dehmelt, *IEEE Trans. Instrum. Meas.* **IM-31**, 83 (1982).
34. D. J. Wineland, *Science* **226**, 395 (1984).
35. W. Neuhauser, M. Hohenstatt, P. E. Toschek, H. Dehmelt, *Phys. Rev. A* **22**, 1137 (1980); W. Nagourney and H. Dehmelt, personal communication.
36. H. G. Dehmelt, *Bull. Am. Phys. Soc.* **20**, 60 (1975).
37. G. Janik, W. Nagourney, H. Dehmelt, *J. Opt. Soc. Am. B* **2**, 1251 (1985).
38. W. M. Itano and D. J. Wineland, *Phys. Rev. A* **24**, 1364 (1981).
39. J. J. Bollinger, J. D. Prestage, W. M. Itano, D. J. Wineland, *Phys. Rev. Lett.* **54**, 1000 (1985).
40. R. J. Cook and H. J. Kimble, *ibid.*, p. 1023.
41. J. Javanainen, *Phys. Rev. A* **33**, 2121 (1986); A. Schenzle, R. G. DeVoe, R. G. Brewer, *ibid.*, p. 2127; C. Cohen-Tannoudji and J. Dalibard, *Europhys. Lett.* **1**, 441 (1986); D. T. Pegg, R. Loudon, P. L. Knight, *Phys. Rev. A* **33**, 4085 (1986); A. Schenzle and R. G. Brewer, *ibid.* **34**, 3127 (1986); H. J. Kimble, R. J. Cook, A. L. Wells, *ibid.*, p. 3190; P. Zoller, M. Marte, D. F. Walls, *ibid.* **35**, 198 (1987).
42. L. R. Brewer, J. D. Prestage, J. J. Bollinger, D. J. Wineland, in *Strongly Coupled Plasma Physics*, F. J. Rogers and H. E. De Witt, Eds. (Plenum, New York, 1987).
43. D. J. Wineland and W. M. Itano, *Phys. Today* **40**, 34 (June 1987).

44. We gratefully acknowledge the support of the Air Force Office of Scientific Research and the Office of Naval Research. This article is not subject to copyright in the United States.

ION SITS STILL FOR SHARP 'PICTURE' OF ITS OPTICAL TRANSITION

A single atom, isolated and motionless, should be an excellent clock. It can radiate signals that are free of Doppler shifts and distortions introduced by its interactions with the environment. Just such thinking has motivated much work on ion traps, and that research is now bearing fruit: A group working at the National Institute of Standards and Technology in Boulder has measured the frequency of an ultraviolet transition in a single mercury atom with a linewidth under 180 Hz. The work was reported by James Bergquist, Frank Dietrich (now at Gsänger Optoelectronik, FRG), Wayne Itano and David Wineland at the Ninth International Conference on Laser Spectroscopy, held in Bretton Woods, New Hampshire, last June.[1] Before this recent feat, the narrowest width measured for an optical frequency had been on the order of a few kilohertz.

The NIST researchers report that their resolution is limited only by the stability of the laser driving the transition. They expect to improve this resolution by a factor of 100 by further stabilizing the laser. The linewidth measured by the NIST team corresponds to a fractional resolution of about 2×10^{13}. Higher fractional resolutions have been achieved in Mössbauer spectroscopy, Wineland told us, but single-ion spectroscopy allows more precise determination of the center of the resonance.

At the University of Washington, Warren Nagourney, Nan Yu and Hans Dehmelt have observed an infrared transition at 1.762 μm in a single barium ion, but with a lower resolution (38 kHz).[2] A group led by Peter Toschek at the University of Heidelberg observed[3] a single-particle spectrum in 1981, and Toschek continues this work on single trapped ions with colleagues at the University of Hamburg.

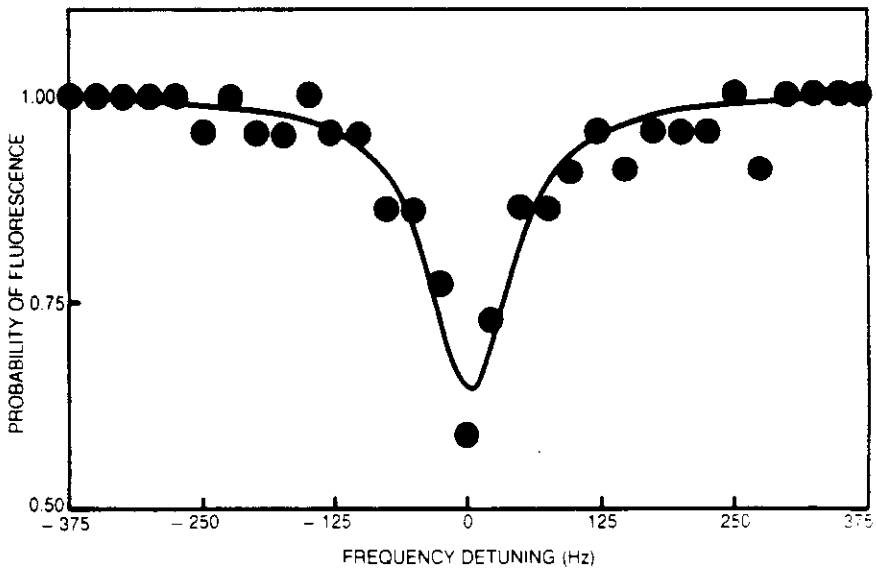

High-resolution optical frequency spectrum of an atomic resonance. The signal here shows the fluorescence stimulated in a single mercury ion by a 194-nm laser after the ion is first irradiated with another oscillator, tuned near the transition from the ground state to a metastable state. If the oscillator excites the ion to this metastable state, it will no longer fluoresce. The 563-nm laser driving the transition is frequency doubled, so that the full width at half-maximum shown here corresponds to a 172-Hz linewidth for the ultraviolet atomic transition. (Adapted from a figure provided by the National Institute of Standards and Technology.)

Holding the ion still

To confine the $(Hg^{199})^+$ ion nearly at rest, Bergquist and his colleagues used techniques developed over the years to trap and cool ions. They placed the ion in a miniature Paul trap—a few hundred microns on a side—where the ion oscillated in the harmonic potential well created by the trap's particular configuration of electrodes. The researchers then slowed the ion's motion by laser cooling, a technique developed by Dehmelt and Wineland and independently by Theodor Hänsch (University of Munich) and Arthur Schawlow (Stanford University). (See the article by Wineland and Itano in PHYSICS TODAY June 1987, page 34.) In this technique, the ion is illuminated with two orthogonal laser beams that are tuned just below the frequency for the transition to one of the excited electronic states. The ion absorbs the radiation only when it is moving toward the laser beam (due to the Doppler effect), and thus slows in that direction to conserve momentum. As the ion reradiates, it does so symmetrically. Thus, on the average, it acquires no momentum in the emisson process.

Once the atom was trapped and cooled, the remaining problem was to detect efficiently the lone photon from a single radiating ion. The metastable state at 282 nm the NIST scientists hoped to excite lives for about 0.1 sec, so that the one photon emitted in that time is virtually impossible to see. Instead of looking for this transition directly, Bergquist and his colleagues exploited the high fluorescence rate of the 194-nm transition in the same ion. In the method they used, which was proposed by Dehmelt in 1975, the absence or presence of 194-nm fluorescence indicates whether light of a particular

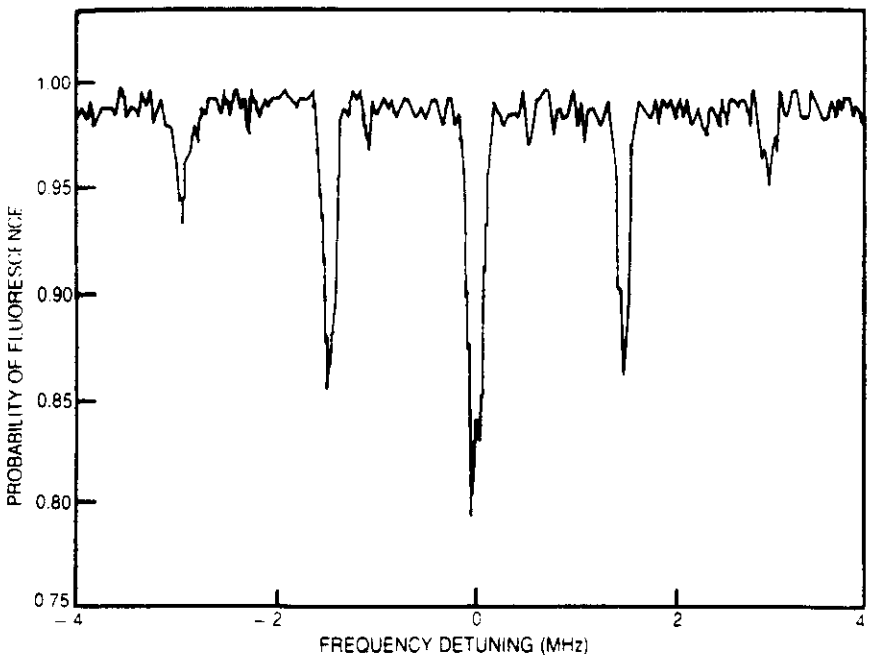

Fluorescence of a single mercury ion as a function of the detuning of a driving laser from its carrier frequency of 563 nm. The figure on page 17 is a high-resolution scan of this spectrum. The Doppler-free resonance in the center might provide the reference for an optical frequency standard. The other two dips are the sidebands caused by vibrational motion of the ion in the trap. (Adapted from a figure provided by the National Institute of Standards and Technology.)

frequency near 282 nm has or has not excited the ion to the target metastable state. First the cooling laser irradiates the ion at 194 nm, exciting the ion from the $5d^{10}6s\ ^2S_{1/2}$ to the $5d^{10}6p\ ^2P_{1/2}$ state. As the ion absorbs and then emits this radiation, it fluoresces at a high rate. The researchers then switch off the cooling lasers and turn on another laser, tuned to about 282 nm, to excite up and down jumps between the $^2S_{1/2}$ state and the metastable $^2D_{5/2}$ state. (The 282-nm radiation was obtained by doubling the frequency of a narrow-band cw ring dye laser operating at 563 nm.) After about 5 msec, they turn off the 282-nm laser and switch on the 194-nm lasers, which serve as state monitors. If the ion has been excited into the $^2D_{5/2}$ state, it will not fluoresce; otherwise, it will.

Using this method, the NIST researchers varied the (doubled) frequency of the driving laser in 50-Hz steps across the region of the expected transition and recorded whether the fluorescence was or was not seen. They averaged all measurements at the same frequency. The figure on page 17 shows a high-resolution scan through the central region; the overall spectrum is pictured in the figure on page 18. The full spectrum manifests not only the carrier frequency, unshifted by the Doppler effect, but also sidebands, generated by the Doppler effect, at frequencies corresponding to the oscillatory motion of the ion in the potential well. The full width at half-maximum is about 86 Hz. (Because the laser is frequency doubled, the linewidth is twice this amount.)

The driving laser was electronically stabilized using an optical reference cavity that was mechanically, acoustically and thermally quiet. Still, the frequency fluctuations of the laser due to instabilities in this cavity currently limit the resolution. The linewidth of the atomic state is 1.7 Hz. Bergquist told us that he and his colleagues hope to spectrally narrow the 563-nm laser to better than 1 Hz. Doing so will require them to hold the relative motion between the cavity mirrors to less than the width of one nucleus!

Clock standards

The NIST experiment is part of research aimed at making atomic standards more accurate and stable. Bergquist told us that there is great interest in moving toward an optical standard as the basis for the atomic clock. One reason is to gain higher resolution: Because the uncertainty in measuring frequency is fixed by the lifetime of the atomic transition, the larger the frequency is, the larger is the ratio of the frequency to the uncertainty (the Q value). The biggest challenge in making an optical frequency serve as a clock lies in finding some method fast enough to count the cycles of optical radiation.

The single trapped ion offers intriguing possibilities for research as well. The NIST investigators have already cooled the mercury ion to the zero-point energy in two degrees of freedom of the motion. They first reduce the ion's temperature to a few millikelvin with 194-nm radiation. Then they cool the ion further by using a cooling transition at which the optical sidebands are fully resolved, so that the laser can be tuned to the first lower vibrational sideband (see the figure on page 18). The ion absorbs photons of this frequency but, on average, reemits photons with the (higher) carrier frequency. For each absorption—emission cycle, the ion's vibration energy is reduced by one quantum.

With the ion at the zero-point energy of motion, the quantum mechanical ion-trap system permits some interesting studies. One might surround the ion with an optical cavity and study the interaction between the single ion and a single optical mode. It may also be possible to produce squeezed states of the atom's motion, in which the uncertainty in either position or momentum is greatly reduced while that in its conjugate variable is enlarged to comply with the uncertainty principle. One way to do this in an ion trap would be to change the potential well rapidly from very deep to very wide and shallow. As soon as the ion, whose position is well resolved in the deep well, was cast into the shallow well, its locational uncertainty would begin to grow. As the ion oscillated in this wide well, the uncertainty in position would swing from narrow to wide, with the uncertainty in momentum oscillating in counterpoint.

—Barbara Goss Levi

References

1. J. Bergquist, F. Dietrich, W. Itano, D. Wineland, in *Proc. 9th International Conf. on Laser Spectroscopy, Bretton Woods, N. H., June 1989*, M. Feld, J. Thomas, A. Mooradian, eds., Academic, San Diego, Calif. (to be published).
2. W. Nagourney, N. Yu, H. Dehmelt, in *Frequency Standards and Metrology*, A. DeMarchi, ed., Springer-Verlag, Berlin (1989), p. 312.
3. W. Neuhauser, M. Hohenstatt, P. E. Toschek, in *Spectral Line Shapes*, B. Wende, ed., Walter de Gruyter, Berlin (1981), p. 1066. ■

References
Trapped Ion Frequency Standards

1. D.J. Wineland, W.M. Itano, and R.S. Van Dyck, Jr., "High-resolution spectroscopy of stored ions," in Advances in Atomic and Molecular Physics, edited by D. Bates and B. Bederson (Academic, New York, 1983), Vol. 19, pp. 135-186.

2. D.J. Wineland and W.M. Itano, "Laser cooling of atoms," Phys. Rev. A 20, 1521-1540 (1979).

3. W.M. Itano and D.J. Wineland, "Laser cooling of ions stored in harmonic and Penning traps," Phys. Rev. A 25, 35-54 (1982).

4. D.J. Larson, J.C. Bergquist, J.J. Bollinger, W.M. Itano, and D.J. Wineland, "Sympathetic cooling of trapped ions: A laser-cooled two-species nonneutral ion plasma," Phys. Rev. Lett. 57, 70-73 (1986).

5. J.J. Bollinger, J.D. Prestage, W.M. Itano, and D.J. Wineland, "Laser-cooled-atomic frequency standard," Phys. Rev. Lett. 54, 1000-1003 (1985).

6. J.C. Bergquist, R.G. Hulet, W.M. Itano, and D.J. Wineland, "Observation of quantum jumps in a single atom," Phys. Rev. Lett. 57, 1699-1702 (1986).

7. D.J. Wineland, W.M. Itano, J.C. Bergquist, and R.G. Hulet, "Laser cooling limits and single ion spectroscopy," Phys. Rev. A 36, 2220-2232 (1987).

8. J.C. Bergquist, W.M. Itano, and D.J. Wineland, "Recoilless optical absorption and Doppler sidebands of a single trapped ion," Phys. Rev. A 36, 428-430 (1987).

Tests of Quantum Mechanics with Laser-Cooled Ions

W. M. Itano
D. J. Heinzen
J. J. Bollinger
S. L. Gilbert
D. J. Wineland

Time and Frequency Division
National Institute of Standards and Technology
(formerly the National Bureau of Standards)
Boulder, Colorado 80303

Supported in part by the Air Force Office of Scientific Research and the Office of Naval Research

OUTLINE

I. Introduction

II. Nonlinear quantum mechanics

- Weinberg's theory
- Experiment with $^9Be^+$ in Penning trap
- Results

III. Quantum Zeno effect

- Basic ideas
- Cook's proposed experiment
- Experiment with $^9Be^+$ in Penning trap
- Results

Precision Tests of Quantum Mechanics

- Measurements of energy levels (e.g. hydrogen) are tests of specific Hamiltonians, Lagrangians, etc. **within** the framework of conventional quantum theory.

- Bell inequality expts. test Q.M. only to 2%.

- Would like **precision** test.

- Need "generalized" theory which $\rightarrow$ ordinary Q.M. when $\epsilon \rightarrow 0$.

- Possibility: Try relaxing linearity postulate [Steven Weinberg, Phys. Rev. Lett. **62**, 485 (1989)]

Weinberg's Nonlinear Quantum Mechanics

- For discrete (e.g. spin) system:

$$\psi = \begin{pmatrix} \psi_1 \\ \psi_2 \\ \vdots \\ \psi_n \end{pmatrix}$$

- Equation of motion:

$$i\hbar \frac{d\psi_k}{dt} = \frac{\partial h(\psi, \psi^*)}{\partial \psi_k^*}$$

- Ordinary quantum mechanics:

$$h(\psi, \psi^*) = \sum_{k,\ell} \psi_k^* H_{k\ell} \psi_\ell$$

$$i\hbar \frac{d\psi_k}{dt} = \frac{\partial h(\psi, \psi^*)}{\partial \psi_k^*} = \sum_\ell H_{k\ell} \psi_\ell$$

$$i\hbar \frac{d\psi}{dt} = H\,\psi$$

Nonlinear 2-Level System

- Definitions:

$$h = n\bar{h}(a)$$

$$n = |\psi_1|^2 + |\psi_2|^2$$

$$a = \frac{|\psi_2|^2}{n}$$

- Equations of motion ($\hbar = 1$):

$$\frac{d\psi_1}{dt} = -i\frac{\partial h}{\partial \psi_1^*} = \left[\bar{h}(a) - a\frac{d\bar{h}(a)}{da}\right]\psi_1$$

$$\frac{d\psi_2}{dt} = -i\frac{\partial h}{\partial \psi_2^*} = \left[\bar{h}(a) + (1-a)\frac{d\bar{h}(a)}{da}\right]\psi_2$$

- Solutions:

$$\psi_k(t) = c_k \exp(-i\omega_k(a)t) \qquad k = 1, 2$$

where

$$\omega_1 = \bar{h}(a) - a\frac{d\bar{h}(a)}{da}$$

$$\omega_2 = \bar{h}(a) + (1-a)\frac{d\bar{h}(a)}{da}$$

- Assume a small nonlinearity:

$$\bar{h}(a) = \omega_0 a + 2\epsilon a^2$$

  where $\mid \epsilon/\omega_0 \mid \ll 1$

- Time development of coherence (observable):

$$\psi_1^* \psi_2 \propto \exp(-i(\omega_0 + 4\epsilon a)t)$$

- "Precession" frequency:

$$\omega_p \equiv \omega_0 + 4\epsilon a$$

Bloch Vector Representation of 2-Level System

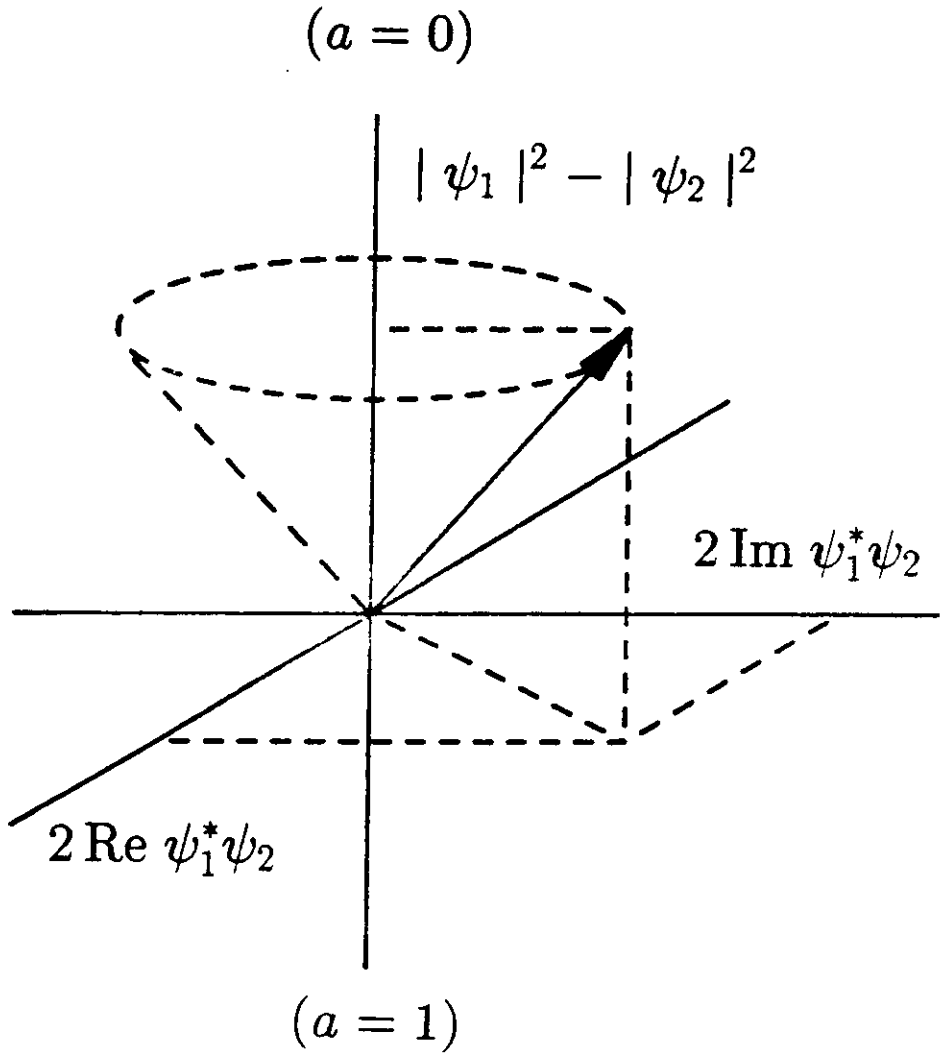

other experimental trial unscathed.

With LEP's present complement of 128 copper rf accelerating cavities, its energy cannot exceed 55 GeV per beam. (See the cover of this issue.) Over the next several years the copper cavities will gradually be replaced by superconducting niobium rf cavities being developed at CERN. By the end of 1992 the schedule calls for 196 superconducting rf cavities to be in place, yielding beams of 96-GeV electrons and positrons.

—BERTRAM SCHWARZSCHILD

References

1. G. S. Abrams *et al.* (Mark II collaboration), Phys. Rev. Lett. **63**, 724 (1989).
2. F. Abe *et al.* (CDF collaboration), Phys. Rev. Lett. **63**, 720 (1989).

DOES QUANTUM MECHANICS HAVE NONLINEAR TERMS?

One hears about testing quantum electrodynamics or relativity theory, but the theoretical basis of quantum mechanics is rarely questioned. Nevertheless, Steven Weinberg (University of Texas) has recently called for high-precision tests of quantum mechanics that are independent of any particular quantum mechanical theory.[1] To pave the way for an examination of quantum mechanics, he has suggested one possible way of generalizing quantum mechanics to make it nonlinear. As Eugene Wigner pointed out in a 1939 paper, the linearity of quantum mechanics is an important assumption and one that may not necessarily always prove true. Weinberg stressed to us that he does not really feel that quantum mechanics is in any immediate danger, but he does believe that we can learn by questioning it: If we find that quantum mechanics cannot be generalized any further, we may come to understand better why it works so well. If we find that the theory can be generalized in a plausible way, then we must ask why ordinary quantum mechanics is so nearly valid—and we may discover some hidden physics in the process.

Weinberg has suggested one particular example in which a nonlinearity might manifest itself, and several experimental groups have taken up the search for it. The first results are now in: John Bollinger, Daniel Heinzen, Wayne Itano, Sarah Gilbert and David Wineland of the National Institute of Standards and Technology (Boulder, Colorado) have set a very low upper limit on the size of a possible nonlinear term in the hyperfine splitting of a beryllium atom. Bollinger presented these results at the annual meeting of the APS division of atomic, molecular and optical physics, held in Windsor, Ontario, last May.[2]

Quantum mechanics has been tested in several ways before. One set of experiments aimed to distinguish it from local hidden-variable theories. (See the article by David Mermin in PHYSICS TODAY, April 1985, page 38.) These experiments succeeded in ruling out hidden variables, but Weinberg points out that they did not test quantum mechanics to better than about one percent. Another approach to testing quantum mechanics dealt with the incorporation of nonlinear terms into the Schrödinger equation. In 1980, at the suggestion of Abner Shimony[3] (Boston University), a team led by Clifford Shull[4] (MIT) used neutron interferometry to search for possible nonlinear terms of a form suggested by Iwo Bialynicki-Birula and Jan Mycielski[5] (University of Warsaw). Roland Gahler (Technical University of Munich), Anthony G. Klein (University of Melbourne, Australia) and Anton Zeilinger[6] (Technical University of Vienna), working at the Laue–Langevin Institute in Grenoble, followed with a similar experiment that set more stringent limits on the size of the nonlinear term.

Nonlinear formulation

Weinberg set out to make the most general formulation possible that is still consistent with essential properties of quantum mechanics. A key requirement was to preserve homogeneity—to ensure that if one wavefunction is a solution of the Schrödinger equation, then so is another wavefunction that is just a constant multiple of the first. The nonlinear term introduced by the Polish theorists did not satisfy this condition. Weinberg assumes that the time dependence of the wavefunction is given by:

$$i\hbar\frac{d\Psi_k}{dt} = \frac{\partial h(\Psi,\Psi^*)}{\partial \Psi_k^*}$$

This equation reduces to the standard form if the Hamiltonian function h has the bilinear form $\Psi_k^* H_{kl} \Psi_l$, but allows for treatment of possible terms in the Hamiltonian that are not bilinear. In the example of a generalized two-component system, Weinberg shows that the Hamiltonian function h can be put in the form $n\,\bar{h}(a)$, where n is the norm $|\Psi_1|^2 + |\Psi_2|^2$ and $\bar{h}$ is an arbitrary function of the variable $a = |\Psi_2|^2/n$.

For an atom undergoing a radiative transition (such as that between two hyperfine levels), Weinberg's equation predicts that the resonant transition frequency will be sensitive to the occupancy of the two levels. This transition frequency will change as these occupancies change. If one drives a certain transition with an applied monochromatic oscillator, detuning will result because the resonant transition frequency will shift as the oscillator continues to populate the upper levels. For a weak nonlinearity, the shift in frequency will be small. To detect it, one must make the coupling between the oscillator and the atom as weak as possible so that the transition takes a long time. The sensitivity of the technique thus varies inversely with the time of perturbation.

Weinberg used data from a 1985 experiment performed at NIST[7] (then called the National Bureau of Standards) to estimate an upper limit on the size of the nonlinear term. In that experiment, Be^9 ions were driven from one state to the other with a single pulse about 1 second long. Because the transition could be driven with such a pulse, Weinberg inferred that the nonlinearity could not lead to a shift of more than the inverse of that pulse length, or 1 Hz, which corresponds to a nonlinear term on the order of 10^{-15} eV.

Norman Ramsey (Harvard University) in 1949 originated a technique for measuring atomic resonant transitions and hence for setting frequency standards. This so-called method of separated oscillatory fields gives a sensitive way to detect changes in transition frequencies. First, an rf pulse is applied to an atom and then turned off. This creates a superposition state, with specific populations of the two atomic levels, that depends on the amplitude, frequency and length of the pulse. After a certain time interval, a second rf pulse of the same length, coherent with the first, is applied. If the two rf pulses are at the resonant transition frequency, the second pulse will be in phase with the superposition state and it will continue to transfer the ions to the upper state. The rf frequency is changed until this resonant condition is met.

If a nonlinearity is present, the phase of the superposition state will not be determined simply by the difference between the energy eigenvalues of the two levels but will also depend on the state amplitudes creat-

ed by the first pulse. Thus the resonant frequency measured by the Ramsey method will depend on the length of the first pulse. In this method for detecting a nonlinearity, the accuracy is inversely related to the time between pulses.

Experimental tests

Bollinger and his colleagues decided that, by using unequal pulses, they could improve considerably on the estimate Weinberg had extracted from their earlier data. They undertook a new experiment on $(Be^9)^+$ ions, using a collection of 5000–10 000 ions stored in a Penning trap and cooled below 250 mK. The design of their experiment is best viewed in terms of the precession of the $(Be^9)^+$ nucleus in an applied magnetic field. The precession rate does not vary with the angle between the spin and the magnetic field vector. In a nonlinear quantum theory, however, the precession rate does vary with angle, because the angle is a measure of the particular mixture of states.

To measure the precession rate the researchers applied the Ramsey method with unequal rf pulses. First they prepared the ions in the $(-\frac{1}{2}, +\frac{1}{2})$ state by a combination of optical pumping and rf resonance techniques. (The state is specified by quantum numbers denoting the nuclear and electronic spins, respectively.) The first Ramsey pulse was then applied to create a superposition with the $(-\frac{3}{2}, +\frac{1}{2})$ state. The length of this pulse determined the amplitude of each eigenstate in the superposition, and hence the tipping angle of the Be^9 nuclear spin. After a period of time, typically 100 sec, the second Ramsey pulse was applied. The ion population in the $(-\frac{1}{2}, +\frac{1}{2})$ state was detected by laser-induced fluorescence. The more ions remaining in the $(-\frac{3}{2}, +\frac{1}{2})$ state, the lower the fluorescence signal. The fluorescence thus peaks as a function of the frequency of the Ramsey pulses. The resonance (precession) frequency was determined from the average of the frequencies at half of the maximum intensity. The NIST team measured the precession rate at two angles (see the figure on this page). The precession frequency did not change significantly with angle. Averaging over 25 runs, the researchers found that the frequency difference was 2.7 ± 6.0 μHz, corresponding to an upper limit of 2.4×10^{-20} eV on the nonlinear term.

To judge how stringent this upper limit is, one needs to compare it with some energy scale, but what scale is appropriate? Weinberg maintains that the proper energy for comparison in this case is the nuclear energy. When compared with the binding energy per nucleon for the beryllium atom, the fractional upper limit on the nonlinearity becomes 4×10^{-27}.

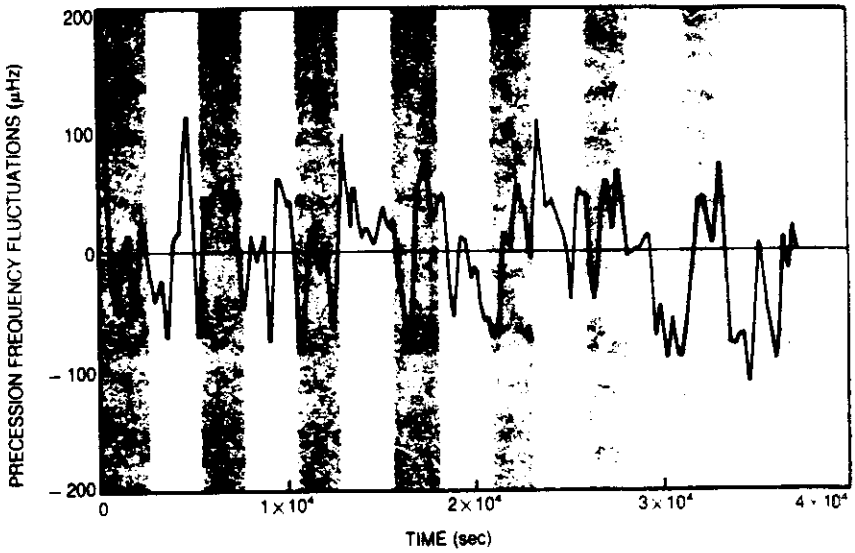

Precession frequency is not expected to vary with tipping angle if quantum mechanics is without nonlinearities. An experiment on Be^9 ions measured the precession frequency during alternating time intervals in which the tipping angle had values of 1.02 rad (blue shading) and 2.12 rad. The frequencies are plotted relative to the time-averaged frequency. The precession frequencies for the two tipping angles, averaged over many runs like that shown above, differed by less than 8.7 μHz. (Adapted from ref. 2.)

Work in progress

At least three other research teams are seeking nonlinearities. One of these—a group led by Norval Fortson at the University of Washington—is looking for the variation with angle of the precession frequency of a spin-$\frac{3}{2}$ nucleus, in this case, Hg^{201}. The investigators sense the precession rate through its modulation of an optical signal. Actually the precession rate is the superposition of three frequencies corresponding to the energy separations between four hyperfine levels. If the frequencies remain constant, independent of the amplitude in each state, linear quantum mechanics holds. At Harvard, Timothy Chupp is conducting a similar experiment but with a different nucleus Ne^{21} and a different experimental method.

Isaac Silvera (Harvard University) and his student Ronald Walsworth, in collaboration with Robert Vessot and Edward Mattison of the Smithsonian Astrophysical Observatory, are working with quite a different tool—the hydrogen maser. However, the nonlinear effect Weinberg identified shows up only in a particle of spin greater than or equal to 1, whereas the spin of the hydrogen nucleus is $\frac{1}{2}$. Walsworth has worked out a treatment for this case and applied it to existing data from hydrogen masers. He hopes to improve the accuracy by at least two orders of magnitude by conducting an experiment directly aimed at sensing the nonlinearities. So far he estimates an upper limit in terms of eV that is a factor of ten higher than that of the NIST team. However, compared with what might be the appropriate energy scale for the hydrogen atom—13.6 eV—this fractional upper limit on the nonlinearity is on the order of 10^{-20}.

—Barbara Goss Levi

References

1. S. Weinberg, Nucl. Phys. B (Proc. Suppl.) **6**, 67 (1989); Phys. Rev. Lett. **62**, 485 (1989); Ann. Phys. (N. Y.) **194**, 336 (1989).
2. J. J. Bollinger, D. J. Heinzen, W. M. Itano, S. L. Gilbert, D. J. Wineland, Phys. Rev. Lett. **63**, 1031 (1989).
3. A. Shimony, Phys. Rev. A **20** 394 (1979).
4. C. G. Shull, D. K. Atwood, J. Arthur, M. A. Horne, Phys. Rev. Lett. **44**, 765 (1980).
5. I. Bialynicki-Birula, J. Mycielski, Ann. Phys. N. Y. **100**, 62 (1976).
6. R. Gahler, A. G. Klein, A. Zeilinger, Phys. Rev. A **23**, 1611 (1981).
7. J. J. Bollinger, J. D. Prestage, W. M. Itano, D. J. Wineland, Phys. Rev. Lett. **54**, 1000 (1985). ■

PHYSICAL REVIEW

LETTERS

VOLUME 63 4 SEPTEMBER 1989 NUMBER 10

Test of the Linearity of Quantum Mechanics by rf Spectroscopy of the $^9Be^+$ Ground State

J. J. Bollinger, D. J. Heinzen, Wayne M. Itano, S. L. Gilbert, and D. J. Wineland

National Institute of Standards and Technology, Boulder, Colorado 80303

(Received 15 May 1989)

A hyperfine transition in the ground state of $^9Be^+$ was used to test a nonlinear generalization of quantum mechanics recently formulated by Weinberg. We searched for a dependence of the frequency of a coherent superposition of two hyperfine states on the populations of the states. We are able to set a limit of 4×10^{-27} on the fraction of binding energy per nucleon of the $^9Be^+$ nucleus that could be due to nonlinear corrections to quantum mechanics.

PACS numbers: 03.65.Bz, 06.30.Ft, 32.30.Bv

Since the 1920s, quantum mechanics has passed numerous tests as illustrated by the agreement between the predictions of specific quantum-mechanical theories and experimental measurements. For example, the measured energy levels of the hydrogen atom are in excellent agreement with the predictions of quantum-mechanical theory. However, this could be regarded as a test of the accuracy of the Hamiltonian rather than a test of quantum mechanics itself. It should be possible to test the basic framework of quantum mechanics independently of and more precisely than any particular quantum-mechanical theory. Recently, Weinberg[1,2] has formulated a general framework for introducing nonlinear corrections to quantum mechanics which enables such a test. He has suggested that a sensitive way to search for possible nonlinearities is to look for a change in a transition frequency as the wave function of a system changes between initial and final states. Monochromatic radiation used to drive the transition would therefore not stay in resonance throughout the entire transition. If the transition can be driven experimentally in time T, then the maximum frequency shift due to the nonlinearity must be on the order of $1/T$. Because nuclear magnetic resonance transitions in $^9Be^+$ have been observed with T as long as 1 s, Weinberg sets a limit of $\sim10^{-15}$ eV on the magnitude of any such nonlinear corrections to the energy of the ^9Be nucleus. In this Letter we report an experiment which improves this limit by 5 orders of magnitude.

In the formalism developed in Refs. 1 and 2, the equation which describes the time evolution of the wave function $\psi(t)$ is nonlinear and derivable from a Hamiltonian function $h(\psi,\psi^*)$. For a discrete system, it takes the form

$$i\hbar\frac{d\psi_k}{dt}=\frac{\partial h(\psi,\psi^*)}{\partial\psi_k^*}, \tag{1}$$

where ψ_k is the amplitude of state k. In general, h is not a bilinear function of ψ and ψ^* as in ordinary quantum mechanics, but the property of homogeneity $[h(\lambda\psi,\psi^*)=h(\psi,\lambda\psi^*)=\lambda h(\psi,\psi^*)$ for any complex $\lambda]$ is retained. Homogeneity guarantees that if $\psi(t)$ is a solution of Eq. (1) then $\lambda\psi(t)$ is also a solution representing the same physical state. Homogeneity ensures the proper treatment of physically separated systems and distinguishes this formalism from previous nonlinear generalizations[3,4] and tests[5,6] of quantum mechanics.

Consider a two-level system which in the absence of nonlinear corrections has eigenvalues E_k, $k=1,2$. Because any nonlinear corrections to quantum mechanics are expected to be small, it is reasonable to write the Hamiltonian function as the sum of the bilinear term $h_0(\psi,\psi^*)=\sum_{k=1,2}E_k\psi_k^*\psi_k$ of ordinary quantum me-

der of magnitude longer than this.]

For the test of nonlinearities, Ramsey's method with unequal rf pulses was used to drive the clock transition and measure ω_p for different values of θ. First an rf θ pulse of duration τ_θ was applied. This prepared the ions into a coherent superposition of the $(-\frac{1}{2},\frac{1}{2})$ and $(-\frac{1}{2},\frac{1}{2})$ states given by Eq. (2) for a particular value of θ. The value of θ was determined from $\theta=(\tau_\theta,\tau_\pi)\pi$, where τ_π was the length of time to drive a π pulse at the same rf power. After the rf θ pulse, the ions freely precessed for a time T. This was followed by an rf $\pi/2$ pulse coherent with the first pulse which completed the Ramsey excitation. In the limit that $T\gg\tau_\theta,\tau_{\pi/2}$, the Ramsey line shape [specifically, the number of ions remaining in the $(-\frac{1}{2},\frac{1}{2})$ state as a function of the rf frequency ω in the Ramsey excitation] is proportional to

$$1-\sin\theta\cos\{[\omega-\omega_p(\theta)]T\},$$

where $\omega_p(\theta)$ is given by Eq. (4). The center frequency of the Ramsey line shape is the precession frequency $\omega_p(\theta)$. Figure 2 shows a Ramsey signal obtained with $T=150$ s and $\theta=\pi/2$.

The Ramsey signal was used to steer the frequency of a synthesized rf source.[11] Ramsey-signal measurements were taken near both of the full-width-at-half-maximum frequencies $\omega_+\equiv2\pi\nu_+$ and $\omega_-\equiv2\pi\nu_-$, where ν_+ and ν_- are indicated in Fig. 2. The difference in the measured signal strengths on either side of the line center was used to electronically steer the average frequency of the synthesizer to $\omega_p(\theta)$. Eight pairs of measurements were taken with an angle $\theta_A=1.02$ rad followed by eight pairs of measurements with an angle $\theta_B=2.12$ rad. This pattern was repeated for the length of an entire run as indicated in Fig. 3. The average frequency of the synthesizer for $\theta=\theta_A$ was then subtracted from the average frequency of the synthesizer for $\theta=\theta_B$. Run lengths varied between 4 and 10 h. The uncertainty was due to the frequency instability of the reference oscillator used with the synthesizer. Most runs were taken with a commercial cesium beam clock [fractional frequency stability[14] $\sigma_y(\tau)\sim6\times10^{-12}\tau^{-1/2}$ for measurement time τ in seconds] as the reference oscillator. For a limited time we had access to a passive hydrogen maser[15] [$\sigma_y(\tau)\sim(2\text{–}3)\times10^{-12}\tau^{-1/2}$] and a few runs were taken with the passive hydrogen maser as the reference oscillator.

Runs were taken with free-precession periods of $T=30$, 60, and 100 s and rf pulse lengths of $\tau_A=0.65\tau_{\pi/2}$, $\tau_B=1.35\tau_{\pi/2}$ with $\tau_{\pi/2}=0.5$, 1, and 2 s. A weighted average of the synthesizer frequency differences for $\theta=\theta_A$ and $\theta=\theta_B$ from 25 runs is 2.7(6.0) μHz. The uncertainty (in parentheses) is the external error calculated from the scatter of the 25 measurements from the weighted average and is in good agreement with the internal error of 5.7 μHz calculated from the uncertainties of each of the 25 runs. The time constant of the servo would have decreased the apparent size of a real frequency difference by 28%. This results in a possible dependence of the precession frequency on θ of $[\omega_p(\theta_B)-\omega_p(\theta_A)]/2\pi=3.8(8.3)$ μHz and from Eq. (4) a value for the parameter ϵ of

$$\epsilon/2\pi\hbar=1.8(4.0)\,\mu\text{Hz}. \tag{5}$$

The error is a 1 standard deviation uncertainty. A few runs were also taken with $\theta=\pi/2$. The frequency $\omega_p(\pi/2)/2\pi$ was compared with the frequencies $\omega_p(\theta_A)/2\pi$ and $\omega_p(\theta_B)/2\pi$ for runs taken within a few days of each other. The standard deviation of the frequencies from their average was 6 μHz, consistent with the 7-μHz uncertainty of the frequencies. The $\theta=\pi/2$ runs do not improve the limit of Eq. (5) on a possible correction to ω_p linear in a, but in general can be used to help place limits

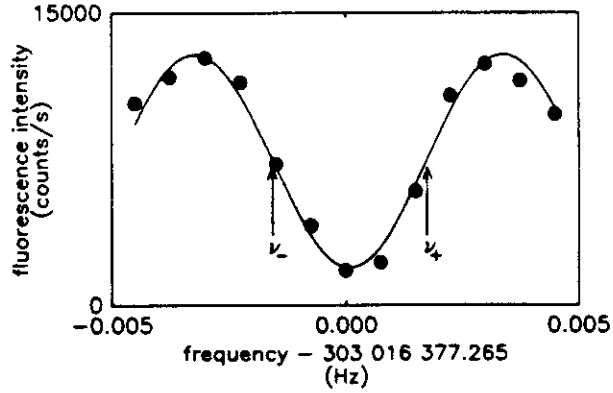

FIG. 2. Ramsey signal of the clock transition with $T=150$ s and $\theta=\pi/2$. The data are the result of one sweep (that is, one measurement per point). The sweep width is 9 mHz and the frequency interval between points is 0.750 mHz. The dots are experimental and the curve is a least-squares fit. The signal-to-noise ratio is limited by the frequency stability of the reference oscillator. The full-width-at-half-maximum frequencies are indicated by ν_+ and ν_-.

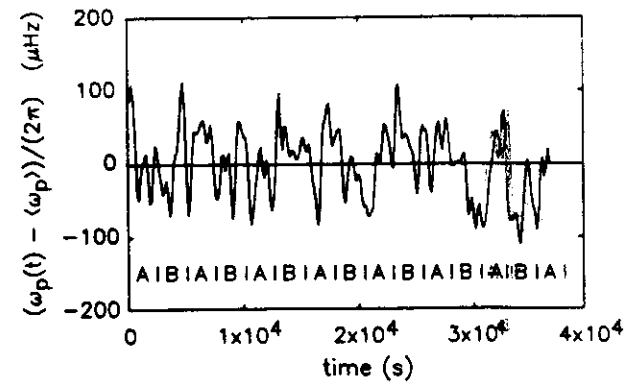

FIG. 3. $^9Be^+$ precession frequency $\omega_p(t)$, referred to a passive hydrogen maser, as a function of time for a single run with $T=100$ s. The periods A (B) during which the initial Rabi pulse created a mixed state with angle $\theta_A=1.02$ rad ($\theta_B=2.12$ rad) are indicated.

chanics and a term $h_{nl}(\psi,\psi^*)$ that is not bilinear and contains the small nonlinear corrections. A form of h_{nl} appropriate for the work discussed here is $h_{nl}=n\bar{h}(a)$, where $n\equiv|\psi_1|^2+|\psi_2|^2$, $a\equiv|\psi_2|^2/n$, and $\bar{h}$ is a real function.[1,2] The nonlinear time-dependent Schrödinger equation then takes the form

$$i\hbar\frac{d\psi_1}{dt}=\left[E_1+\bar{h}-a\frac{d\bar{h}}{da}\right]\psi_1\equiv\hbar\omega_1(a)\psi_1,$$

$$i\hbar\frac{d\psi_2}{dt}=\left[E_2+\bar{h}+(1-a)\frac{d\bar{h}}{da}\right]\psi_2\equiv\hbar\omega_2(a)\psi_2,$$

which has solutions

$$\psi_k(t)=c_k e^{-i\omega_k(a)t},\quad k=1,2, \tag{2}$$

where a and the c_k's can be parametrized by $c_1=\sin(\theta/2)$ and $c_2=a^{1/2}=\cos(\theta/2)$. The relative phase of the two components of the wave function (specifically, the time dependence of the coherence $\psi_1\psi_2^*$) evolves with a frequency

$$\omega_p\equiv\omega_1(a)-\omega_2(a)=\omega_0-(d\bar{h}/da)/\hbar,$$

where $\omega_0=(E_1-E_2)/\hbar$ is the atomic transition frequency in the absence of nonlinearities. A two-level system is mathematically equivalent to a spin-$\frac{1}{2}$ system in an external, uniform magnetic field, where θ is the angle by which the spin is tipped with respect to the magnetic field and ω_p is the precession frequency of the spin about the magnetic field.[7] In the language of the equivalent spin-$\frac{1}{2}$ system, the effect of the nonlinear correction $d\bar{h}/da$ is to create a dependence of the precession frequency ω_p on the tipping angle θ between the spin and the magnetic field.

We searched for a θ dependence of the precession frequency of the $(m_I,m_J)=(-\frac{1}{2},+\frac{1}{2})\rightarrow(-\frac{3}{2},+\frac{1}{2})$ hyperfine transition at $\sim$303 MHz in the ground state of $^9Be^+$ (see Fig. 1). At a magnetic field B of 0.8194 T, this transition, referred to as the clock transition, depends only quadratically on magnetic field fluctuations. With $\psi_1\equiv\psi(-\frac{3}{2},+\frac{1}{2})$ and $\psi_2\equiv(-\frac{1}{2},+\frac{1}{2})$ the simplest nonbilinear addition to the Hamiltonian function of the free $^9Be^+$ nucleus for the two states is[1,2]

$$\bar{h}(a)=2\epsilon a^2, \tag{3}$$

where ϵ is a measure of the strength of the nonlinear correction. This gives rise to a dependence of ω_p on θ of

$$\omega_p=\omega_0-4(\epsilon/\hbar)\cos^2(\theta/2). \tag{4}$$

This discussion assumes that the $^9Be^+$ nuclear spin is decoupled from the valence electron spin and therefore the $(-\frac{1}{2},\frac{1}{2})$ and $(-\frac{3}{2},\frac{1}{2})$ states are pure (m_I,m_J) states. At a magnetic field of 0.8194 T these states have a 0.02 to 0.03 amplitude admixture of $m_J=-\frac{1}{2}$ states. This creates small corrections to Eqs. (3) and (4) which we neglect.

Between 5000 and 10000 $^9Be^+$ ions and 50000 to 150000 $^{26}Mg^+$ ions were simultaneously stored in a cylindrical Penning trap[8] with $B\simeq0.8194$ T under conditions of high vacuum ($\lesssim10^{-8}$ Pa). To minimize second-order Doppler shifts of the clock transition, the $^9Be^+$ ions were cooled to less than 250 mK. The $^{26}Mg^+$ ions were directly laser cooled and compressed by a narrow-band ($\sim$1 MHz) radiation source at 280 nm.[9] The $^9Be^+$ ions were then sympathetically cooled[10] by their Coulomb interaction with the cold Mg^+ ions. A narrow-band 313-nm radiation source was used to optically pump and detect the $^9Be^+$ ions.[11,12] With the 313-nm source tuned to the $2s\,^2S_{1/2}(m_I=\frac{3}{2},m_J=\frac{1}{2})$ to $2p\,^2P_{3/2}(\frac{3}{2},\frac{3}{2})$ transition, 94% of the $^9Be^+$ ions were optically pumped into the $2s\,^2S_{1/2}(\frac{3}{2},\frac{1}{2})$ ground state.[11,12] The 313-nm source was then turned off to avoid optical pumping and ac Stark shifts. The sympathetic cooling of the $^9Be^+$ ions by the Mg^+ ions provided a steady cooling source independent of the 313-nm radiation and therefore permitted the use of long transition times.

The clock transition was detected by the following method. After the 313-nm source was turned off, the ions in the $(\frac{3}{2},\frac{1}{2})$ state were transferred to the $(\frac{1}{2},\frac{1}{2})$ state and then to the $(-\frac{1}{2},\frac{1}{2})$ state by two successive rf π pulses. Each pulse was 0.2 s long and resonant with the appropriate transition frequency (around 321 and 311 MHz, respectively). The clock transition was then driven by Ramsey's method of separated oscillatory fields[13] with rf pulses of about 1-s duration and a free-precession time on the order of 100 s. This transferred some of the ions from the $(-\frac{1}{2},\frac{1}{2})$ state to the $(-\frac{3}{2},\frac{1}{2})$ state. Those ions remaining in the $(-\frac{1}{2},\frac{1}{2})$ state were then transferred back to the $(\frac{3}{2},\frac{1}{2})$ state by reversing the order of the two rf π pulses. The 313-nm source was then turned back on, and the population of ions in the $(-\frac{3}{2},\frac{1}{2})$ state was registered as a decrease in the $^9Be^+$ fluorescence, relative to the steady-state fluorescence, during the first second that the 313-nm source was on. [The optical repumping time of the ions from the $(-\frac{3}{2},\frac{1}{2})$ state to the $(\frac{3}{2},\frac{1}{2})$ state was an or-

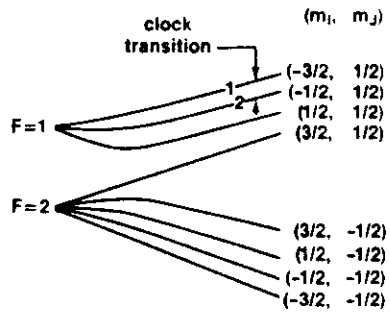

FIG. 1. Hyperfine energy levels (not drawn to scale) of the $^9Be^+$ $2s\,^2S_{1/2}$ ground state as a function of magnetic field. At $B=0.8194$ T the 303-MHz clock transition is independent of magnetic field to first order.

on a more complicated form for $\bar{h}(a)$.

Equation (5) sets an upper limit of $|\epsilon| < 2.4\times10^{-20}$ eV (5.8 μHz) for a nonlinear contribution to the $^9Be^+$ nuclear Hamiltonian. This is less than 4 parts in 10^{27} of the binding energy per nucleon of the $^9Be^+$ nucleus and improves the limit set in Ref. 1 by roughly 5 orders of magnitude. The limit on $|\epsilon|$ is also 5 orders of magnitude smaller than experimental limits placed by neutron interferometry[5,6] on $|b|$, where b is the coefficient of a logarithmic addition $-b\psi(\mathbf{x})\ln|\psi(\mathbf{x})|^2$ to the one-particle Schrödinger equation. However, this nonlinearity does not satisfy the property of homogeneity and therefore these experiments[5,6] test for a nonlinearity which does not satisfy the requirements of the framework developed by Weinberg. Our experimental result is limited by statistics due to the frequency instability of the reference oscillator. The largest known systematic error of our measurement of $\omega_p(\theta)$ is the second-order Doppler (time dilation) frequency shift due to the temperature and $\mathbf{E}\times\mathbf{B}$ rotation of the ions in the trap.[11] Its size is less than 3 μHz (1×10^{-14}). We believe it can be held constant to significantly better than 10% over the time required to make a frequency difference measurement. With a better reference oscillator or a second $^9Be^+$ clock, it should therefore be possible to improve our limit on $|\epsilon|$ by more than an order of magnitude. Improvements on this measurement may also be possible using nuclear magnetic resonance techniques on neutral atoms.[16,17]

We gratefully acknowledge the support of the U.S. Air Force Office of Scientific Research and the U.S. Office of Naval Research. We thank S. Weinberg for a number of helpful discussions clarifying the theory, and J. C. Bergquist and S. R. Lundeen for their comments on the manuscript.

[1]S. Weinberg, Phys. Rev. Lett. **62**, 485 (1989).

[2]S. Weinberg, Ann. Phys. (N.Y.) **194**, 336 (1989).

[3]I. Bialynicki-Birula and J. Mycielski, Ann. Phys. (N.Y.) **100**, 62 (1976).

[4]A. Shimony, Phys. Rev. A **20**, 394 (1979).

[5]C. G. Shull, D. K. Atwood, J. Arthur, and M. A. Horne, Phys. Rev. Lett. **44**, 765 (1980).

[6]R. Gahler, A. G. Klein, and A. Zeilinger, Phys. Rev. A **23**, 1611 (1981).

[7]R. P. Feynman, F. L. Vernon, Jr., and R. W. Hellwarth, J. Appl. Phys. **28**, 49 (1957).

[8]S. L. Gilbert, J. J. Bollinger, and D. J. Wineland, Phys. Rev. Lett. **60**, 2022 (1988).

[9]W. M. Itano and D. J. Wineland, Phys. Rev. A **24**, 1364 (1981); W. M. Itano, L. R. Brewer, D. J. Larson, and D. J. Wineland, Phys. Rev. A **38**, 5698 (1988).

[10]D. J. Larson, J. C. Bergquist, J. J. Bollinger, W. M. Itano, and D. J. Wineland, Phys. Rev. Lett. **57**, 70 (1986).

[11]J. J. Bollinger, J. D. Prestage, W. M. Itano, and D. J. Wineland, Phys. Rev. Lett. **54**, 1000 (1985).

[12]L. R. Brewer, J. D. Prestage, J. J. Bollinger, W. M. Itano, D. J. Larson, and D. J. Wineland, Phys. Rev. A **38**, 859 (1988).

[13]N. F. Ramsey, *Molecular Beams* (Oxford Univ. Press, London, 1956).

[14]$\sigma_y^2(\tau)=\langle[f_{i+1}(\tau)-f_i(\tau)]^2/2\bar{f}^2\rangle$, where $f_i(\tau)$ is the ith measurement of the frequency over a measurement time interval τ, the brackets denote an average over all measurements, and $\bar{f}=\langle f_i\rangle$. See J. A. Barnes *et al.*, IEEE Trans. Instrum. Meas. **20**, 105 (1971).

[15]F. L. Walls, IEEE Trans. Instrum. Meas. **36**, 596 (1987).

[16]S. K. Lamoreaux, J. P. Jacobs, B. R. Heckel, F. J. Raab, and E. N. Fortson, Phys. Rev. A **39**, 1082 (1989).

[17]T. E. Chupp, E. R. Oteiza, J. M. Richardson, and T. R. White, Phys. Rev. A **38**, 3998 (1988).

Test of Zeno Effect
(R. J. Cook, 1988)

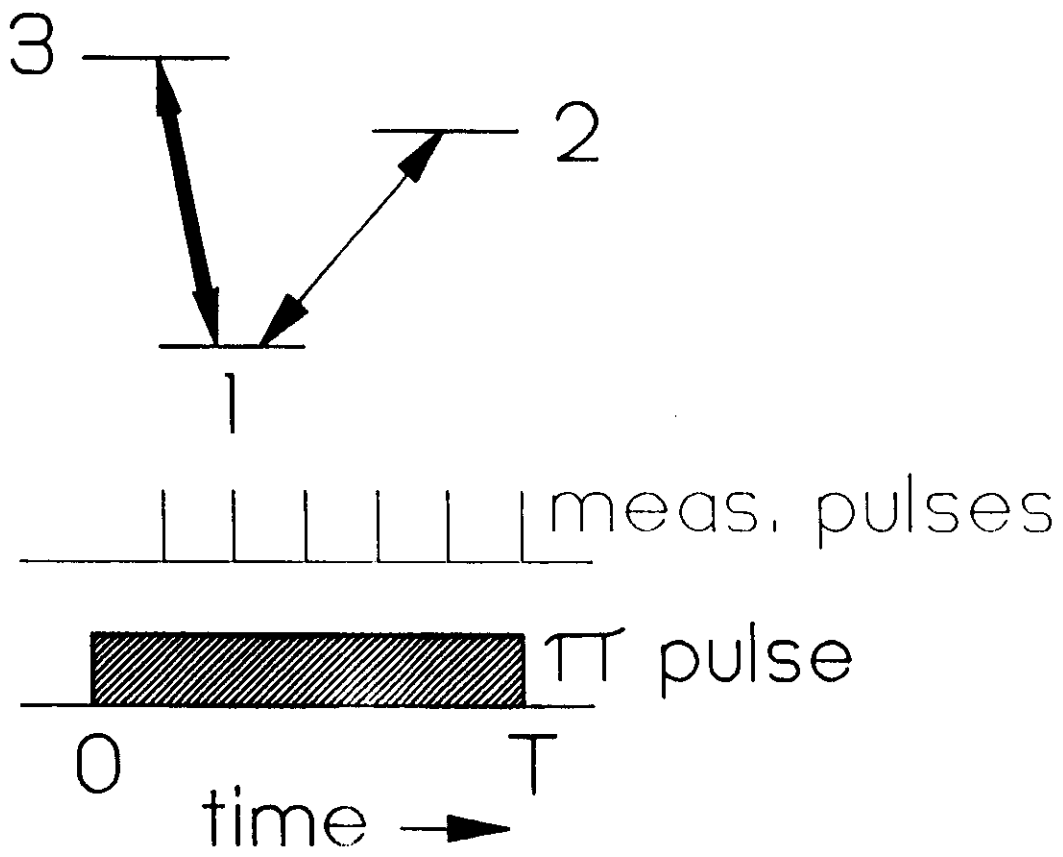

Inhibition of $1 \rightarrow 2$ Transition by Measurement Pulses

Bloch vector picture

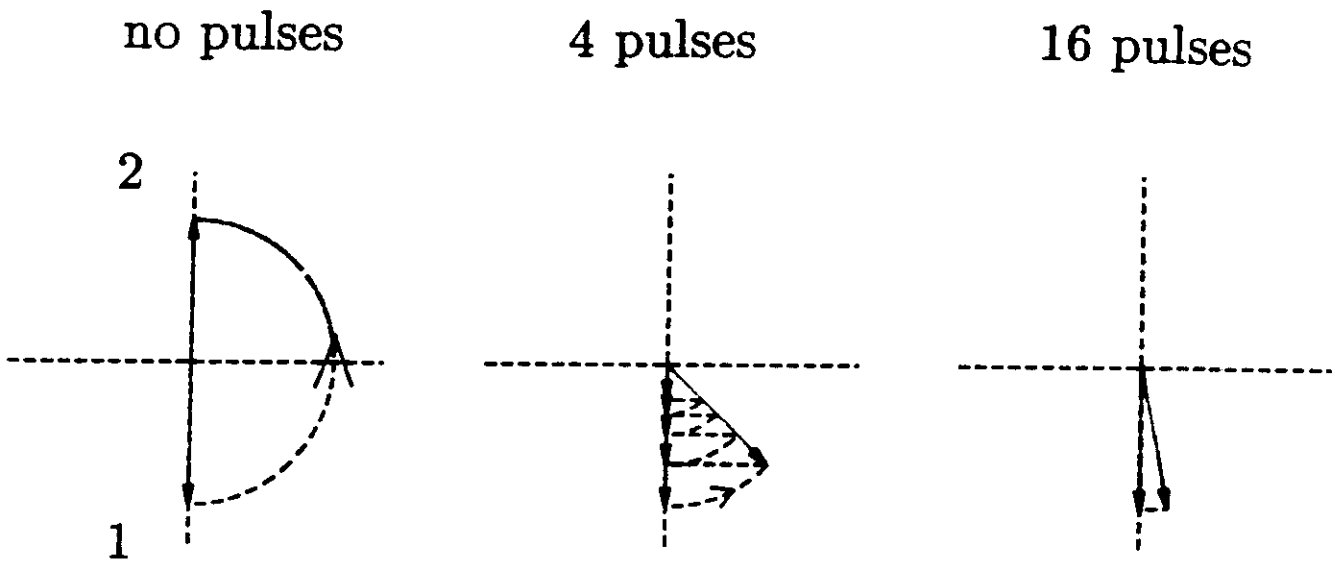

$$P_2(T) = \tfrac{1}{2}\left[1 - \cos^n(\pi/n)\right]$$

$$\approx \tfrac{1}{2}\left[1 - \exp(-\tfrac{1}{2}\pi^2/n)\right]$$

$2 \rightarrow 1$ process essentially the same

Quantum Pot Watching

A test of how observation affects a quantum system verifies theoretical predictions and proves the truth of an old maxim

A WATCHED POT NEVER BOILS, at least not if it's a quantum pot. That's the gist of a recent experiment by Wayne Itano, Daniel Heinzen, John Bollinger, and David Wineland at the National Institute of Standards and Technology in Boulder, Colorado. The work is the first unambiguous confirmation of a phenomenon that theorists had predicted in the 1970s, and it highlights one of the strangest aspects of quantum physics—the way an observer can influence the behavior of a system merely by sneaking a peek.

The pot that the NIST scientists watched was a magnetic trap holding several thousand beryllium-9 ions—the "water." At the beginning of the experiment, the ions were ordered so that they were almost all in a single electronic state, which was called Level 1. By exposing the ions to a radio-frequency field for exactly 256 milliseconds, the researchers caused them to move to another state, Level 2. The water had boiled.

At least that's what happened when no one was watching. It was a different story if someone took a look before the 256 milliseconds were up, says Wayne Itano, a member of the NIST team.

The researchers made their observations by exposing the beryllium ions to very short pulses of laser light whose photons had an energy equal to the energy difference between Level 1 and a third atomic state of the beryllium ions, Level 3.

When the laser light hit the ions in Level 1, it would force them briefly into Level 3. The ions would then quickly decay back to Level 1, each emitting a photon that could be counted with a photon detector. In this way, the researchers could tell how many of the 5000 or so beryllium ions in their pot were in Level 1 at any given time, and could thus estimate the number in Level 2. (The Level 2 ions were not affected by the laser pulses.)

Itano and his colleagues found that the number of ions in Level 2 at the end of 256 milliseconds depended on how often they looked at the ions. If they waited the full period to shine a laser pulse at the ions, all had moved to Level 2. If they looked once after 128 milliseconds and then again at 256 milliseconds, only half of the ions were in Level 2 at the second measurement. If they made four evenly spaced observations, only about a third of the ions were in Level 2 at the end. And if they peeked 64 times—or once every 4 milliseconds—almost none of the ions were found in Level 2. The pot refused to boil.

The reason, Itano explains, lies in the way in which this quantum "water" boils. When an individual atom in Level 1 is exposed to the radio-frequency field, its quantum state gradually shifts from Level 1 to Level 2. If one waits the full 256 milliseconds before taking a look, the ion will be completely in the Level 2 state when the laser pulse hits it.

But what happens if someone peeks early—say after only 128 milliseconds? At this point, an ion is in a composite state, half Level 1 and half Level 2. Observing it forces it to be in either one state or the other, much as a tossed coin suddenly goes from an indefinite state to being either heads or tails once it hits the ground. A single ion observed after 128 milliseconds will have equal probability of going into Level 1 or Level 2, so roughly half of the several thousand ions in the trap will be seen to be in Level 1 and the other half in Level 2.

After only 4 milliseconds, however, the quantum state of any given ion is about 99.99% Level 1. This means that shining the laser at the trap will reveal all but about 0.01% of the ions to still be in Level 1. The water has not yet started to boil.

But the act of looking has done more than reveal the state of the system. It has also sent all the ions, except for the few that made it to level 2, back to the starting point in Level 1. If the observer continues to peek every 4 milliseconds, the system is reset again and again, with an average of only 0.01% of the ions moving to Level 2 each time. At the end of 256 milliseconds, only about 0.6% of the ions have moved to Level 2, and the system looks very nearly the same as at the beginning. Making more frequent observations would reduce the percentage in Level 2 even more, Itano says.

The NIST experiment provides experimental confirmation of an effect noted by several observers, including B. Misra and Ennackel Sudarshan at the University of Texas in Austin in the late 1970s. These two researchers showed that in theory a continuously observed quantum state can never decay and called this the "quantum Zeno effect." That was in reference to a famous paradox conceived by the ancient Greek philosopher Zeno, in which he argued that motion is impossible. Consider an arrow in flight, Zeno said: At any given instant it cannot be at two places, so it must be at one point, but if it is in one spot it is at rest. This implies that the arrow is at rest at every moment of its flight, so it cannot be moving after all.

Until the NIST experiment, no researchers had demonstrated the quantum Zeno effect directly and unambiguously, although some experiments involving continuous observation of certain quantum systems may have exhibited it indirectly, Itano says. The key to the NIST group's success was use of a system in which the transition from one state to another proceeded slowly enough so that observations could significantly reduce the probability of it happening. For instance, in order to slow radioactive decay, researchers would have to make measurements that are less than one-trillionth the duration of the 2.4-millisecond pulses used in the NIST work. This is way out of the range of experimental capabilities.

Although in theory one could suspend any quantum transition—even the decay of a radioactive atom—by keeping a constant watch on it, in practical terms this is impossible, Itano notes. Because any observation takes a finite period of time, there will always be in-between times when the atom is not being watched and can decay. The NIST researchers could probably improve their result by several orders of magnitude by using a more powerful laser, which would permit shorter laser pulses and more observations, Itano says, but even then a few atoms would still make it to Level 2. And please don't call their experiment the "quantum pot-watching effect." To Itano *et al*, "Quantum Zeno effect" sounds more erudite and catchy. ■ ROBERT POOL

To be published in Physical Review A

Quantum Zeno Effect*

Wayne M. Itano, D. J. Heinzen, J. J. Bollinger, and D. J. Wineland
Time and Frequency Division, National Institute of Standards and Technology, Boulder, Colorado 80303

(Received 12 October 1989)

The quantum Zeno effect is the inhibition of transitions between quantum states by frequent measurements of the state. The inhibition arises because the measurement causes a collapse (reduction) of the wave-function. If the time between measurements is short enough, the wave-function usually collapses back to the initial state. We have observed this effect in an rf transition between two $^9Be^+$ ground-state hyperfine levels. The ions were confined in a Penning trap and laser cooled. Short pulses of light, applied at the same time as the rf field, made the measurements. If an ion was in one state, it scattered a few photons; if it was in the other, it scattered no photons. In the latter case the wave-function collapse was due to a null measurement. Good agreement was found with calculations.

1990 PACS numbers: 03.65.Bz, 32.30.Bv, 32.80.Pj

I. INTRODUCTION

The quantum Zeno effect (or paradox) is the inhibition of transitions between quantum states by frequent measurements.[1-7] Misra and Sudarshan[1] were the first to call the effect by that name, but closely related work was done much earlier.[8]

Consider the decay of an unstable state, such as an unstable particle. An observation that the state has not decayed causes a collapse (reduction) of the wave-function to the undecayed state. The probability that the state decays after this collapse grows quadratically with time, for short enough times. Suppose n measurements, spaced in time by T/n, are made. The probability that the state will survive for a time T goes to 1 in the limit $n \rightarrow \infty$. Hence, Misra and Sudarshan argued, a continuously observed state can never decay.[1] This effect is difficult to observe in spontaneous decay because the interval during which the probability grows quadratically is very short compared to the time required to make a measurement. Ghirardi *et al.*[3] have shown, by general arguments based on the time-energy uncertainty relations, that the dependence of the lifetime on the frequency of measurements, although present in principle, would be extremely difficult to observe. Deviations from an exponential decay law, expected theoretically for very short and very long times, have not yet been observed experimentally.[9]

The term "quantum Zeno effect" is applied also to the inhibition of *induced* transitions by frequent measurements. This effect can easily be observed experimentally, in contrast to the inhibition of spontaneous transitions. Consider a system made up of two levels, labeled 1 and 2. Assume that the system can be driven from level 1 to level 2 by applying a resonant perturbation for a given length of time. Assume that it is possible to make measurements of the state of the system, which project the system into one of the two levels, and which take a negligible amount of time. If the system is initially in level 1, and we make n equally spaced measurements while the perturbation is applied, the probability of finding the system in level 2 at the end of the period decreases as n increases. Various cases of this type have been examined theoretically.[10-12]

II. THEORY

Cook[12] proposed an experiment on a single, trapped ion to demonstrate the quantum Zeno effect on an induced transition. Trapped ions provide very clean systems for testing calculations of the dynamics of quantum transitions. They can be observed for long periods, free from perturbations and relaxations. Their levels can be manipulated easily with rf and optical fields.

In Cook's proposed experiment, the ion was assumed to have the level structure shown in Fig. 1. Level 1 is the ground state. Level 2 is an excited metastable state. Spontaneous decay from level 2 to level 1 is assumed to be negligible. If the ion is in level 1 at time $\tau = 0$, and a perturbation having the resonance frequency $(E_2 - E_1)/\hbar$ is applied, a coherent superposition state is created. Let P_1 and P_2 be the probabilities for the ion to be in levels 1 and 2. Then $P_2(\tau) = \sin^2(\Omega\tau/2)$

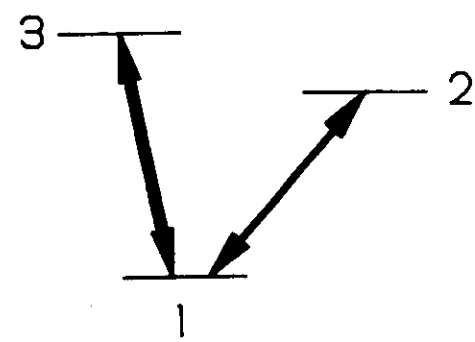

FIG. 1. Energy-level diagram for Cook's proposed demonstration of the quantum Zeno effect.

and $P_1(\tau) = \cos^2(\Omega\tau/2)$, where Ω, the Rabi frequency, is proportional to the amplitude of the applied field. If a measurement of the state of the ion is made after a short time, such that $\Omega\tau \ll 1$, then $P_1(\tau) \approx 1$ and $P_2(\tau) \approx \frac{1}{4}\Omega^2\tau^2 \ll 1$. If, instead, the ion starts out in level 2, the situation is reversed, so that $P_2(\tau) \approx 1$ and $P_1(\tau) \approx \frac{1}{4}\Omega^2\tau^2$.

Assume that level 3 is connected by a strongly allowed transition to level 1 and that it can decay *only* to level 1. The state measurement is carried out by driving the $1 \rightarrow 3$ transition with an optical pulse. This pulse causes a collapse of the wave-function. The wave-function of the ion is projected by the measurement into level 1 or 2 with probabilities equal to the squares of the wave-function amplitudes for being in level 1 or 2. If the ion is projected into level 1 at the beginning of the pulse, it cycles between level 1 and level 3, and emits a series of photons until the pulse is turned off. If it is projected into level 2, it scatters no photons. The latter case is an example of what Porrati and Putterman have called a wave-function collapse due to a null measurement.[13] That is, the *absence* of scattered photons when the optical pulse is applied is enough to cause a collapse of the wave-function to level 2. The pulse must be long enough so that an ion in level 1 would have time to scatter a few photons. It does not matter whether a switched-on detector capable of detecting the photons is actually present. The state of the ion is recorded in the electromagnetic field. The measurement (and the subsequent wave-function collapse) takes place after the field has interacted with the ion for a sufficient amount of time.[12,14] If a measurement finds the ion to be in level 1, the ion returns to level 1 after the end of the measurement, within a time approximately equal to the lifetime of level 3. If a measurement finds the ion to be in level 2, the ion never leaves that level during the measurement. If this measurement is followed immediately by a second one, the result will *almost* always be the same. Thus the optical pulses make nearly ideal, nondestructive measurements. However, since a finite time is required to make a measurement, the wave-function can evolve between measurements. Therefore, it is possible for the result of the second measurement to differ from that of the first.

Cook's proposed experiment was to drive the $1 \rightarrow 2$ transition with an on-resonance π pulse (a square pulse of duration $T = \pi/\Omega$) while simultaneously applying a series of short measurement pulses. The duration of a measurement pulse was assumed to be much less than the time between pulses. Suppose the ion is in level 1 at time $\tau = 0$. The π pulse is then applied. Without the measurement pulses, the probability $P_2(T)$ to be in level 2 at $\tau = T$ is 1. Let n measurement pulses be applied at times $\tau = kT/n = k\pi/(n\Omega)$, where $k = 1, \ldots, n$. The level populations at the end of the π pulse are easily calculated with the use of the vector representation of a two-level system.[15] The equations simplify if we transform to a coordinate system in which the rotating component of the rf perturbation is stationary. (We ignore the counter-rotating component.) The system is described by a vector $\mathbf{R} \equiv (R_1, R_2, R_3)$, whose components can be expressed in terms of the density matrix ρ:

$$\begin{aligned} R_1 &\equiv \rho_{12} + \rho_{21}, \\ R_2 &\equiv i(\rho_{12} - \rho_{21}), \\ R_3 &\equiv \rho_{22} - \rho_{11} \equiv P_2 - P_1. \end{aligned} \tag{1}$$

The equation of motion for $\mathbf{R}$ is

$$d\mathbf{R}/dt = \boldsymbol{\omega} \times \mathbf{R}, \tag{2}$$

where $\boldsymbol{\omega} = (\Omega, 0, 0)$. The geometrical interpretation of Eq. (2) is that $\mathbf{R}$ precesses about $\boldsymbol{\omega}$ with fixed magnitude and angular velocity $|\boldsymbol{\omega}| = \Omega$. At $\tau = 0$, $\mathbf{R} = (0, 0, -1)$. Just before the first measurement pulse at $\tau = \pi/(n\Omega)$,

$$\begin{aligned} \mathbf{R} &= [0, \sin(\Omega\tau), -\cos(\Omega\tau)] \\ &= [0, \sin(\pi/n), -\cos(\pi/n)]. \end{aligned} \tag{3}$$

The measurement pulse projects an ion into level 1 or 2. Its effect on the density matrix, which corresponds to an ensemble average, is to set the coherences (ρ_{12} and ρ_{21}) to zero, while leaving the populations (ρ_{22} and ρ_{11}) unchanged. Hence, R_1 and R_2 are set to zero, while R_3 remains unchanged:

$$\mathbf{R} = [0, 0, -\cos(\pi/n)]. \tag{4}$$

Thus, at $\tau = \pi/(n\Omega)$, just after the first measurement pulse, $\mathbf{R}$ is the same as it was at $\tau = 0$, except that its magnitude has been decreased by a factor of $\cos(\pi/n)$. After the second measurement [$\tau = 2\pi/(n\Omega)$], $|\mathbf{R}|$ is decreased by another factor of $\cos(\pi/n)$. This follows from the fact that Eq. (2) is linear with respect to $\mathbf{R}$. After n measurements, ($\tau = \pi/\Omega$),

$$\mathbf{R}(T) = [0, 0, -\cos^n(\pi/n)]. \tag{5}$$

We use Eq. (1) to express P_2 in terms of R_3 :

$$\begin{aligned} P_2 &= R_3 + P_1 = R_3 + (1 - P_2) \\ &= \tfrac{1}{2}(1 + R_3). \end{aligned} \tag{6}$$

In deriving Eq. (6), we used the conservation of probability for a closed two-level system: $P_1 + P_2 = 1$. Substituting the value of $R_3(T)$ from Eq. (5) into Eq. (6), we have

$$P_2(T) = \tfrac{1}{2}[1 - \cos^n(\pi/n)]. \tag{7}$$

It can be shown from Eq. (7) that $P_2(T)$ decreases monotonically toward zero as n goes to infinity. For large n,[12]

$$P_2(T) \approx \tfrac{1}{2}[1 - \exp(-\tfrac{1}{2}\pi^2/n)]. \tag{8}$$

Equation (8) was derived from Eq. (7) by expanding $\cos(\pi/n)$ in a power series and using

$$\lim_{n\to\infty} (1 - x/n)^n = e^{-x}. \tag{9}$$

III. EXPERIMENT

Our experiment is very similar to that proposed by Cook. Levels 1 and 2 are the $(m_I,\ m_J) = (\frac{3}{2},\ \frac{1}{2})$ and $(\frac{1}{2},\ \frac{1}{2})$ hyperfine sublevels in the ground $2s\ ^2S_{1/2}$ state of $^9Be^+$ (see Fig. 2). These levels are separated by 320.7 MHz at the magnetic field used in the experiment ($B \approx 0.8194$ T). Level 3 is the $(m_I = \frac{3}{2},\ m_J = \frac{3}{2})$ sublevel of the $2p\ ^2P_{3/2}$ state, which decays only to level 1. Spontaneous decay from level 2 to level 1 is negligible.

The experimental apparatus has been described previously.[16-18] About 5000 $^9Be^+$ ions were stored in a cylindrical Penning trap. The pressure in the trap was about 10^{-8} Pa. The storage time of the ions in the trap was several hours. A frequency-doubled cw dye laser generated 313-nm radiation to drive the $1 \rightarrow 3$ transition in order to optically pump, detect, and laser cool the $^9Be^+$ ions. The 313-nm fluorescence from the ions was detected by an imaging photon-counting detector.[16] About 100 000 $^{26}Mg^+$ ions were confined together with the $^9Be^+$ ions. The $^{26}Mg^+$ ions were laser-cooled by 280 nm radiation from a frequency-doubled cw dye laser. The $^9Be^+$ were kept cold ($\lesssim 250$ mK) by long-range Coulomb collisions with the $^{26}Mg^+$ ions even when they were not directly laser-cooled by the 313-nm source.[19]

The polarization of the 313-nm beam was perpendicular to the magnetic field. When the 313-nm radiation was nearly resonant with the $1 \rightarrow 3$ transition and no rf field was applied, about $\frac{16}{17}$ of the population was optically pumped to the $(\frac{3}{2},\ \frac{1}{2})$ ground-state sublevel (level 1).[20-22] The remaining population was in the $(\frac{3}{2},\ -\frac{1}{2})$ sublevel. When the 313-nm radiation was on continuously, the populations approached the steady state with a time constant of about 1 s.

The measurement sequence for the $1 \rightarrow 2$ transition was as follows: The 313-nm radiation was left on for about 5 s to prepare most of the $^9Be^+$ ions in level 1 and to empty level 2. The 313-nm radiation was then turned off. The 320.7-MHz rf field was turned on for $T = 256$ ms. Its frequency and amplitude were adjusted to make this an on-resonance π pulse. During the rf pulse, n pulses of length $\tau_p = 2.4$ ms and wavelength 313-nm were applied, where n was 1, 2, 4, 8, 16, 32, or 64. The pulses were long enough to collapse each ion's wave-function without causing significant optical pumping. The delay from the beginning of the rf pulse to the beginning of the first 313-nm pulse was $(T/n - 1.3)$ ms. The time between the beginning of one 313-nm pulse and the beginning of the next one was T/n.

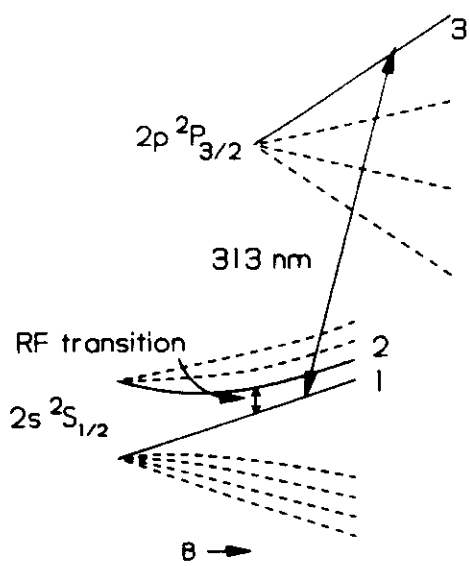

FIG. 2. Diagram of the energy levels of $^9Be^+$ in a magnetic field B. The states labeled 1, 2, and 3 correspond to those in Fig. 1

After the end of the rf π pulse, the 313-nm radiation was turned on and left on to prepare the state. The number of photons counted in the first 100 ms was recorded. This signal was roughly proportional to the number of ions remaining in level 1. However, background counts, counter deadtime, and optical pumping during the 100 ms cause deviations from this proportionality. In order to calibrate the signal, known level populations were created by applying rf pulses of lengths $\tau = 0, 32, 64, \ldots, 544$ ms. The population of level 1 (per ion in the subsystem made up of levels 1 and 2) was then given by $\cos^2(\Omega\tau/2)$. From these data, the precise value of Ω and also the calibration of the signal as a function of the population of level 1 were obtained. The deviations of the calibration points from a smooth curve gave an indication of the measurement errors.

The 313-nm radiation was turned on and off with an electromechanical shutter that had a rise or fall time of about 0.2 ms. The 320.7-MHz rf field was turned on and off with a semiconductor diode switch, which had a switching time of about 150 ns and an on-to-off ratio of about 75 dB. The 280-nm beam was left on continuously. The measurement sequence was the same for the $2 \rightarrow 1$ transition, except that first an rf π pulse, free from 313-nm pulses, transferred the level 1 population to level 2 immediately after the 313-nm radiation was shut off.

The $1 \rightarrow 2$ transition frequency decreases by 22 Hz for a 1-μT increase in B. If the transition frequency shifts by more than a small fraction of $1/T \approx 4$ Hz, the observed transition probabilities will deviate significantly from the calculated ones. The center frequency of the $1 \rightarrow 2$ resonance was measured before and after each run. If the frequency shifted by more than about 0.1 Hz, the data from that run were not used. Drift of the magnetic field was the main obstacle to increasing T. Relaxations of the ground-state hyperfine levels are very weak when the 313-nm radiation is not applied. This was shown in studies of the $(m_I,\ m_J) = (-\frac{1}{2},\ \frac{1}{2})$ to $(-\frac{3}{2},\ \frac{1}{2})$ transition. The derivative of this transition frequency with respect to B goes to zero at $B \approx 0.8194$ T. At this value of B, weak relaxation processes due, for example, to collisions or to the 280-nm radiation can be studied. This transition showed no sign of population or coherence relaxations for times up to 550 s.[17]

The average number of photons scattered by an ion in

TABLE I. Predicted and observed values of the $1 \rightarrow 2$ and $2 \rightarrow 1$ transition probabilities for different values of the number of measurement pulses n. The uncertainties of the observed transition probabilities are about 0.02. The second column shows the transition probabilities that result from a simplified calculation, in which the measurement pulses are assumed to have zero duration and in which optical pumping is neglected.

		$1 \rightarrow 2$ transition		$2 \rightarrow 1$ transition	
n	$\frac{1}{2}[1-\cos^n(\pi/n)]$	Predicted	Observed	Predicted	Observed
1	1.0000	0.995	0.995	0.999	0.998
2	0.5000	0.497	0.500	0.501	0.496
4	0.3750	0.351	0.335	0.365	0.363
8	0.2346	0.201	0.194	0.217	0.209
16	0.1334	0.095	0.103	0.118	0.106
32	0.0716	0.034	0.013	0.073	0.061
64	0.0371	0.006	−0.006	0.080	0.075

level 1 during a single 313-nm pulse of length τ_p is approximately $\tau_p R_c/(\epsilon_d N)$, where R_c is the observed steady-state photon count rate, ϵ_d is the probability of detecting a scattered photon, and N is the total number of $^9Be^+$ ions. The photon detection efficiency ϵ_d was estimated from the solid angle of the lens system and the quantum efficiency of the detector to be about 2×10^{-4}. For typical experimental values $\tau_p = 2.4$ ms, $R_c = 30\,000$ s^{-1}, and $N = 5000$, the number of scattered photons per ion per pulse was therefore about 72, more than enough to cause the collapse of the wave-function. We emphasize that it is the number of scattered photons which is important, not the number that can be detected by the apparatus. The number of photons detected per ion per pulse is much less than 1. As a further check that the pulses were long enough, some runs were taken with τ_p decreased to 1.4 ms (the shortest that the shutter could make). The results indicated that these pulses were still long enough to collapse the wave-functions. These data are not reported here because the pulse shapes were not the same for different pulse repetition rates. This made quantitative interpretation of the data difficult.

With a faster optical shutter, such as an acousto-optic modulator, the 313-nm pulses could be decreased in length and still be long enough to collapse the wave-functions. However, the minimum time required for a measurement pulse depends not only on the *average* photon scattering rate, but also on the time required to ensure that every ion will pass through the 313-nm beam. The $^9Be^+$ ions occupied a cylindrical volume with a height of about 1000 μm and a radius of about 350 μm. The 313-nm beam was focused to a radius of about 50 μm. It propagated perpendicular to the axis of the cylinder and intersected the $^9Be^+$ ions near the center of the volume. If the 313-nm beam were expanded radially and directed along the axis, so that it intersected the entire volume, this problem could be avoided.

IV. RESULTS

Table I shows the calculated and observed values of the probabilities of making the $1 \rightarrow 2$ and $2 \rightarrow 1$ transitions for values of $n = 1, 2, \ldots, 64$. The predicted and observed values agree within the measurement error of about 0.02 estimated from the scatter of the signal calibration data. The general decrease of the probabilities with n demonstrates the quantum Zeno effect. Probabilities must take values from 0 to 1. However, with our method of determining the transition probability, random fluctuations in the photon count rate can lead to an *apparent* transition probability which is less than zero or greater than 1. The value of −0.006 for the observed $1 \rightarrow 2$ transition probability for $n = 64$ just means that the number of photons detected was slightly higher than the number expected for a transition probability of 0. Figures 3 and 4 show the probabilities for the $1 \rightarrow 2$ and $2 \rightarrow 1$ transitions, respectively.

The assumptions made in the calculations are as follows: When the rf field is present and the 313-nm radiation is not, the transition between levels 1 and 2 is assumed to proceed without relaxations. During the 313-

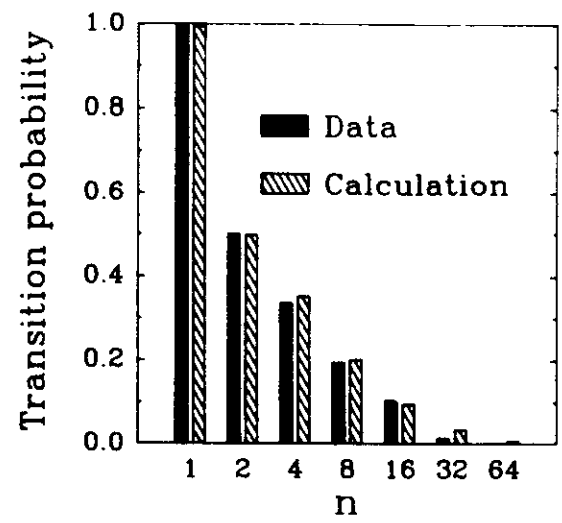

FIG. 3. Graph of the experimental and calculated $1 \rightarrow 2$ transition probabilities as a function of the number of measurement pulses n. The decrease of the transition probabilities with increasing n demonstrates the quantum Zeno effect.

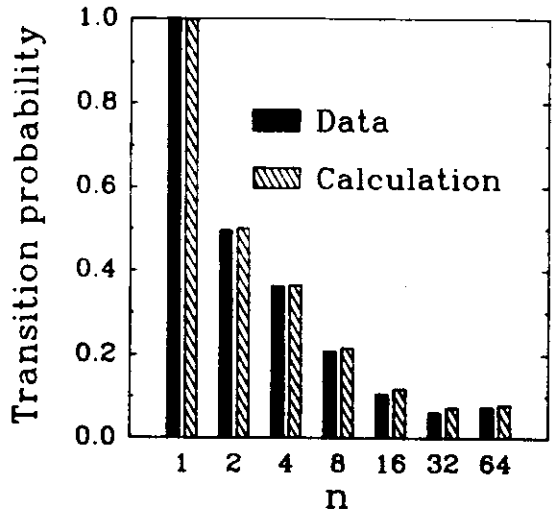

FIG. 4. Graph of the experimental and calculated $2 \rightarrow 1$ transition probabilities as a function of the number of measurement pulses n. The transition probabilities for $n = 32$ and $n = 64$ are higher than the corresponding ones for the $1 \rightarrow 2$ transition because of an optical pumping effect discussed in the text.

nm pulses, the coherence between levels 1 and 2 is assumed to be destroyed so quickly that the rf field can be ignored. The 313-nm radiation causes optical pumping from level 2 to level 1 with a time constant of about 1 s. This rate was measured by using an rf π pulse to prepare the ions in level 2, turning on the 313-nm radiation, and recording the 313-nm fluorescence as a function of time. Optical pumping by the 313-nm pulses can have an observable effect on the measured transition probabilities, especially for large n. This optical pumping causes a decrease in the $1 \rightarrow 2$ transition probability and an increase in the $2 \rightarrow 1$ transition probability. The decrease in the $1 \rightarrow 2$ transition probability is not noticeable in our data, since the transition probability is already small for large n. The increase in the $2 \rightarrow 1$ transition probability is noticeable for $n = 32$ and 64. The predicted transition probabilities shown in Table I and plotted in Figs. 3 and 4 take into account optical pumping, the finite 313-nm pulse durations, and the measured value of Ω. The measured value of Ω differed by less than 3% from the ideal value $\Omega = \pi/T$. For comparison, $\frac{1}{2}[1 - \cos^n(\pi/n)]$, the transition probability calculated if these effects are not included, is also shown in Table I.

For the larger values of n, the sum of the measurement periods, $n\tau_p$, is not negligible compared to T. Therefore, part of the decrease in the transition probability is due merely to the decrease in the time during which rf field can act. For the most extreme case ($n = 64$) $n\tau_p$ is 60% of T. However, even for this case, the decrease in the transition probability is much more than could be accounted for by the decrease in time. For $n = 16$, $n\tau_p$ is only 15% of T, but the transition probability is decreased by about 90%.

V. DISCUSSION

Cook[12] originally proposed an experiment with a single ion. Such an experiment should be feasible, since single ions have been observed in Penning traps[21,23] and in Paul traps.[24,25] The ensemble average, which is needed for comparison with calculations of the density matrix, would be obtained by repeating the experiment many times. In the present experiment, each measurement is an average over an ensemble of about 5000 independent ions, since their mutual interactions can be neglected. An experiment might be done with a single Hg^+ ion. Level 1 would be the ground $5d^{10}6s\ ^2S_{1/2}$ state, level 2 would be the metastable $5d^96s^2\ ^2D_{5/2}$ state, and level 3 would be the $5d^{10}6p\ ^2P_{1/2}$ state. The $1 \rightarrow 2$ transition at 282 nm and the $1 \rightarrow 3$ transition at 194 nm have already been observed in a single Hg^+ ion.[25]

It might be argued that previous observations of effects such as collisional relaxation of rf transitions already contain the quantum Zeno effect. This is possible, but we know of no experiment in which the effect has been demonstrated simply and unambiguously. Collisions cannot usually be interpreted as quantum measurements. That is, they do not necessarily project a single quantum system, such as an atom, into one state or the other. Rather, in many cases, they perturb the phase of the coherence, represented by R_1 and R_2 in the vector model, for each system. For the ensemble average, R_1 and R_2 are driven to zero, just as in our experiment, but the underlying physics is different. Collisions may also perturb R_3, which is not desirable for a demonstration of the quantum Zeno effect.

Some experiments that involve continuous measurements have, in a sense, already demonstrated the quantum Zeno effect. Although the measurements are continuous, it takes a finite amount of time to make a measurement with a given degree of uncertainty. Thus a continuous measurement might be regarded as a series of measurements, one after the other. In such experiments, the measurement times are not separated from the free evolution periods, so the analysis is more difficult than for the present experiment. One example of such an experiment is the spin flip resonance of a single, trapped electron.[10] The spin state is detected by coupling the electron to an electronic circuit. As the time required to make a measurement is decreased by increasing the degree of coupling, noise broadens the spin-flip resonance. This broadening decreases the rate of transitions induced by a weak microwave field. Another example is the three-level Hg^+ system described previously.[25] Radiation resonant with the $5d^{10}6s\ ^2S_{1/2}$ to $5d^{10}6p\ ^2P_{1/2}$ ($1 \rightarrow 3$) transition performs a continuous state measurement. Photons are not scattered if the ion is in the $5d^96s^2\ ^2D_{5/2}$ state (level 2); otherwise they are. We have observed a decrease of the rate of the $1 \rightarrow 2$ transition, induced by a narrow-band laser, when radiation at the $1 \rightarrow 3$ transition frequency is applied.

Normally, the probability for spontaneous emission of

a photon by an atom grows quadratically only for extremely short times, approximately the inverse of the frequency of the emitted photon. However, it might be possible to increase this time by placing the atom inside a resonant cavity. Jaynes and Cummings[26] showed that a two-level atom coupled to a single mode of a resonant, lossless cavity oscillates between the ground and excited states. Suppose an excited atom is placed in a cavity that initially contains no photons. Then the probability for the atom to be in the excited state is $\cos^2(g\tau)$, where g is the coupling constant (the vacuum field Rabi frequency) and τ is the time that the atom has been in the cavity. The probability for the atom to be in the ground state is proportional to τ^2 for τ short compared to g^{-1}.

If the atom is coupled to a single ***damped*** cavity mode, the probability to be in the ground state is still proportional to τ^2, provided that τ is short compared to both g^{-1} and γ_c^{-1}, where γ_c is the dissipation rate of the cavity.[27] It might be possible to demonstrate the quantum Zeno effect on the decay of an atom in a cavity. This would not contradict the results of Ghirardi *et al.*,[3] since they did not consider such a system.

VI. ACKNOWLEDGMENTS

This research was supported in part by the U. S. Air Force Office of Scientific Research and the Office of Naval Research. We thank Dr. S. L. Gilbert and Dr. M. G. Raizen for reading the manuscript.

---

[1] B. Misra and E. C. G. Sudarshan, J. Math. Phys. **18**, 756 (1977).

[2] C. B. Chiu, E. C. G. Sudarshan, and B. Misra, Phys. Rev. D **16**, 520 (1977).

[3] G. C. Ghirardi, C. Omero, T. Weber, and A. Rimini, Nuovo Cimento **52A**, 421 (1979).

[4] A. Peres, Am. J. Phys. **48**, 931 (1980).

[5] E. Joos, Phys. Rev. D **29**, 1626 (1984).

[6] K. Kraus, Found. Phys. **11**, 547 (1981).

[7] D. Home and M. A. B. Whitaker, J. Phys. A **19**, 1847 (1986).

[8] L. A. Khalfin, Zh. Eksp. Teor. Fiz. **33**, 1371 (1957) [Sov. Phys.-JETP **6**, 1053 (1958)]; R. G. Winter, Phys. Rev. **123**, 1503 (1961); W. Yourgrau, in *Problems in the Philosophy of Science*, edited by I. Lakatos and A. Musgrave (North-Holland, Amsterdam, 1968), pp. 191 and 192.

[9] E. B. Norman, S. B. Gazes, S. G. Crane, and D. A. Bennett, Phys. Rev. Lett. **60**, 2246 (1988).

[10] H. Dehmelt, Proc. Natl. Acad. Sci. U.S.A. **83**, 2291 (1986); **83**, 3074 (1986).

[11] G. J. Milburn, J. Opt. Soc. Am. B **5**, 1317 (1988).

[12] R. J. Cook, Phys. Scr. **T21**, 49 (1988).

[13] M. Porrati and S. Putterman, Phys. Rev. A **36**, 929 (1987).

[14] H. J. Carmichael, S. Singh, R. Vyas, and P. R. Rice, Phys. Rev. A **39**, 1200 (1989).

[15] I. I. Rabi, N. F. Ramsey, and J. Schwinger, Rev. Mod. Phys. **26**, 167 (1954); R. P. Feynman, F. L. Vernon, Jr. , and R. W. Hellwarth, J. Appl. Phys. **28**, 49 (1957).

[16] S. L. Gilbert, J. J. Bollinger, and D. J. Wineland, Phys. Rev. Lett. **60**, 2022 (1988); S. L. Gilbert, J. C. Bergquist, J. J. Bollinger, W. M. Itano, and D. J. Wineland, in ***Atomic Physics 11***, Proceedings of the International Conference, Paris, 1988, edited by S. Haroche, J. C. Gay, and G. Grynberg (World Scientific, Singapore, 1989), p. 261.

[17] J. J. Bollinger, S. L. Gilbert, W. M. Itano, and D. J. Wineland, in *Frequency Standards and Metrology*, Proceedings of the Fourth Symposium, Ancona, Italy, 1988, edited by A. De Marchi (Springer-Verlag, Berlin, 1989), p. 319.

[18] J. J. Bollinger, D. J. Heinzen, W. M. Itano, S. L. Gilbert, and D. J. Wineland, Phys. Rev. Lett. **63**, 1031 (1989).

[19] D. J. Larson, J. C. Bergquist, J. J. Bollinger, W. M. Itano, and D. J. Wineland, Phys. Rev. Lett. **57**, 70 (1986).

[20] D. J. Wineland, J. C. Bergquist, W. M. Itano, and R. E. Drullinger, Opt. Lett. **5**, 245 (1980).

[21] R. G. Hulet, D. J. Wineland, J. C. Bergquist, and W. M. Itano, Phys. Rev. A **37**, 4544 (1988).

[22] L. R. Brewer, J. D. Prestage, J. J. Bollinger, W. M. Itano, D. J. Larson, and D. J. Wineland, Phys. Rev. A **38**, 859 (1988).

[23] D. J. Wineland and W. M. Itano, Phys. Lett. **82A**, 75 (1981).

[24] W. Neuhauser, M. Hohenstatt, and P. E. Toschek, Phys. Rev. A **22**, 1137 (1980); W. Nagourney, G. Janik, and H. Dehmelt, Proc. Natl. Acad. Sci. U.S.A., **80**, 643 (1983); F. Diedrich and H. Walther, Phys. Rev. Lett. **58**, 203 (1987); R. G. DeVoe, J. Hoffnagle, and R. G. Brewer, Phys. Rev. A **39**, 4362 (1989); J. D. Sankey and A. A. Madej, Appl. Phys. B **49**, 69 (1989).

[25] J. C. Bergquist, R. G. Hulet, W. M. Itano, and D. J. Wineland, Phys. Rev. Lett. **57**, 1699 (1986); J. C. Bergquist, W. M. Itano, and D. J. Wineland, Phys. Rev. A **36**, 428 (1987).

[26] E. T. Jaynes and F. W. Cummings, Proc. IEEE **51**, 89 (1963).

[27] S. Sachdev, Phys. Rev. A **29**, 2627 (1984).

References
Tests of Quantum Mechanics with Laser-Cooled Ions

1. S. Weinberg, "Precision tests of quantum mechanics," Phys. Rev. Lett. 62, 485-488 (1989).

2. S. Weinberg, "Testing quantum mechanics," Ann. Phys. (New York) 194, 336-386 (1989).

3. J.J. Bollinger, D.J. Heinzen, W.M. Itano, S.L. Gilbert, and D.J. Wineland, "Test of the linearity of quantum mechanics by rf spectroscopy of the $^{9}Be^{+}$ ground state," Phys. Rev. Lett. 63, 1031-1034 (1989).

4. R. J. Cook, "What are quantum jumps?" Phys. Scripta T21, 49-51 (1988).

5. W.M. Itano, D.J. Heinzen, J.J. Bollinger, and D.J. Wineland, "Quantum Zeno effect," Phys. Rev. A (in press).

Quantum Optics of Single, Trapped Ions

W. M. Itano
J. C. Bergquist
F. Diedrich
D.J. Wineland

Time and Frequency Division
National Institute of Standards and Technology
(formerly the National Bureau of Standards)
Boulder, Colorado 80303

Supported in part by the Air Force Office of Scientific Research and the Office of Naval Research

OUTLINE

I. Introduction

II. Apparatus

III. 1 (or 2) ion quantum jumps

- Density matrix equations
- Photon antibunching
- Sub-Poissonian statistics
- Chaos?

IV. QM of 1 ion in a harmonic well

- Sideband laser cooling
- Zero-point confinement
- Coherent or squeezed matter states

QUANTUM OPTICS OF SINGLE, TRAPPED IONS*

Wayne M. Itano, J.C. Bergquist, F. Diedrich,† and D.J. Wineland

Time and Frequency Division
National Institute of Standards and Technology
Boulder, CO 80303

INTRODUCTION

Single ions in ion traps can be localized in small volumes and held for long periods of time. This makes it easier to observe certain nonclassical properties of the electromagnetic field, such as photon antibunching and sub-Poissonian photon statistics, which are reduced when large numbers of atoms are present. Such properties can be observed in atomic beams so dilute that the probability of having more than one atom in the observation volume is low.[1,2] Trapped ions can be studied for much longer times. This makes it possible, for example, to observe repeated quantum jumps of the *same* atom.[3–5] When there are only a few (or one) ions in the trap, their number can be known and kept fixed. Thus, sub-Poissonian photon statistics can be observed[6,7] *without* the time gating which is necessary with atomic beams.[2] Another advantage of trapped ions is that, thanks to their isolation from collisions and other perturbations, they can be laser-cooled to low temperatures and studied spectroscopically with great precision. A single ion has even been cooled to the ground energy level of the harmonic well of the trap, so its motion must be treated quantum mechanically.[8]

EXPERIMENT

Hg^+ ions were confined in a Paul trap that consists of a toroidal ring electrode, with an inner diameter slightly less than 1 mm, and two endcap electrodes, which are placed symmetrically on opposite sides of the hole through the ring.[9] A combination of static and rf potentials applied between the electrodes effectively creates a three-dimensional harmonic well. The classical motion consists of a small-amplitude oscillation, at the frequency of the applied rf potential, superimposed on a large-amplitude, harmonic motion, called the secular motion. The frequencies of the secular motion were 1–4 MHz.

A cw, tunable 194 nm radiation source[10] with a power of about 5 μW was used to excite the $^2S_{1/2}$ to $^2P_{1/2}$ first resonance line of Hg^+. In order to cool the ions, the frequency of the 194 nm source was tuned slightly lower than the atomic resonance. The radiation pressure force increases when the ion's velocity is opposed to the direction of 194 nm propagation, because the Doppler shift brings the light frequency closer to resonance. This form of laser cooling is called Doppler cooling. The 194 nm fluorescence

†Present address: Gsänger Optoelektronik GmbH, Planegg, Federal Republic of Germany.

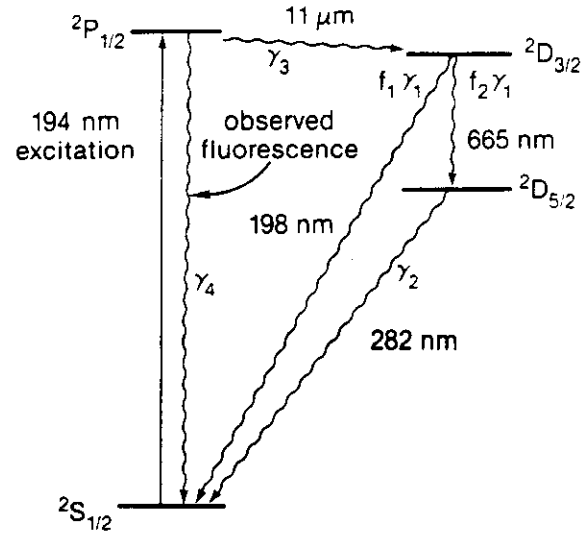

Figure 1: The lowest four energy levels of Hg^+.

from a single, cooled ion was easily observed. The photon detection efficiency was about 5×10^{-4}. Approximately 50 000 photons/s from a single ion were detected with a photomultiplier tube.

QUANTUM JUMPS

Quantum jumps of single, trapped ions have been observed in Ba^+,[3,4] Hg^+,[5] and Mg^+.[11] In this context, the term "quantum jump" refers to a sudden change in the fluorescence intensity when the atom makes a transition to or from a metastable level. We have observed photon antibunching and sub-Poissonian statistics in the system shown in Fig. 1. Measurements of the radiative decay rates were reported previously.[7] The 194 nm source drives the Hg^+ ion from the ground $^2S_{1/2}$ level to the $^2P_{1/2}$ level, which decays at a rate of 4×10^8 s^{-1}. Usually, the ion decays back to the ground state, emitting a 194 nm photon. However, about once in 10^7 times, it decays instead to the metastable $^2D_{3/2}$ level, and emits an 11 μm photon. The $^2D_{3/2}$ level decays with a total rate of $\gamma_1 = 109 \pm 5$ s^{-1}. It decays directly to the ground state with probability $f_1 = 0.491 \pm 0.015$ and to the metastable $^2D_{5/2}$ level with probability $f_2 = 1 - f_1$. The $^2D_{5/2}$ level decays to the ground state at a rate $\gamma_2 = 11.6 \pm 0.4$ s^{-1}.

Figure 2 shows the 194 nm fluorescence from a single Hg^+ ion as a function of time. When the ion makes transitions between the $^2S_{1/2}$ level and the $^2P_{1/2}$ level, the fluorescence has a high, steady level. When the ion makes a transition (quantum jump) to the $^2D_{3/2}$ level and emits an 11 μm photon, the fluorescence drops to the background level. When the ion returns to the ground state, the fluorescence goes back to the high level. We call the sudden drops in fluorescence "on-to-off" quantum jumps and the sudden increases "off-to-on" quantum jumps.

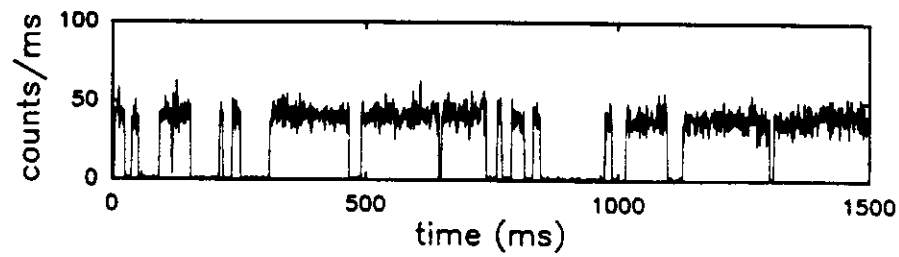

Figure 2: 194 nm fluorescence of a single Hg^+ ion as a function of time.

Table 1: Table of observed and calculated values of $Np(n)$ and Q. Values of $Np(n)$ and Q for Poissonian distributions having the same $\langle n \rangle$ are shown for comparison.

		$p(n)$								Q
	$n =$	0	1	2	3	4	5	6	7	
1-ion	Obs.	350	785	572	222	58	12	0	1	-0.253 ± 0.025
	Calc.	360.3	771.5	568.3	228.2	59.2	10.9	1.5	0.2	-0.243
	Poiss.	470.5	680.9	492.6	237.6	86.0	24.9	6.0	1.2	0.000
2-ion	Obs.	796	1503	1118	445	99	35	2	2	-0.194 ± 0.019
	Calc.	775.0	1558.1	1077.1	436.8	122.3	25.8	4.3	0.6	-0.198
	Poiss.	969.0	1373.8	973.9	460.2	163.1	46.3	10.9	2.2	0.000

Let $g^{(2)}(\tau)$ be the normalized intensity correlation function of the 11 μm field generated by the radiative decay from the $^2P_{1/2}$ level to the $^2D_{3/2}$ level. Reference 7 used a solution of the density-matrix equations of the four-level atomic system, valid for times long compared to the lifetime of the $^2P_{1/2}$ level, to show that

$$g^{(2)}(\tau) = 1 - C_+ e^{-\gamma_+ \tau} - C_- e^{-\gamma_- \tau}, \tag{1}$$

where

$$\gamma_\pm \equiv \frac{1}{2}\{(\gamma_0 + \gamma_1 + \gamma_2) \pm [(\gamma_0 + \gamma_1 + \gamma_2)^2 - 4f_2\gamma_0\gamma_1 - 4\gamma_1\gamma_2 - 4\gamma_0\gamma_2]^{\frac{1}{2}}\}, \tag{2}$$

$$C_\pm \equiv \pm\gamma_\mp(f_1\gamma_\pm - \gamma_2)/[\gamma_2(\gamma_+ - \gamma_-)]. \tag{3}$$

Here, γ_0 is the transition rate from the "on" to the "off" state. It depends on the intensity and frequency detuning of the 194 nm source. Since $g^{(2)}(\tau) \to 0$ as $\tau \to 0$, the 11 μm light is antibunched. The calculated and measured $g^{(2)}(\tau)$ are in good agreement [see Fig. 2(a) of Ref. 7]. Photon antibunching was also observed with two Hg^+ ions separated by about 3 μm.[7] The observed $g^{(2)}(\tau)$ was consistent with the assumption that the two ions were independent.

Given $g^{(2)}(\tau)$, we can compute the complete photon counting distribution. Let $p(m)$ be the probability that m, 11 μm photons are emitted in an interval of length T. It can be shown that

$$p(m) = \frac{1}{m!}\sum_{r=0}^{\infty}\frac{(-1)^r}{r!}\langle n^{(m+r)}\rangle, \tag{4}$$

where the rth factorial moment of n is defined for $r = 1, 2, 3\ldots$, by

$$\langle n^{(r)}\rangle \equiv \langle n(n-1)\ldots(n-r+1)\rangle \equiv \sum_{n=0}^{\infty} n(n-1)\ldots(n-r+1)p(n) \tag{5}$$

and $\langle n^{(0)}\rangle = 1$.[13] With the assumption that the ion loses memory of its previous history after each 11 μm photon emission, the factorial moments are given by

$$\langle n^{(r)}\rangle = \langle\hat{I}\rangle^r r!\int_0^T dt_r \ldots \int_0^{t_2} dt_1\, g^{(2)}(t_r - t_{r-1})\ldots g^{(2)}(t_2 - t_1), \quad r = 2, 3, \ldots,$$

$$\langle n^{(1)}\rangle = \langle n\rangle = \langle\hat{I}\rangle T, \qquad \langle n^{(0)}\rangle = 1, \tag{6}$$

where $\langle\hat{I}\rangle$ is the average number of 11 μm photons emitted per unit of time.[13] The normalized second factorial moment Q is given by Eq. (11a) of Ref. 13. This parameter measures the departure of the variance of a distribution from that of a Poissonian distribution. Negative values of Q indicate sub-Poissonian statistics.

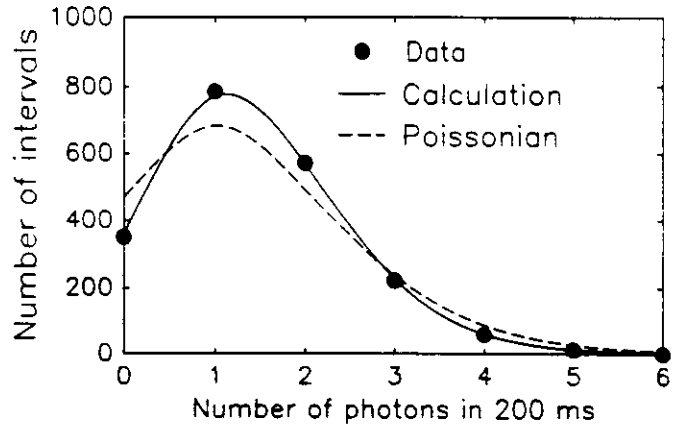

Figure 3: Observed and calculated photon count distributions. The uncertainties are less than or approximately equal to the radii of the dots. A Poissonian distribution is shown for comparison.

Observed and calculated values of $Np(n)$ and Q for one and two ions are shown in Table 1. Here, $Np(n)$ is the number of intervals in which n photons were detected, where N is the total number of intervals. For the one-ion data, $N = 2000$, $T = 200$ ms, $\gamma_0 = 12.55$ s^{-1}. For the two-ion data, $N = 4000$, $T = 100$ ms, $\gamma_0 = 12.1$ s^{-1}. The observed and calculated values are in good agreement with each other and clearly differ from the values for a Poissonian distribution. The statistical uncertainties of $Np(n)$ are approximately the square roots of the measured values. The values of Q depend on the value of T. For example, Q was measured to be -0.242 ± 0.025 for $T = 200$ ms.[7] Values of $p(n)$ were calculated by computing $\langle n^{(r)} \rangle$ for $r = 0, \ldots, 11$ from Eq. (6) and using Eq. (4). Figure 3 shows the observed and calculated values of $Np(n)$ for one ion. The dots represent the experimental data. The solid line is a smooth curve connecting the calculated values.

If the atom loses all memory after each quantum jump, then the lengths of successive intervals between jumps should show no correlation. Let $T_1, T_2, \ldots, T_n$ be the successive intervals between off-to-on or on-to-off quantum jumps. A nonrandom pattern in the scatter plot of T_n vs T_{n+1} would be an indication that the seemingly random sequence of quantum jumps was actually governed by a low-dimensional chaotic attractor. Such patterns have been observed, for example, in the time sequence of drips from a leaky faucet.[14] Plots of T_n vs T_{n+1} for both the off-to-on and the on-to-off quantum jumps are shown in Fig. 4. No nonrandom structure is apparent.

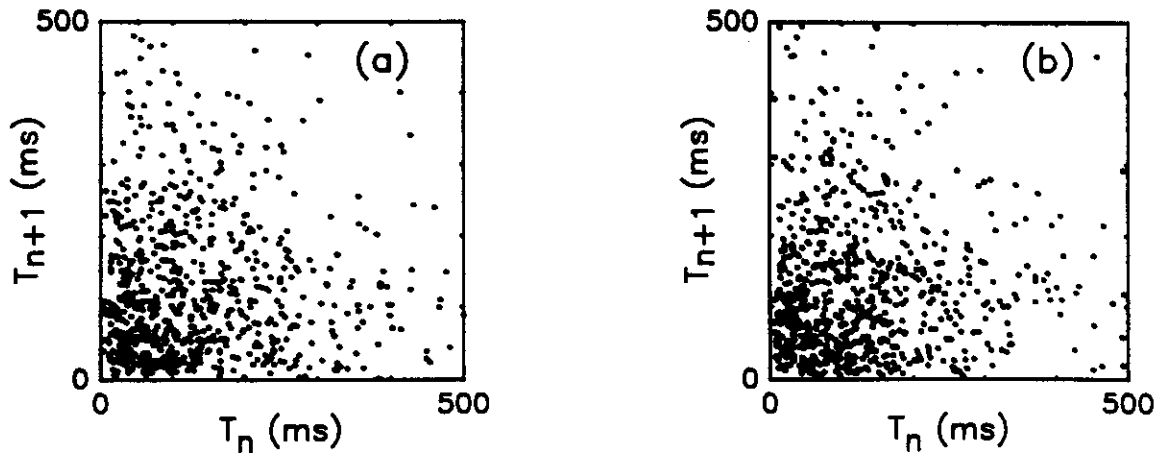

Figure 4: Scatter plot of T_{n+1} vs T_n, where T_n is the nth interval between successive (a) on-to-off quantum jumps and (b) off-to-on quantum jumps.

QUANTUM HARMONIC OSCILLATOR

The wavefunctions of a single charged particle in a Paul trap have been calculated in Refs. 15 and 16. Since the Hamiltonian is time dependent, stationary states do not exist. However, quasi-stationary states, obtained by solving for the eigenvalues of the Floquet operator, do exist. They correspond in some sense to the stationary states of the secular harmonic oscillator potential.

The absorption spectrum of a narrow optical resonance of an ion in a Paul trap consists of an unshifted carrier, surrounded by discrete motional sidebands. The sidebands are spaced by multiples and combinations of the secular frequencies. We have observed these sidebands in the absorption spectrum of the $^2S_{1/2}$-to-$^2D_{5/2}$ transition of a single trapped Hg^+ ion.[9] The carrier results from transitions in which the vibrational quasi-energy is unchanged. The upper and lower sidebands correspond to transitions which increase or decrease the quasi-energy.

Recently, we have cooled a single Hg^+ ion almost to the lowest ($n_v = 0$) vibrational quasi-energy state, by a method called sideband cooling.[8] First, the ion was Doppler cooled to about 2 mK with the $^2S_{1/2}$-to-$^2P_{1/2}$ transition, so that the mean value of n_v was about 12 at a secular frequency of 2.96 MHz. Laser radiation tuned to the first lower sideband of the narrow $^2S_{1/2}$-to-$^2D_{5/2}$ transition was then applied to the ion, lowering n_v by one for each photon absorbed. After the sideband cooling period, laser radiation of saturating intensity was applied at the lower sideband frequency. Absence of absorption, detected by optical double resonance,[9] indicated that the ion was in the $n_v = 0$ state. The ion was found to be in the ($n_v = 0$) state about 95% of the time.

Starting from the $n_v = 0$ state, other quantum harmonic oscillator states could be prepared by manipulation of the electric potentials applied to the trap. A coherent state could be prepared by quickly shifting the static potential of one endcap relative to the other, thus shifting the center of the potential well. A squeezed state could be prepared by shifting the static potential on both of the endcaps relative to the ring.

Acknowledgments

We wish to acknowledge the generous support of the Air Force Office of Scientific Research and the Office of Naval Research.

1. H. J. Kimble, M. Dagenais, and L. Mandel, Phys. Rev. Lett. **39**, 691 (1977); M. Dagenais and L. Mandel, Phys. Rev. A **18**, 2217 (1978).
2. R. Short and L. Mandel, Phys. Rev. Lett. **51**, 384 (1983).
3. W. Nagourney, J. Sandberg, and H. Dehmelt, Phys. Rev. Lett. **56**, 2797 (1986).
4. Th. Sauter, W. Neuhauser, R. Blatt, and P. E. Toschek, Phys. Rev. Lett. **57**, 1696 (1986).
5. J. C. Bergquist, R. G. Hulet, W. M. Itano, and D. J. Wineland, Phys. Rev. Lett. **57**, 1699 (1986).
6. F. Diedrich and H. Walther, Phys. Rev. Lett. **58**, 203 (1987).
7. W. M. Itano, J. C. Bergquist, and D. J. Wineland, Phys. Rev. A **38**, 559 (1988).
8. F. Diedrich, J. C. Bergquist, W. M. Itano, and D. J. Wineland, Phys. Rev. Lett. **62**, 403 (1989).
9. J. C. Bergquist, W. M. Itano, and D. J. Wineland, Phys. Rev. A **36**, 428 (1987).
10. H. Hemmati, J. C. Bergquist, and W. M. Itano, Opt. Lett. **8**, 73 (1983).
11. R. G. Hulet, D. J. Wineland, J. C. Bergquist, and W. M. Itano, Phys. Rev. A **37**, 4544 (1988).
12. W. M. Itano, J. C. Bergquist, R. G. Hulet, and D. J. Wineland, Phys. Rev. Lett. **59**, 2732 (1987).
13. L. Mandel, Opt. Lett. **4**, 205 (1979).
14. P. Martien, S. C. Pope, P. L. Scott, and R. S. Shaw, Phys. Lett. **110A**, 399 (1985).
15. R. J. Cook, D. G. Shankland, and A. L. Wells, Phys. Rev. A **31**, 564 (1985).
16. M. Combescure, Ann. Inst. Henri Poincaré **44**, 293 (1986).

4-Level Density-Matrix Equations

$$\frac{d\rho_{11}}{dt} = -\gamma_1\rho_{11} + \gamma_3\rho_{44}$$

$$\frac{d\rho_{22}}{dt} = f_2\gamma_1\rho_{11} - \gamma_2\rho_{22}$$

$$\frac{d\rho_{33}}{dt} = f_1\gamma_1\rho_{11} + \gamma_2\rho_{22} + \gamma_4\rho_{44} - i(\rho_{34} - \rho_{43})\mu E(t)/\hbar$$

$$\frac{d\rho_{44}}{dt} = -(\gamma_4 + \gamma_3)\rho_{44} + i(\rho_{34} - \rho_{43})\mu E(t)/\hbar$$

$$\frac{d\rho_{34}}{dt} = [i\omega_{43} - \tfrac{1}{2}(\gamma_3 + \gamma_4)]\rho_{34} + i(\rho_{44} - \rho_{33})\mu E(t)/\hbar$$

ω_{43} is $^2S_{1/2}$ to $^2P_{1/2}$ transition frequency,

μ is electric dipole matrix element,

$E(t) = E\cos(\omega t)$.

Effective 3-State Rate Equations

For time scales much longer than the $^2P_{1/2}$ lifetime (2 ns), the system can be described by 3 population variables:

$$P_1 \equiv \rho_{11}, \quad P_2 \equiv \rho_{22}, \quad \text{and} \quad P_0 \equiv \rho_{33} + \rho_{44}.$$

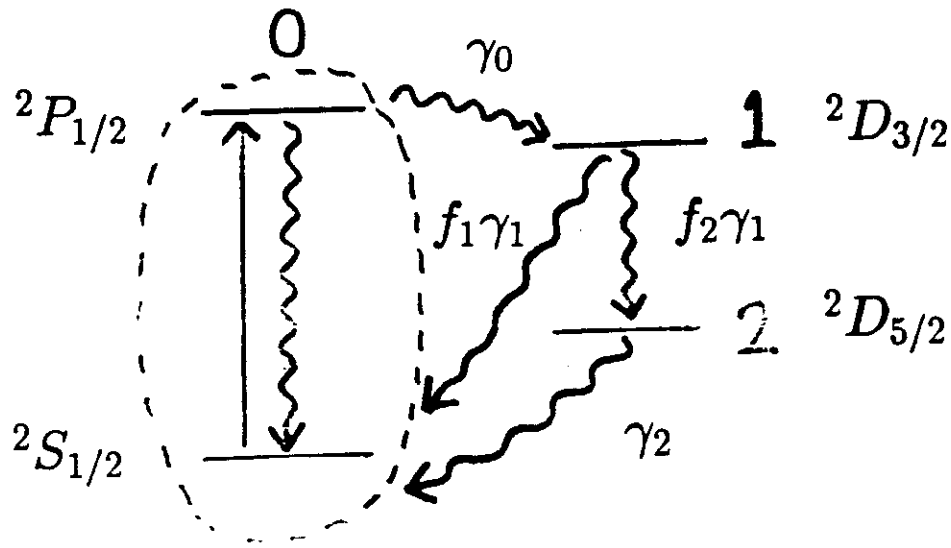

$$\frac{dP_1}{dt} = -\gamma_1 P_1 + \gamma_0 P_0$$

$$\frac{dP_2}{dt} = f_2\gamma_1 P_1 - \gamma_2 P_2$$

$$\frac{dP_0}{dt} = f_1\gamma_1 P_1 + \gamma_2 P_2 - \gamma_0 P_0$$

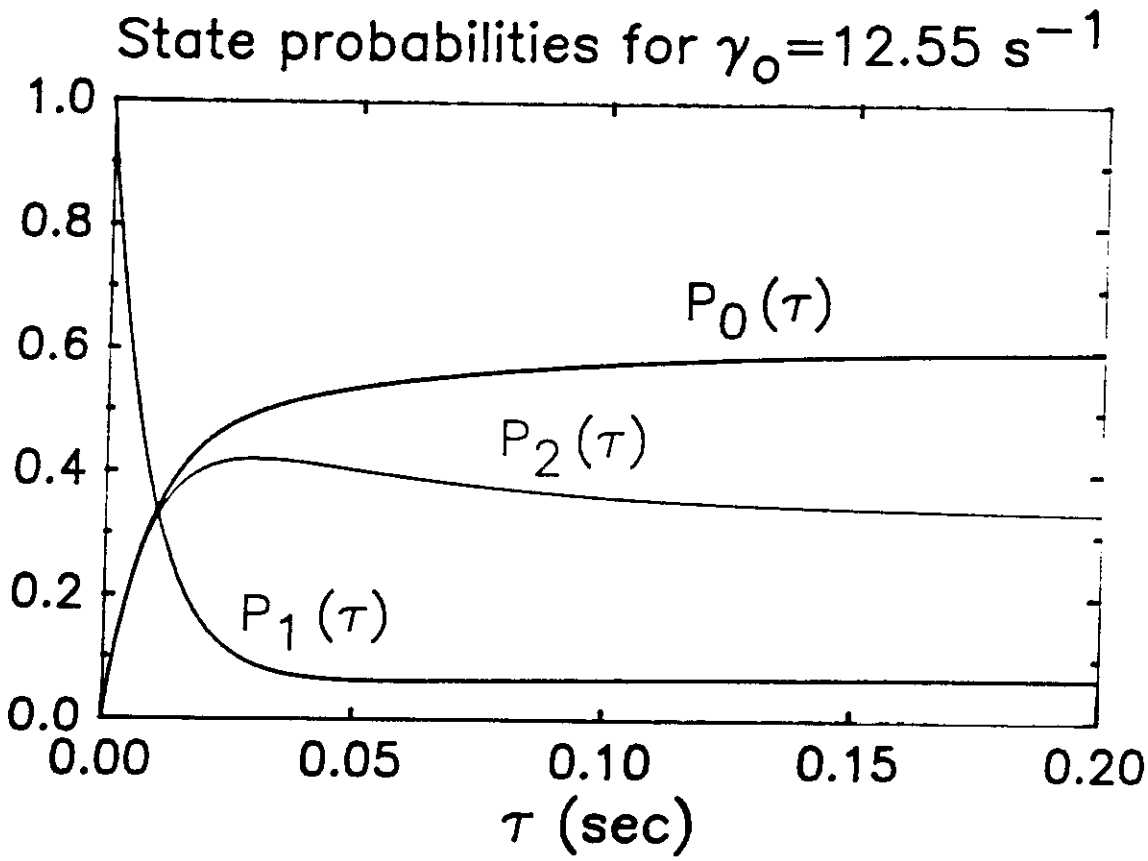
State probabilities for γ_o=12.55 s^{-1}
1.0
0.8
0.6
0.4
0.2
0.0
$P_0(\tau)$
$P_2(\tau)$
$P_1(\tau)$
0.00
0.05
0.10
0.15
0.20
τ (sec)

Calculation of $g^{(2)}(\tau)$ for 1 Ion

$g^{(2)}(\tau)$ = intens. correl. function of 11 μm field.
11 μm photons emitted at rate $\gamma_0 P_0$.
$g^{(2)}(\tau) \propto P_0(\tau)$.

For initial conditions at $\tau = 0$:

$$P_0 = 0, \quad P_1 = 1, \quad P_2 = 0.$$

(i.e., at $\tau = 0$, the ion is in the $^2D_{3/2}$ state.)

Solution:

$$g^{(2)}(\tau) = 1 - C_+ e^{-\gamma_+ \tau} - C_- e^{-\gamma_- \tau},$$

$\{C_+, C_-, \gamma_+, \gamma_-\}$ depend on $\{\gamma_0, \gamma_1, \gamma_2, f_1, f_2\}$.

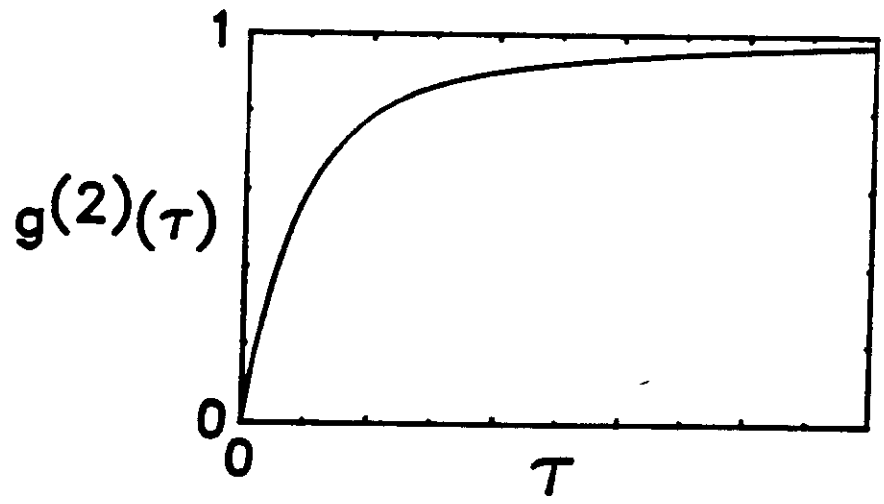

$$g^{(2)}(\tau) \longrightarrow 0 \text{ as } \tau \longrightarrow 0$$

(photon antibunching)

WHAT IS PHOTON ANTIBUNCHING?

Define the intensity correlation function $C(\tau)$ to be:

$$C(\tau) = \langle I(t)I(t+\tau)\rangle,$$

and the normalized intensity correlation function to be:

$$g^{(2)}(\tau) = \frac{C(\tau)}{\langle I(t)\rangle^2} = \frac{\langle I(t)I(t+\tau)\rangle}{\langle I(t)\rangle^2}.$$

Examples:

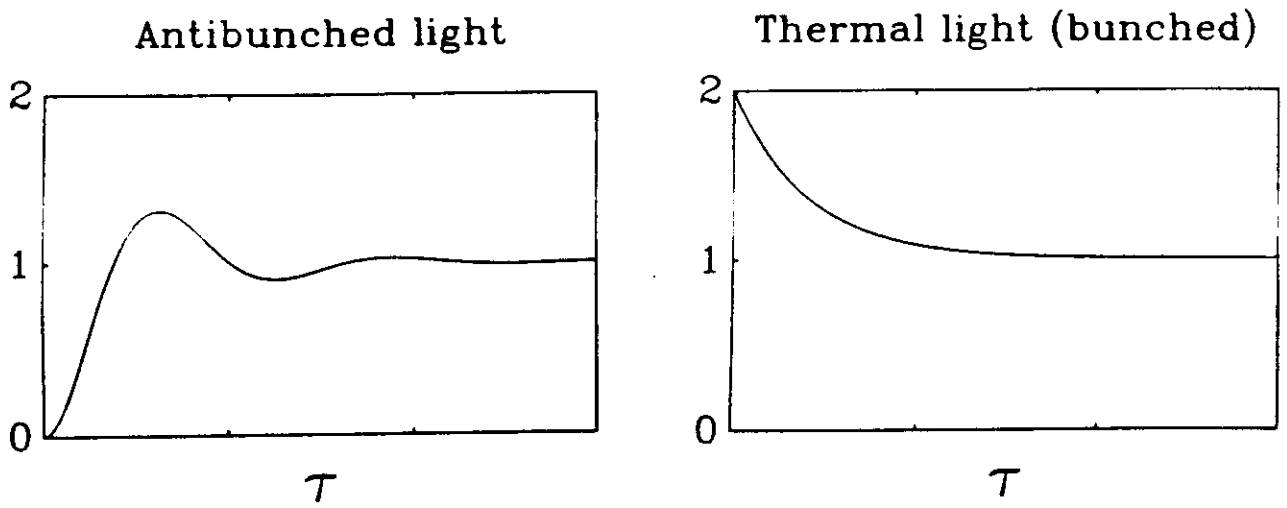

For antibunched light, $g^{(2)}(0) < 1$. The photons tend to avoid each other. For thermal (chaotic) light, $g^{(2)}(0) > 1$ (photon bunching).

A CLASSICAL FIELD CANNOT BE ANTIBUNCHED

Consider an arbitrary, stationary, classical $I(t)$:

$$I(t) = I_o + \Delta I(t),$$

where $I_o \equiv \langle I(t) \rangle$ and $\langle \Delta I(t) \rangle = 0$.

Intensity correlation function:

$$C(\tau) = \langle I(t) I(t+\tau) \rangle$$

$$\begin{aligned} C(\infty) &= \langle I(t) \rangle^2 \\ &= (I_o)^2 \end{aligned}$$

$$\begin{aligned} C(0) &= \langle I(t)^2 \rangle \\ &= \langle (I_o + \Delta I(t))^2 \rangle \\ &= \langle (I_o)^2 + \underbrace{2\Delta I(t)\ I_o}_{=0} + (\Delta I(t))^2 \rangle \\ &= (I_o)^2 + \underbrace{\langle (\Delta I(t))^2 \rangle}_{\geq 0} \end{aligned}$$

Therefore,

$$C(0) \geq C(\infty)$$

Calculation of Photon Count Distribution $P(m)$

$P(m)$ = prob. m photons detected in time T.
It can be shown that

$$P(m) = \frac{1}{m!} \sum_{r=0}^{\infty} \frac{(-1)^r}{r!} \langle n^{(m+r)} \rangle,$$

where the $\langle n^{(r)} \rangle$ defined by:

$$\begin{aligned} \langle n^{(0)} \rangle &= 1 \\ \langle n^{(1)} \rangle &= \langle n \rangle \\ \langle n^{(2)} \rangle &= \langle n(n-1) \rangle \\ \langle n^{(3)} \rangle &= \langle n(n-1)(n-2) \rangle \\ &\vdots \end{aligned}$$

and $\langle n^{(r)} \rangle$ is given by the r-fold integral:

$$\langle n^{(r)} \rangle = \langle \hat{I} \rangle^r r! \int_0^T dt_r \ldots \int_0^{t_2} dt_1 \, g^{(2)}(t_r - t_{r-1}) \ldots g^{(2)}(t_2 - t_1),$$

where $\langle \hat{I} \rangle$ = avg. # photons/sec.

Calculation of Q

The Poissonian distribution is:

$$P_{Poiss}(m, \langle n \rangle) \equiv \frac{\langle n \rangle^m}{m!} e^{-\langle n \rangle}$$

Q measures the deviation from Poissonian statistics:

$$Q \equiv \frac{\langle (\Delta n)^2 \rangle - \langle n \rangle}{\langle n \rangle} = \frac{\langle n^{(2)} \rangle - \langle n \rangle^2}{\langle n \rangle}$$

$$Q = \frac{2\langle \hat{I} \rangle}{T} \left\{ \int_0^T dt_2 \int_0^{t_2} dt_1 [g^{(2)}(t_1) - 1] \right\}$$

$$= -2\langle \hat{I} \rangle \left\{ \frac{C_+}{\gamma_+} \left[1 - \frac{1 - e^{-\gamma_+ T}}{\gamma_+ T} \right] + \frac{C_-}{\gamma_-} \left[1 - \frac{1 - e^{-\gamma_- T}}{\gamma_- T} \right] \right\}$$

Laser Cooling to the Zero-Point Energy of Motion

F. Diedrich,[a] J. C. Bergquist, Wayne M. Itano, and D. J. Wineland
Time and Frequency Division, National Institute of Standards and Technology, Boulder, Colorado 80303
(Received 28 July 1988)

A single trapped $^{198}Hg^+$ ion was cooled by scattering laser radiation that was tuned to the resolved lower motional sideband of the narrow $^2S_{1/2}$-$^2D_{5/2}$ transition. The different absorption strengths on the upper and lower sidebands after cooling indicated that the ion was in the ground state of its confining well approximately 95% of the time.

PACS numbers: 32.80.Pj, 32.30.Jc, 35.10.−d

The subject of laser cooling of ions and neutral atoms is currently of great experimental and theoretical interest.[1] It has been applied to high-resolution spectroscopy, low-energy collisions, quantum jumps, and photon antibunching.[2] In all cooling experiments done so far, the oscillation frequency ω_r of the particle in its confining well was less than the linewidth Γ of the cooling transition. This condition also applies to free-atom experiments, where $\omega_r \to 0$. The lowest temperatures T have been obtained in recent free-atom experiments,[3,4] where kinetic energies near or below that corresponding to the recoil of a single photon from an atom at rest have been achieved ($T \approx 1$ μK). In this Letter we report, for the first time, laser cooling of a single bound atom in the resolved sideband regime $\Gamma \ll \omega_r$. An ion has been cooled so that it occupies the ground state of its confining potential most of the time.

The idea of laser cooling in the resolved sideband regime is as follows[5]: Let the rest frequency of the atom's cooling transition be ω_0. If the atom oscillates at frequency ω_r in its confining well, the atom's absorption and emission spectrum (as viewed in the laboratory) has resolved components at ω_0 and $\omega_0 \pm m\omega_r$ (m an integer). If we irradiate the atom with narrow-band radiation tuned to the first lower sideband at $\omega_0 - \omega_r$, the atom absorbs photons of frequency $\hbar(\omega_0 - \omega_r)$ and reemits photons of average energy $\hbar\omega_0$. Hence, on the average, each scattered photon reduces the atom's vibrational energy by $\hbar\omega_r$, or reduces the atom's vibrational quantum number n_r by 1. In this way, we can obtain $\langle n_r \rangle \ll 1$ and have the atom most of its time in the ground-state level of its confining potential.[6–8] When $\langle n_r \rangle \ll 1$, T is no longer proportional to $\langle n_r \rangle$ but depends logarithmically[7,8] on $\langle n_r \rangle$. The technique of sideband cooling has previously been applied to cool the magnetron motion of trapped electrons with an rf electronic excitation of the axial motion that was coupled to a cooled resistor.[9] The final temperature in this experiment was limited by thermal excitation and the energy of the magnetron motion corresponded to $\langle n_r \rangle \gg 1$. In the experiments described here, we achieve $\langle n_r \rangle \ll 1$ by optical sideband cooling. For our value of ω_r, T was about 50 μK. However, to the extent that the particle is in the ground state of its confining potential (about 95% of the time here) the fundamental limit of laser cooling for a confined particle has been reached.

Our experiments were performed with a single $^{198}Hg^+$ ion stored in a Paul (rf) trap[10,11] which had $\omega_r/2\pi = 2.96$ MHz (see Fig. 1). In order to optimize the cooling, a two-stage process[8] was used. First, the ion was cooled to near the Doppler cooling limit[1] ($T = \hbar\Gamma/2k_B$, where k_B is the Boltzmann constant) by scattering light of wavelength 194 nm on the strong $^2S_{1/2}$-$^2P_{1/2}$ transition [(A) in Fig. 1(a)].[12] At the Doppler cooling limit, $\langle n_r \rangle \approx 12$ ($T = 1.7$ mK) for each degree of freedom.[8] In the next stage of cooling, the 194-nm radiation was turned off and the narrow $^2S_{1/2}$-$^2D_{5/2}$ electric quadrupole transition [(B) in Fig. 1 (a)] was driven on the first lower sideband frequency $\omega_0 - \omega_r$. Since the natural lifetime of the $^2D_{5/2}$ state limits the maximum scatter rate to approximately $\frac{1}{2}\Gamma(^2D_{5/2}) \approx 6$ photons/s,[10,13] a cooling time of at least 6 s is required to reach $\langle n_r \rangle = 0$ for all degrees of freedom. This time becomes even longer, or cooling is prevented, if external heating is present. Therefore, in order to enhance the sideband cooling rate, the lifetime of the $^2D_{5/2}$ state was shortened by coupling it to the fast decaying $^2P_{3/2}$ state by 398-nm radiation [(C) in Fig. 1(a)]. From the $^2P_{3/2}$ state, the ion has high probability

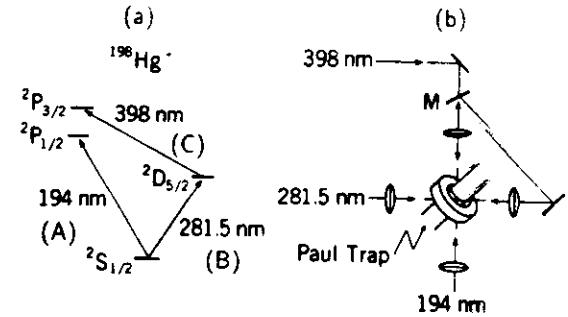

FIG. 1. (a) A simplified energy level scheme of Hg II showing the optical transitions involved in our sideband cooling experiment. (b) The geometrical arrangement of the laser beams. The 194-nm fluorescence is detected normal to the plane of the figure. Mirror M reflects 194-nm radiation while transmitting 398-nm radiation.

of rapidly decaying to the ground state. When $\langle n_r \rangle \ll 1$, a quantitative measurement of $\langle n_r \rangle$ from the absorption spectrum becomes very simple. The strength of absorption S_L on the lower sideband is proportional to $\langle n_r \rangle$, while the strength S_U of the upper sideband is proportional to $\langle n_r \rangle + 1$.[8] When $\langle n_r \rangle$ approaches zero, the lower sideband disappears because no more vibrational quanta can be extracted from the ion. If the sideband absorption spectrum is probed with saturating power, the ratio of the strengths of lower to upper sidebands becomes independent of power[14] and directly gives $\langle n_r \rangle$.

To simplify our discussion, we have assumed the trap states and associated wave functions are those of a harmonic potential which is equal to the classical pseudopotential of the rf trap. In the quantum treatment of the rf trap,[15,16] the relevant states are not energy eigenstates because of the time dependence of the potential. However, when the trap drive frequency $\Omega \gg \omega_r$, the atom's optical spectrum and transition matrix elements relevant for cooling closely approximate those for a harmonic potential equal to the classical pseudopotential. The states which represent the cooled ion look like harmonic-oscillator states whose dimensions oscillate with small amplitude at frequency Ω. These states are of the form $\exp[-i\omega_r(n+\frac{1}{2})t]f_n(x,t)$ where the f_n are periodic in time with period $2\pi/\Omega$.[16]

Our trap[10,11] ($r_0 \simeq 466$ μm, $z_0 \simeq 330$ μm) was operated at a trapping field frequency $\Omega/2\pi = 23.189$ MHz. With an rf peak voltage amplitude $V_0 \approx 1.2$ kV and a static potential $U_0 = +71.4$ V applied to the ring electrode, the trap potential was approximately spherical. In order to cool all motional degrees of freedom to near the Doppler cooling limit for the (A) transition, two orthogonal beams of 194-nm radiation, both at an angle of 55° with respect to the trap symmetry (z) axis, were used (Fig. 1). The radiation to drive the (B) transition was derived from a frequency stabilized dye laser ($\lambda = 563$ nm) with a linewidth less than 20 kHz. The output radiation from this narrow-band laser was frequency doubled and focused to as much as 25 W/cm^2 at the position of the ion; this allows strong saturation on the cooling transition. The radiation to drive the (C) transition was derived from a frequency stabilized LD 700 dye laser whose output radiation was frequency doubled and focused to give approximately 1 mW/cm^2 at the position of the ion.

Before the sideband cooling experiment was started, an absorption spectrum of the (B) transition was taken[17] to determine the carrier frequency as well as the sideband frequencies (inset Fig. 2). We made sure that the 282-nm source had equal power at both the upper and lower sideband frequencies. For the sideband cooling and the probing of the absorption spectrum, the following computer-controlled sequence was run repeatedly. First, the 398- and 194-nm radiation were turned on simultaneously for a 20-ms interrogation period. If the 194-nm fluorescence exceeded a preset value during this

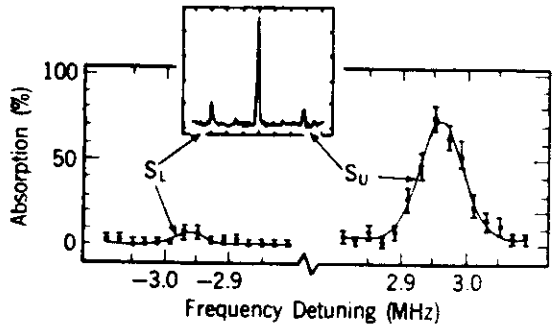

FIG. 2. Absorption spectrum of the $^2S_{1/2}$-$^2D_{5/2}$ electric quadruple transition of $^{198}Hg^+$. The inset spectrum was taken before sideband cooling was applied. It shows the carrier at zero detuning (frequency ω_0) and the first sidebands (at frequencies $\omega_0 - \omega_r$ and $\omega_0 + \omega_r$) generated by the ion's motion in the approximately spherical well. For this spectrum, the bandwidth of the 282-nm radiation was broadened to 120 kHz to reduce the number of required data points and the laser power was reduced in order to avoid saturation. The enlarged part of the figure shows the absorption strength S_L (S_U) on the lower (upper) motional sideband 15 ms after the end of the sideband cooling. Values for S_L and S_U were obtained from Gaussian fits to the data points which are averaged over 41 sweeps.

period, it could be assumed that the ion was laser cooled and cycling between the $^2S_{1/2}$ and the $^2P_{1/2}$ states. This 20-ms interrogation period was repeated until this condition was satisfied. Then the 194-nm radiation was switched off and the 282-nm radiation, tuned to the first lower sideband at $\omega_0 - \omega_r$, was switched on for a cooling time τ_c (typically 200–500 ms). After the 282-nm radiation was switched off, the 398-nm radiation was kept on for a relaxation time τ_r (typically 5 ms) in order to empty the $^2D_{5/2}$ state. After this, the cooled ion was in the electronic ground state and the probing of the absorption spectrum was done as follows: The 282-nm source was switched on at saturating intensity for 10 ms at a frequency corresponding to one point near the upper or lower sideband frequency. After this, the 282-nm beam was switched off and the 194-nm radiation was switched on to see if the ion had made the transition to the $^2D_{5/2}$ state.[11] The result was averaged with the results of previous measurements at the same probe frequency. The frequency of the 282-nm source was stepped to the next value and the cooling and probing cycle was repeated until about 40 cycles for each value of the probe frequency were completed. The results of a typical run are shown in Fig. 2.

In order to deduce $\langle n_r \rangle$ for the different motional degrees of freedom, the geometry of our experiment (Fig. 1) has to be considered. The 282-nm beam enters the trap at an angle of 55° with respect to the z axis. The x and y directions were previously determined by the fixed spatial alignment of two simultaneously stored ions,[17] which we take to be along the x axis. From these data, the squares of the projections p_i of unit vectors along the

trap axes onto the 282-nm beam axis are calculated to be $p_x^2=0.03$, $p_y^2=0.64$, and $p_z^2=0.33$. Since we make the differences between the x, y, and z frequencies bigger than $1/\tau_c$, all directions are cooled simultaneously.[8] However, in the analysis, we assume that the probing absorption strength is due only to the ion's motion in the y and z directions. Since the x axis is nearly perpendicular to the 282-nm beam, no meaningful statement abut the energy in this degree of freedom can be made. By neglecting the contribution of the x motion to the sideband strength we overestimate $\langle n_v\rangle$ for the y and z directions. In order to deduce $\langle n_v\rangle$ for the y and z oscillations from our data (Fig. 2), an assumption about the energy distribution between the two directions has to be made. If we assume temperature equilibrium between the y and z degrees of freedom, both contain an energy corresponding to $\langle n_v\rangle=(1-S_L/S_U)^{-1/2}-1=0.051\pm0.012$ quanta. Therefore, for the y and z degrees of freedom, the ion is in the $n_v=0$ state 95% of the time. The corresponding temperature given by[8] $k_BT=\hbar\omega_v/\ln(1+1/\langle n_v\rangle)$ is $T=47\pm3$ μK. For any other energy partition, $\langle n_v\rangle$ and T for one degree of freedom would be less than these values. Independent of the energy distribution, for both degrees of freedom the temperature is much lower than the 194-nm Doppler cooling limit and the ion spends most of its time in the harmonic-oscillator ground-state level.

The theoretical sideband cooling limit[8] gives a value of $\langle n_v\rangle\approx10^{-6}$. However, since the probing in the experiment is done at saturating power, the measured $\langle n_v\rangle$ corresponds to the energy of the ion at the end of the probing interval, which is typically 15 ms after the end of the sideband cooling, and external heating might have occurred. In order to check for external heating processes, we extended τ_r up to 100 ms and measured S_L/S_U as a function of τ_r. We determined a heating rate (due apparently to pickup of stray noise fields at radio frequencies) of $\langle\dot{n}_v\rangle\approx6$/s. If we assume the heating is due to thermalization of the ion to room temperature by noise at frequency ω_v, the heating time constant is 95 h.[18] This rate varied slightly with ω_v around $\omega_v=3$ MHz, but was substantially higher for $\omega_v\lesssim2.5$ MHz. From these heating data, the measured $\langle n_v\rangle$ is consistent with the theoretical limit at the end of the sideband cooling period. We also measured $\langle n_v\rangle$ for a single degree of freedom directly by changing U_0 to -25 V in order to split the radial and axial sideband frequencies. The 282-nm radiation was tuned so that only the first axial sideband at $\omega_v/2\pi=4.66$ MHz was cooled and probed. From the results, shown in Fig. 3, we calculate $\langle n_v\rangle=0.049\pm0.045$ at the end of the cooling period, consistent with the theoretical cooling limit. The confinement of the axial motion is given by the spread of the zero-point wave function $z(\text{rms})\approx2.4$ nm.

For our data, the uncertainty in the second-order Doppler shift is dominated by the uncertainty in $\langle n_v\rangle$ and

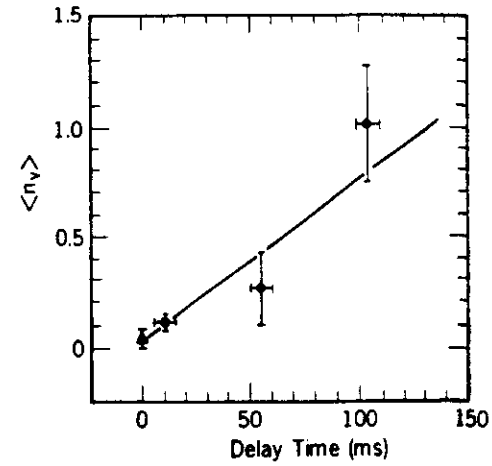

FIG. 3. Vibrational quantum number $\langle n_v\rangle$ for the axial motion ($\omega_v/2\pi=4.66$ MHz) as a function of time delay between the end of the sideband cooling and probing. A linear extrapolation of the data points (circles) to zero delay time yields $\langle n_v\rangle$ (triangle) consistent with the theoretical expectation.

amounts to $\Delta\nu/\nu<10^{-20}$ (Ref. 8). It can be made substantially lower by adiabatically lowering the potential well depth after the ion is cooled into the ground state. With our experiment, the absorption of a single quantum of energy at a (tunable) frequency in the MHz range can be detected with an efficiency of nearly 100%. With appropriate coupling to the ion's motion (for example, via one of the endcaps), a similar apparatus could serve as a very sensitive spectrum analyzer. In another possible application, the motion of a trapped charged particle could be damped by coupling it electronically[19] to a second laser-cooled ion in a separate trap, thereby reducing the first charged particle's kinetic energy to near the zero-point energy. Resonant excitation of the first particle's motion could then be detected very sensitively by its influence on the laser-cooled ion. Such a device might be useful in mass spectroscopy.

In summary, we have realized laser cooling in the resolved sideband regime for the first time. The kinetic energy of a trapped atomic ion was reduced to a value where it spent most of its time in the ground-state level of its confining well. To the extent that the ion is in the zero-point energy state of motion, this realizes for the first time the fundamental limit of laser cooling for a bound particle and the ideal of an isolated atomic particle at rest to within the quantum-mechanical limits imposed by the surrounding apparatus.

We acknowledge the support of the U.S. Air Force Office of Scientific Research and the U.S. Office of Naval Research. F. D. thanks the Deutsche Forschungsgemeinschaft for financial support. We thank C. Wieman, J. Bollinger, and J. Helffrich for comments and suggestions on the manuscript. We thank R. Cook and R.

Blümel for helpful discussions on the quantum-mechanical Paul trap.

---

[a]Present address: Max-Planck-Institut für Quantenoptik, Garching, West Germany.

[1]See, for example, S. Stenholm, Rev. Mod. Phys. **58**, 699 (1986); D. J. Wineland and W. M. Itano, Phys. Today **40**, No. 6, 34 (1987), and references therein.

[2]See, for example, *Laser Spectroscopy VII*, edited by T. W. Haench and Y. R. Shen, Springer Series in Optical Sciences Vol. 49 (Springer-Verlag, Berlin, 1987); "Atomic Physics 11," edited by S. Haroche, J. C. Gay, and G. Gynberg (World Scientific, Singapore, to be published).

[3]P. D. Lett, R. N. Watts, C. I. Westbrook, W. D. Phillips, P. L. Gould, and H. J. Metcalf, Phys. Rev. Lett. **61**, 169 (1988).

[4]A. Aspect, E. Arimondo, R. Kaiser, N. Vansteenkiste, and C. Cohen-Tannoudji, Phys. Rev. Lett. **61**, 826 (1988).

[5]D. J. Wineland and H. Dehmelt, Bull. Am. Phys. Soc. **20**, 637 (1975).

[6]W. Neuhauser, M. Hohenstatt, P. Toschek, and H. Dehmelt, Phys. Rev. Lett. **41**, 233 (1978).

[7]D. J. Wineland and W. M. Itano, Phys. Rev. A **20**, 1521 (1979).

[8]D. J. Wineland, W. M. Itano, J. C. Bergquist, and R. G. Hulet, Phys. Rev. A **36**, 2220 (1987).

[9]R. S. Van Dyck, Jr., P. B. Schwinberg, and H. G. Dehmelt, in *New Frontiers in High-Energy Physics*, edited by B. M. Kursunoglu, A. Perlmutter, and L. F. Scott (Plenum, New York, 1978), p. 159.

[10]J. C. Bergquist, D. J. Wineland, W. M. Itano, H. Hemmati, H. U. Daniel, and G. Leuchs, Phys. Rev. Lett. **55**, 1567 (1985).

[11]J. C. Bergquist, W. M. Itano, and D. J. Wineland, Phys. Rev. A **36**, 428 (1987).

[12]H. Hemmati, J. C. Bergquist, and W. M. Itano, Opt. Lett. **8**, 73 (1983).

[13]W. M. Itano, J. C. Bergquist, R. G. Hulet, and D. J. Wineland, Phys. Rev. Lett. **59**, 2732 (1987).

[14]Ref. 8 is in error on this effect of saturation.

[15]R. J. Cook, D. G. Shankland, and A. L. Wells, Phys. Rev. A **31**, 564 (1985).

[16]M. Combescure, Ann. Inst. Henri Poincaré **44**, 293 (1986).

[17]D. J. Wineland, J. C. Bergquist, W. M. Itano, J. J. Bollinger, and C. H. Manney, Phys. Rev. Lett. **59**, 2935 (1987).

[18]The quantity actually measured is the probability, after a time τ_r, of finding the ion in a state with quantum number n_r, where $1 \leq n_r \leq n^* \simeq 10^4$. Strong, discontinuous heating, such as collisions with neutral atoms, would result in $n_r \gg 1$ after each heating event. Hence, a measurement of S_L/S_U vs τ_r would yield a heating rate lower than the actual one. In contrast, a continuous heating process, such as rf noise, would cause $\langle n_r \rangle$ to increase smoothly with time, and the analysis should be valid.

[19]D. J. Wineland and H. G. Dehmelt, J. Appl. Phys. **46**, 919 (1975).

Published in Proc. Workshop on Crystalline Ion Beams,
edited by R. W. Hasse, I. Hofmann, D. Liesen,
GSI Darmstadt, 1989

Coulomb Clusters of Ions in a Paul Trap*

Wayne M. Itano J. C. Bergquist D. J. Wineland

Time and Frequency Division
National Institute of Standards and Technology
(formerly National Bureau of Standards)
Boulder, Colorado 80303, U.S.A.

Abstract

Ordered structures of as many as 16 laser-cooled Hg^+ ions, confined in a Paul trap, have been observed. These structures, called Coulomb clusters, match those calculated by minimizing the effective potential energy of the system. The $5d^{10}6s\ ^2S_{1/2}$ to $5d^9 6s^2\ ^2D_{5/2}$ transition in Hg^+ has been observed by optical-optical double resonance. The resolution was high enough that Doppler-induced sidebands, due to the harmonic motion of a single ion in the trap, were clearly resolved. Additional sidebands, due to the relative vibration of two ions forming a pseudomolecule, have also been observed.

I. Introduction

A group of a few ions in a Paul (radiofrequency) trap is a system that can be modelled with simple calculations, but which still exhibits phenomena, such as spatial ordering and phase transitions, which are associated with condensed matter. Stimulated in part by recent theoretical predictions that systems of laser-cooled ions would form spatially ordered structures,[1–5] several experimental groups have produced and studied such structures.[6–11]

We have created systems of a few Hg^+ ions, which we call Coulomb clusters, in which the positions of the ions are approximately fixed relative to each other. These relative positions are determined by a balance between the confining forces of the trap and the mutual Coulomb repulsion of the ions. We have also observed a modification of the optical absorption spectrum of the ions by the harmonic vibration of two ions relative to each other. This vibration is an indication that the ions have formed a spatially ordered state. Direct evidence of spatial ordering has been obtained by two-dimensional imaging of the laser-induced fluorescence from the ions. Images of up to 16 ions have been recorded and compared with calculations. These clusters are a novel form of matter, in which the spacing between atoms is larger by about three orders of magnitude than in an ordinary crystal or molecule. Observations of similar structures of ions in a Penning trap have been made recently.[12] Those structures

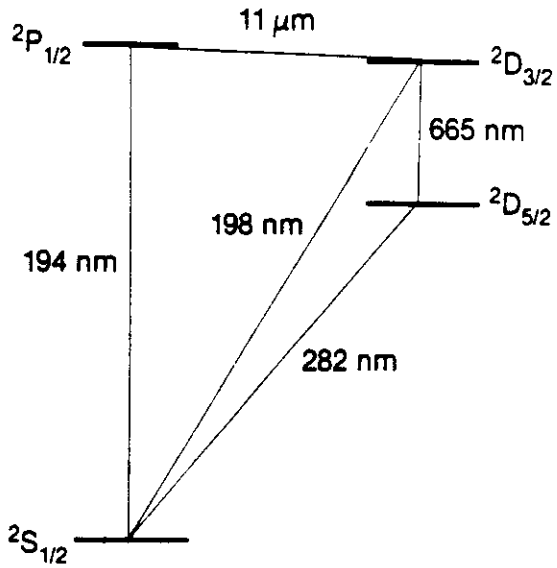

Figure 1: The lowest energy levels of Hg^+.

contained more ions than those described here (as many as 15 000). However, individual ions were not resolved in the Penning trap, as they were in the Paul trap. The smallest clusters studied in the Penning trap had about 20 ions, so that the two experiments taken together cover a range of ion numbers from one to 15 000. We have also observed Coulomb clusters of charged particles with diameters of several micrometers in a large Paul trap. Such clusters of mascroscopic particles are more easily produced and observed than ion clusters. However, the charge-to-mass ratio cannot be made as uniform as for ions. In Thomson's model of the atom, the potential energy function for the electrons was essentially the same as for the ions in a Paul trap. As a result, some of the cluster shapes that we observe are the same as those Thomson calculated for atomic electrons. Preliminary reports of this work have appeared elsewhere.[7,10]

II. Hg^+ levels

The lowest energy states of the mercury ion are shown in Fig. 1. The ground state is $^2S_{1/2}$, as in an alkali atom. The strong $^2S_{1/2}$ to $^2P_{1/2}$ electric dipole transition at 194 nm is used for the laser cooling and fluorescence detection. The lifetime of the $^2P_{1/2}$ state is about 2 ns. Usually, it decays directly back to the ground $^2S_{1/2}$ state. About once in 10^7 times, it decays instead to the metastable $^2D_{3/2}$ state, which has a lifetime of about 9 ms. If this happens the 194 nm fluorescence abruptly turns off. The $^2D_{3/2}$ state decays about half the time directly to the ground state and the rest of the time to the metastable $^2D_{5/2}$ state, which has a lifetime of about 86 ms. After the decay to the ground state the fluorescence turns on again. Thus, the 194 nm fluorescence from a single ion is bistable and switches randomly between zero and a steady level. The statistical properties of this bistable signal

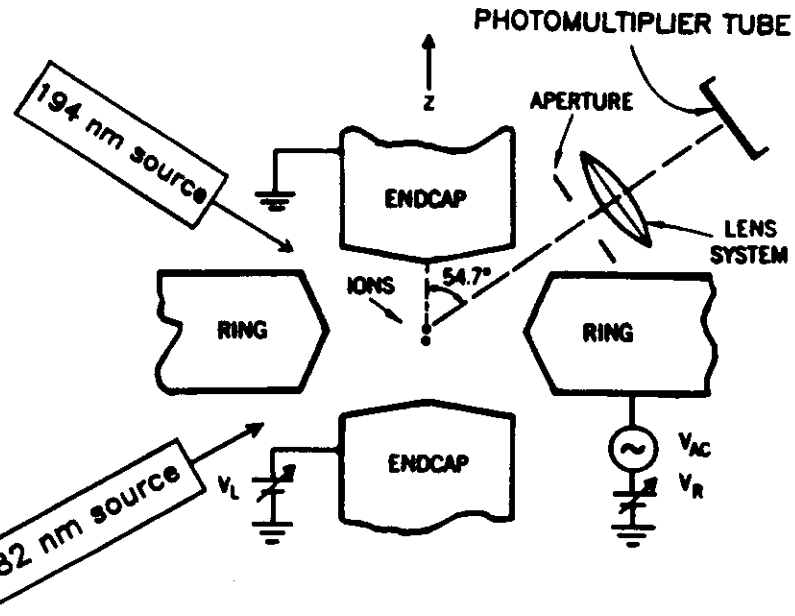

Figure 2: Schematic view of the apparatus. The separation between the endcap electrodes is approximately 625 μm. The inner diameter of the ring electrode is approximately 890 μm.

have been used to measure the decay rates of the metastable states.[13]

III. Apparatus

The experimental apparatus is shown schematically in Fig. 2. The electrodes of the Paul trap are shown in cross section. Radiofrequency and static voltages are applied between the electrodes to control the effective potential well for the ions. The 194 nm laser beam passes along a diagonal between the electrodes. The 194 nm source is required both for detecting the ions and for cooling them (by resonant radiation pressure). The 194 nm fluorescence is detected along another diagonal. For some experiments, the 194 nm detector is a photomultiplier tube. In other cases, a resistive-anode photomultiplier tube that provides two-dimensional positional information from single photoelectrons is used. For optical-optical double resonance experiments, 282 nm light from a frequency-doubled dye laser is focused on the ions.

A. Paul trap

The electric potential inside an ideal Paul trap is given by the expression,

$$\phi(x,y,z) = \frac{U_0 + V_0\cos(\Omega t)}{A^2}(x^2 + y^2 - 2z^2). \tag{1}$$

The potential V applied between the ring electrode and the two endcap electrodes is the sum of a static and a radiofrequency part: $V = U_0 + V_0\cos(\Omega t)$. The parameter A depends

on the geometry of the trap electrodes and has the dimensions of area. The radiofrequency voltage V_0 gives rise to an effective potential which confines in all directions. This potential is four times as strong in the axial (z) direction as in the radial (r) direction. The ratio of the axial to radial confining force can be changed by varying the static voltage U_0. The effective potential energy which governs the average motion, called the secular motion, is

$$q\phi_{\rm eff}(x,y,z) = \left(\frac{q^2V_0^2}{m\Omega^2A^4}+\frac{qU_0}{A^2}\right)(x^2+y^2)+\left(\frac{4q^2V_0^2}{m\Omega^2A^4}-\frac{2qU_0}{A^2}\right)z^2 \quad (2)$$

$$= \frac{m\omega_r^2}{2}(x^2+y^2)+\frac{m\omega_z^2}{2}z^2. \quad (3)$$

We call the harmonic frequencies for the secular motion along the axial and radial directions ω_z and ω_r. The ion also oscillates at the frequency Ω of the applied field. This motion is called the micromotion. Under normal operating conditions, Ω is much greater than ω_z or ω_r. If there is a slight deviation from axial symmetry, we can describe the effective potential in terms of secular frequencies ω_x and ω_y, provided that we align the coordinate axes along the principal axes of the potential. The effective potential is

$$q\phi_{\rm eff}(x,y,z) = \frac{m\omega_x^2}{2}x^2+\frac{m\omega_y^2}{2}y^2+\frac{m\omega_z^2}{2}z^2, \quad (4)$$

where $\omega_x \approx \omega_y$.

The trap used in these experiments has been described previously.[14] The electrodes were made of molybdenum. The design of the electrodes, which were machined with simple straight cuts, has been discussed in detail elsewhere.[15] The inside diameter of the ring electrode was less than 1 mm. This allowed very strong electric field gradients to be applied. The maximum value of V_0 was about 1 kV. The frequency $\Omega/2\pi$ was about 23 MHz. The ions were created inside the trap by electron impact ionization of isotopically purified ^{198}Hg.

B. Lasers

The cw, tunable 194 nm source has been described previously.[16] Radiation at 257 nm was generated by frequency doubling the output of a 515 nm single-mode cw argon ion laser in an ammonium dihydrogen phosphate crystal. This radiation was mixed with the output of a 792 nm cw dye laser in a potassium pentaborate crystal to generate the sum frequency at 194 nm. The efficiencies of the frequency doubling and mixing processes were enhanced by using ring buildup cavities to increase the powers of the input beams circulating through the crystals. About 5 μW were generated at 194 nm. The bandwidth was about 2 MHz.

The narrowband 282 nm source was obtained from a dye laser that was frequency doubled in a deuterated ammonium dihydrogen phosphate crystal. The bandwidth of the dye laser, which was stabilized to a Fabry-Perot cavity, was about 15 kHz for these experiments. Recently, the linewidth of this laser has been decreased further by stabilizing it to a higher-finesse cavity.

C. Photon imaging detection

A three-stage lens system projected an image of the ion fluorescence onto the photocathode of the position-sensitive photon counter with a magnification of about 180. The first stage

was an aberration-corrected multi-element lens with an f-number of 4.5. The positional information from single detected photons was available in either analog or digital form. Images could be observed in real time on an oscilloscope screen, using the analog pulses. The digital information went to a computer, in order to make time exposures. An image of a single ion in the trap, recorded with this apparatus, has been published previously.[17]

IV. High resolution optical spectroscopy

A. Optical-optical double resonance

We have observed the 282 nm $^2S_{1/2}$ to $^2D_{5/2}$ electric quadrupole transition with high resolution. The metastable $^2D_{5/2}$ state has a lifetime of about 86 ms, so the transition has a natural linewidth of about 2 Hz. It would be very difficult to observe this transition in a single ion by detecting the emitted 282 nm photons, since there would be at most about 11 photons per second. To increase the efficiency of observation, we use optical-optical double resonance with quantum amplification.[14,18,19] The method works in the following way. The 194 nm source is turned off and 282 nm source is turned on. Suppose the ion absorbs a 282 nm photon, and is put into the metastable state. When the 194 nm light is then turned on, no fluorescence is observed. If, on the other hand, the ion is still in the ground state when the 194 nm light is turned on, fluorescence is observed at the normal intensity (typically thousands of photons per second detected). After a few milliseconds, the state of the ion can be determined with almost complete certainty. This technique was developed with the goal of making an optical frequency standard. Here it is used to yield information about the temperature and mutual interactions of the trapped ions.

B. Single-ion motional sidebands

The Doppler broadening of an absorption resonance of an ion bound in a harmonic well is modified by the confinement.[20] Instead of a single, broadened resonance line, the spectrum takes the form of a series of discrete resonances, each having a width equal to the natural width of the resonance, which are separated by the frequency of harmonic motion.

Consider an ion moving in the x direction in a harmonic well with frequency ω_x and amplitude X_0, so that

$$x = X_0 \cos(\omega_x t). \tag{5}$$

Let it be irradiated by a monochromatic laser beam of frequency ω propagating along the x axis. The electric field $\vec{E}(x,t)$ of the laser beam is

$$\vec{E}(x,t) = \mathrm{Re}\, \vec{E}_0 e^{i(kx-\omega t)}, \tag{6}$$

where the symbol Re denotes the real part of a complex expression. In the frame of the ion, there is a frequency modulation of the laser field. The electric field in the ion's frame is obtained by substituting the expression for x given by Eq. (5) into Eq. (6):

$$\begin{aligned} \vec{E}(x,t) &= \mathrm{Re}\, \vec{E}_0 e^{i(kX_0 \cos\omega_x t - \omega t)} \\ &= \mathrm{Re}\, \vec{E}_0 \sum_{n=-\infty}^{+\infty} i^n J_n(kX_0) e^{-i(\omega - n\omega_x)t}. \end{aligned} \tag{7}$$

In addition to the carrier at ω, the ion sees sidebands, called motional sidebands, spaced by the harmonic oscillation frequency ω_x. The amplitudes of the sidebands are proportional to the Bessel functions J_n. The ion absorbs light when the laser frequency is equal to one of its resonance frequencies and also when one of the motional sidebands matches a resonance frequency.

The intensities of the sidebands can be used to measure the temperature of the ion. A quantum mechanical treatment, in which a thermal-state-probability distribution was assumed, has been given previously.[21] According to Eq. (44) of Ref. 21, the intensity of the nth sideband $\sigma(n)$, is

$$\sigma(n) = \sigma_0 \exp\left(\frac{n\hbar\omega_x}{2k_BT} - k^2\langle x^2\rangle\right) I_n\left(\exp\left(\frac{\hbar\omega_x}{k_BT}(kx_0)^2\langle n_x\rangle\right)\right). \tag{8}$$

In this notation, the intensity of the carrier is $\sigma(0)$, I_n is a modified Bessel function, and $\langle x^2\rangle$ is the mean squared displacement of the harmonic oscillator, given by

$$\langle x^2\rangle = \frac{\hbar}{m\omega_x}(\langle n_x\rangle + \tfrac{1}{2}) \equiv 2x_0^2(\langle n_x\rangle + \tfrac{1}{2}), \tag{9}$$

where m is the mass of the ion and $\langle n_x\rangle$ is the mean occupation number of the oscillator. The temperature T is related to $\langle n_x\rangle$ by

$$\langle n_x\rangle = \frac{1}{\exp\left(\frac{\hbar\omega_x}{k_BT}\right) - 1}. \tag{10}$$

Equation 8 can easily be generalized to cases where there are two or more distinct frequencies of motion and where the laser beam is not directed along one of the principal axes of the trap. We have measured the temperature of a single, laser-cooled Hg^+ ion from the motional sidebands of the $^2S_{1/2}$ to $^2D_{5/2}$ transition.[22] The measured temperature was about 2 mK, which agrees with theoretical predictions.[21]

Figure 3(a) shows the absorption spectrum of a single Hg^+ ion, observed by the optical-optical double resonance. The carrier (at optical frequency ν_0) and the motional sidebands above and below ν_0 are clearly resolved. The potentials U_0 and V_0 were adjusted so that $\nu_r \approx 2\nu_z \approx 473$ kHz, where $\nu_r \equiv \omega_r/2\pi$ and $\nu_z \equiv \omega_z/2\pi$. This condition helped to simplify the sideband spectrum. The frequencies ν_z and ν_r were determined experimentally by applying a radiofrequency voltage between the electrodes. When the frequency of the applied voltage matched one of the secular frequencies, the fluorescence decreased, due to heating of the ion. In our notation for the sidebands, $(3z, r+z)$, for example, denotes the two overlapping sidebands at the frequencies $\nu_0 + 3\nu_z$ and $\nu_0 + \nu_r + \nu_z$.

C. Two-ion motional sidebands

If $\nu_z < \nu_r$, two ions have the lowest possible potential energy when they are located on the z axis, at $z = \pm z_{\min}$, where $z_{\min} = (q^2/4m\omega_z^2)^{1/3}$. The normal-mode frequencies of vibration about the minimum of the potential have been calculated previously.[3,7,8] The center of mass of the two ions behaves like a particle of mass $2m$ and charge $2q$ and thus has the same

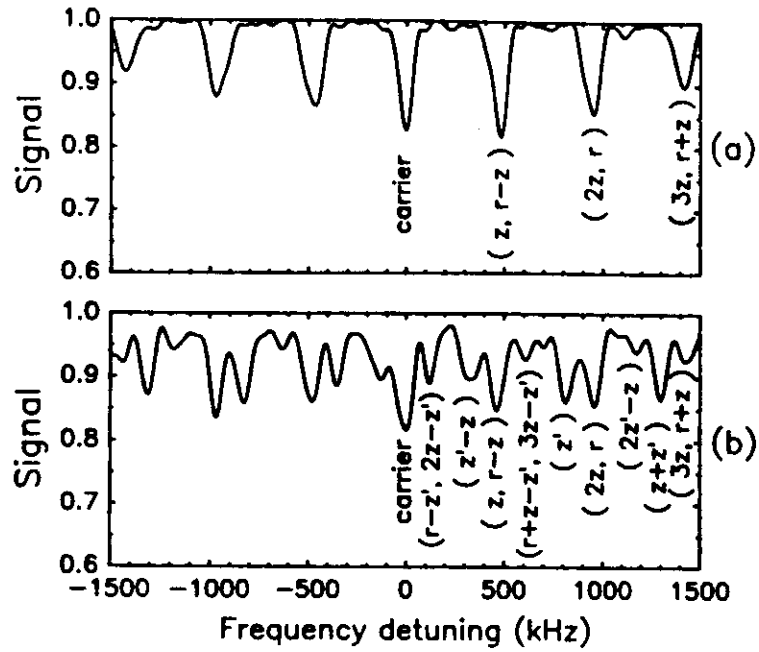

Figure 3: Absorption spectra of the $^2S_{1/2}(m_J = 1/2)$ to $^2D_{5/2}(m_J = -1/2)$ transition for (a) one Hg^+ ion and for (b) two Hg^+ ions. The carrier at optical frequency ν_0 (defined as zero frequency detuning) and the motional sidebands are clearly resolved. The sidebands are labeled in a notation that is explained in the text. The additional sidebands in (b) are due to the vibration of the two ions with respect to each other at frequency ν_z'.

frequencies of motion as a single ion. The frequency at which two ions vibrate with respect to each other along the z axis is $\nu_z' \equiv \sqrt{3}\nu_z$. This mode is like the stretch vibration of a diatomic molecule. The other vibrational frequency is $(\nu_r^2 - \nu_z^2)^{1/2}$, which, for $\nu_r = 2\nu_z$, is also equal to $\sqrt{3}\nu_z$. This vibration is a torsional motion in the x-z or y-z plane. Figure 3(b) shows an absorption spectrum taken with 2 ions in the trap. The trap potentials were the same as for the data of Fig. 3(a). The electronics of the position-sensitive photon detector were adjusted so that the fluorescence from only one of the two ions was detected. The motion of one ion is a superposition of harmonic motions at all of the normal-mode frequencies of the system. Therefore, all of the sidebands in Fig. 3(a) are also present in Fig. 3(b). The additional lines are due to the additional vibrational modes, at frequency ν_z', of the 2-ion pseudomolecule.

This kind of vibrational mode of two trapped ions has been observed by another method described in Ref. 9. Those workers applied a radiofrequency electric field between the trap electrodes, thus directly exciting the vibrational mode. When the frequency of the applied field matched the vibrational resonance, the fluorescence signal decreased.

V. Multi-ion cluster shapes

A. Calculations

The effective potential energy $V_{\rm eff}$ for a system of N ions of mass m and charge q is given by the expression,

$$V_{\rm eff}(\{x_i, y_i, z_i\}) = \underbrace{\frac{m}{2}\sum_{i=1}^{N}(\omega_x^2 x_i^2 + \omega_y^2 y_i^2 + \omega_z^2 z_i^2)}_{\text{effective trap potential}} + \underbrace{\frac{1}{2}\sum_{i\neq j}\frac{q^2}{|\vec{r_i} - \vec{r_j}|}}_{\text{Coulomb repulsion}}. \qquad (11)$$

Here, $\vec{r_i} = (x_i, y_i, z_i)$ is the position of the ith ion. The first term in Eq. (11) is the effective potential of the ions due to the trap fields. The second is the potential energy due to the Coulomb repulsion between the ions. The equilibrium configurations were calculated by finding the set of $3N$ ion coordinates that minimized the potential energy. A variable metric, or quasi-Newton, method was used to find the minimum, as in Ref. 3. We used the FORTRAN subroutine DFPMIN from Ref. 23. For a cylindrically symmetric Paul trap, there is an infinite set of solutions, since $V_{\rm eff}$ is unchanged by an arbitrary rotation about the z axis. To avoid possible convergence problems, and also to simulate the asymmetry of a real trap, ω_x and ω_y were assumed to differ by 0.2 %. Because of the remaining symmetry of the trap, there were in some cases several solutions, which were related by rotations and reflections. The algorithm sometimes converged to a minimum which was not the global minimum. In order to detect such false minima, at least 10 random initial configurations were used for each case. The solution with the lowest final value of $V_{\rm eff}$ was assumed to be a global minimum.

B. Observations

The ions were observed at an angle of approximately 54.7° with respect to the z axis of the trap. This allowed the three-dimensional structure of the clusters to be seen. In the apparatus of Ref. 6, the ions were observed along the z axis, so only the projection on the x-y plane could be seen. Figures 4-10 show the observed ion images and the corresponding calculated configurations. The magnification was the same for all of the experimental images. The scale of the experimental and calculated images is the same. The scale for the experimental images was determined from the separation between two ions, which is easily calculated. An approximate scale can be determined from the caption to Fig. 5. Experimental images of two, three, and four ions, obtained with less optical magnification, were published previously.[7]

Figure 4(a) shows five ions for $\nu_z = 0.308$ MHz and $\nu_r = 0.376$ MHz. Two of the ions lie along the z axis, symmetrically above and below the x-y plane. The other three ions circulate in the x-y plane about the z axis. They are not fixed in position, because the trap's effective potential is nearly cylindrically symmetric. Thus, the small, unintentional torque that the 194 nm beam applies to the system is enough to cause it to rotate. In this case, we determined the number of ions by reducing ν_z, relative to ν_r, until they were clearly separated in a chain along the z axis. Figure 4(b) shows the calculated ion positions for these

trap parameters. The circle in the calculated figure is obtained by rotating the configuration about the z axis.

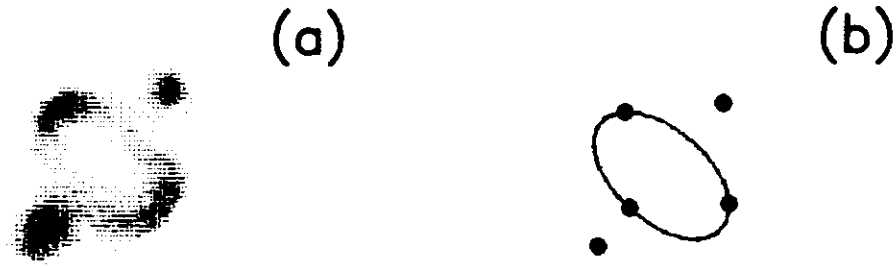

Figure 4: Nonplanar configuration of five ions for $\nu_z = 0.308$ MHz and $\nu_r = 0.376$ MHz. (a) Experimental data. (b) Calculation.

Figure 5 shows six ions for $\nu_z = 0.497$ MHz and $\nu_r = 0.256$ MHz. One is located at the origin. The other five circulate in the x-y plane. For these trap parameters, the configurations calculated for six, seven, and eight ions all have one ion at the origin and the rest in a ring in the x-y plane. In this case, we assume that there were six ions, because that number gives the best agreement between the observed and calculated ring sizes.

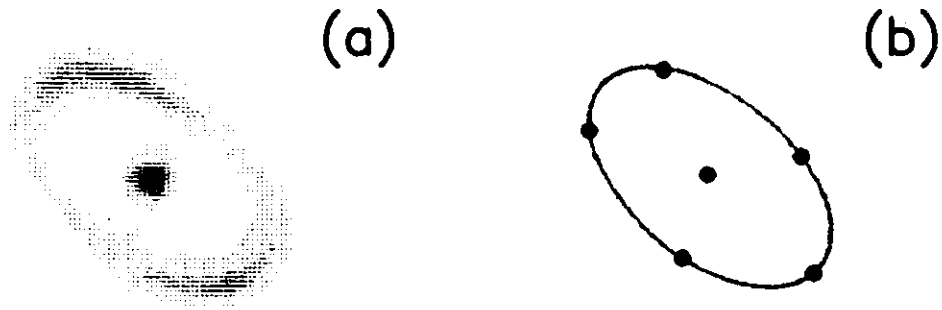

Figure 5: Planar configuration of six ions for $\nu_z = 0.497$ MHz and $\nu_r = 0.256$ MHz. The diameter of the ring is approximately 16 μm. (a) Experimental data. (b) Calculation.

Figure 6 shows six ions for $\nu_z = 0.780$ MHz and $\nu_r = 0.347$ MHz. One is at the origin, and four others lie at the vertices of a pentagon in the x-y plane. The fifth vertex of the pentagon appears to be vacant, but we assume that it is occupied by an ion which does not fluoresce. It may be a heavier isotope of mercury, such as $^{199}Hg^+$, or a molecular ion, such as $HgOH^+$, neither of which would fluoresce. If it had a higher charge-to-mass ratio than $^{198}Hg^+$, it would be more tightly bound to the trap, and would go the center. The additional asymmetry, due to the odd ion, keeps the configuration from rotating.

Figures 7 and 8 show two different configurations of the same nine ions. The secular frequencies for Fig. 7 were $\nu_z = 0.497$ MHz and $\nu_r = 0.256$ MHz; for Fig. 8, they were

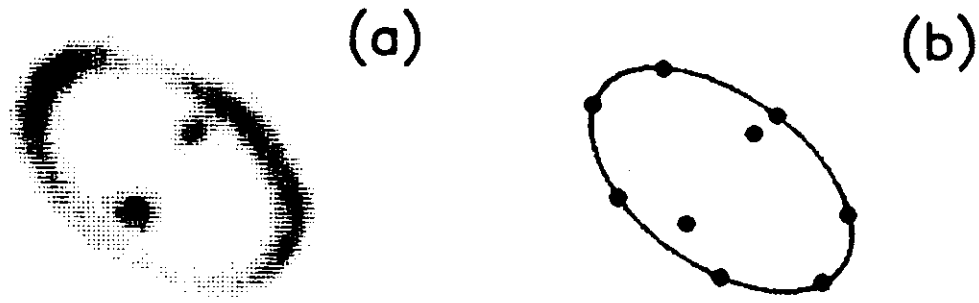

Figure 8: Nonplanar configuration of nine ions for $\nu_z = 0.439$ MHz and $\nu_r = 0.304$ MHz. Seven circulate in the x-y plane. The other two are displaced along the z axis. (a) Experimental data. (b) Calculation.

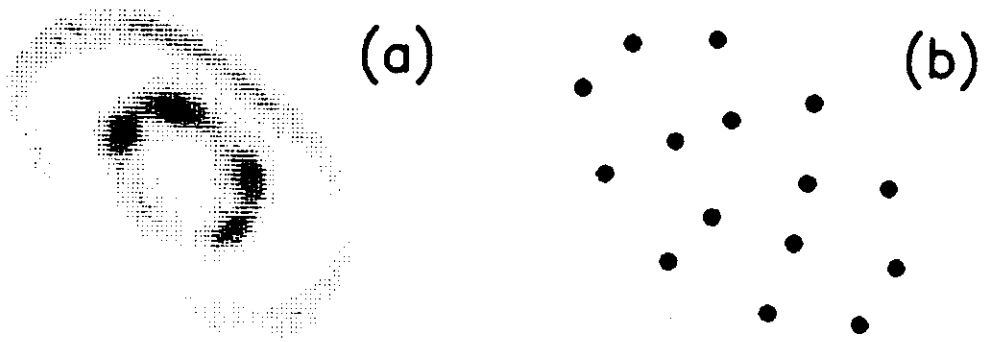

Figure 9: Planar configuration of 15 ions for $\nu_z = 0.780$ MHz and $\nu_r = 0.347$ MHz. (a) Experimental data. (b) Calculation.

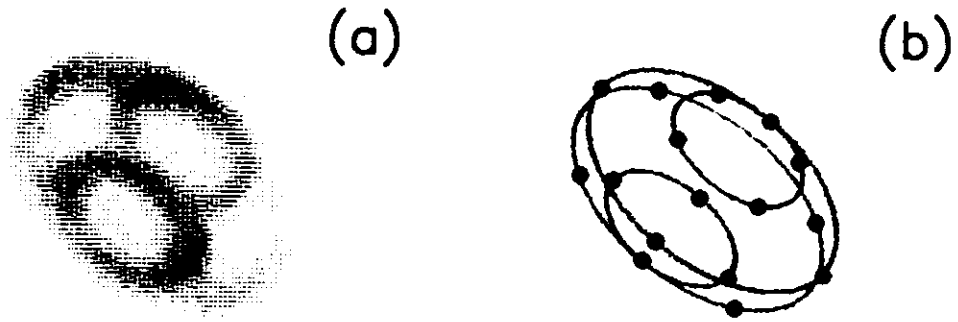

Figure 10: Nonplanar configuration of 16 ions for $\nu_z = 0.626$ MHz and $\nu_r = 0.479$ MHz. (a) Experimental data. (b) Calculation.

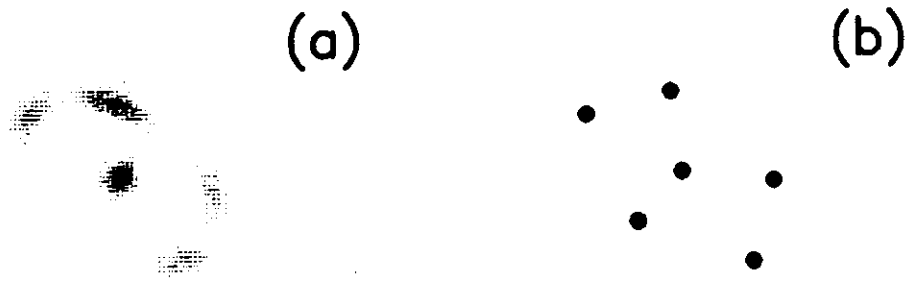

Figure 6: Planar configuration of six ions for $\nu_z = 0.780$ MHz and $\nu_r = 0.347$ MHz. Five ions are presumed to lie at the vertices of a pentagon in the x-y plane, but one does not fluoresce. Another one lies at the origin. (a) Experimental data. (b) Calculation.

$\nu_z = 0.439$ MHz and $\nu_r = 0.304$ MHz. The ions in Fig. 7 lie in the x-y plane. This configuration is the same as the calculated one shown in Fig. 1 of Ref. 3. The outer ring of the experimental image appears to be incomplete in this case because of nonuniform illumination of the cluster by the tightly focused 194 nm beam. In Fig. 8, two ions lie along the z axis, symmetrically above and below the x-y plane. The others form a ring in the x-y plane. The number of ions in Figs. 7 and 8 was determined uniquely from the observed configurations for the two different sets of conditions.

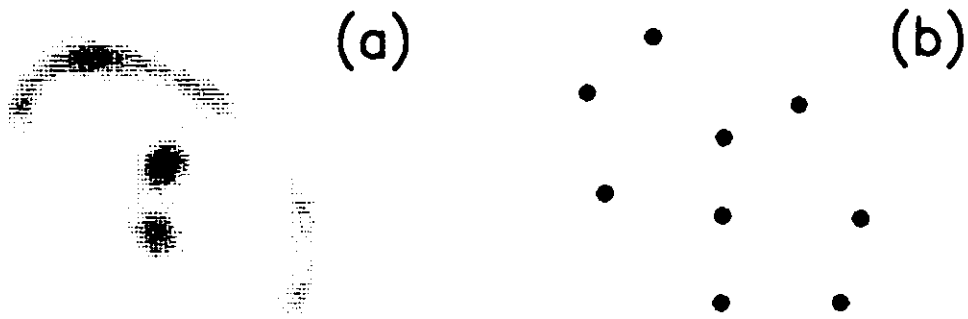

Figure 7: Planar configuration of nine ions for $\nu_z = 0.497$ MHz and $\nu_r = 0.256$ MHz. (a) Experimental data. (b) Calculation.

Figure 9 shows 15 ions for $\nu_z = 0.780$ MHz and $\nu_r = 0.347$ MHz. All of them lie in the x-y plane. Five form a pentagon, and the other ten form the outer ring. The observed pattern is only consistent with the one calculated for 15 ions.

Figure 10 shows 16 ions, for $\nu_z = 0.626$ MHz and $\nu_r = 0.479$ MHz. The large ring of eight ions lies nearly in the x-y plane. Two smaller rings of four ions each are displaced along the z axis, above and below the x-y plane. If another ion is added, at the same trap voltages, then, according to calculations, one ion goes to the center. By using data taken at another set of trap voltages, we could determine the number of ions. The 16 ions lie close to the surface of a spheroid. For larger numbers of ions, one would expect to see a

series of concentric spheroids like those which have been predicted and observed in Penning traps.[12,25]

VI. Related physical systems

A. Macroscopic particle traps

Perhaps the earliest studies of spatially ordered systems of charged particles in a Paul trap were made by Wuerker, Shelton, and Langmuir about 30 years ago.[24] In these studies, aluminum particles that had diameters of a few micrometers were suspended in a large Paul trap and cooled by collisions with gas molecules.

A similar trap has been built in our laboratory.[10] The inner diameter of the ring was about 2.5 cm. Typical trap parameters were $V_0 \approx 350$ V, $U_0 \approx 0$ V, and $\Omega/2\pi \approx 60$ Hz. Aluminum oxide particles of approximate mass 10^{-9} g and charge approximately 10^5 times the proton charge were trapped and observed to form ordered structures.

B. The Thomson model of the atom

In an early model for the atom, first suggested by Kelvin and later studied in detail by Thomson, electrons were assumed to be embedded in a uniform sphere of positive charge.[26] The potential energy of an electron inside the sphere due to the positive charge is proportional to $x^2 + y^2 + z^2$. Thus, the stable spatial configurations of the electrons in such a model are the same as for ions in a Paul trap with a spherically symmetric effective potential. Thomson's calculations of the minimum-energy configurations, which actually were done in two dimensions, showed patterns of concentric rings. He tabulated the configurations for up to 100 electrons. The 100-electron configuration contains seven rings. For $\nu_z > \nu_r$, the three-dimensional configurations for small numbers of particles are the same as for Thomson's two-dimensional calculations. For example, Thomson's 15-electron configuration has five in the inner ring and ten in the outer ring, like the data of Fig. 9. Thomson's calculations are perhaps the earliest predictions of layered structures in a bound Coulomb system. Such layered structures are predicted to occur in one-, two-, and three-dimensional systems[25] and have been observed in the Penning trap, a three-dimensional system.[12]

Thomson discussed experiments with floating magnets, which he used to verify his calculations of the two-dimensional configurations. For these experiments, equally magnetized needles, oriented in the same way, were pushed through corks and floated on water. An attractive force was produced by a large magnet placed above the surface of the water, the lower pole having the opposite sign to that of the upper poles of the floating magnets.

VII. Discussion

The equilibrium shapes of clusters that contain 16 ions or fewer and the intra-cluster vibrational frequencies can be calculated from the effective potential approximation. Other properties, however, such as the Doppler spectrum or the order-chaos transition, are affected by the micromotion, and require a more complete theoretical treatment.

Experiments with charged micrometer-sized particles in Paul traps might be useful in testing calculations, since they are relatively simple to perform, compared to experiments with ions. Large numbers of particles (on the order of 100) can be cooled and optically observed. The melting and freezing phase transitions have been observed previously.[24] Perhaps further experimental work could reveal details of the transition to chaotic behavior.[8,9] Other kinds of traps, with linear or "racetrack" geometries[27] might be useful in simulating ordered structures in ion storage rings. Such structures have been predicted, but not yet observed.[28]

Acknowledgments

We gratefully acknowledge support from the Air Force Office of Scientific Research and the Office of Naval Research.

References

1. J. Mostowski and M. Gajda, Acta Phys. Pol. **A67**, 783 (1985).
2. E. V. Baklanov and V. P. Chebotayev, Appl. Phys. B **39**, 179 (1986).
3. J. Javanainen, J. Opt. Soc. Am. B **5**, 73 (1988).
4. R. Casdorff and R. Blatt, Appl. Phys. B **45**, 175 (1988).
5. J. D. Prestage, M. J. Djomehri, and L. Maleki, Bull. Am. Phys, Soc. **33**, 914 (1988).
6. F. Diedrich, E. Peik, J. M. Chen, W. Quint, and H. Walther, Phys. Rev. Lett. **59**, 2931 (1987).
7. D. J. Wineland, J. C. Bergquist, W. M. Itano, J. J. Bollinger, and C. H. Manney, Phys. Rev. Lett. **59**, 2935 (1987).
8. J. Hoffnagle, R. G. DeVoe, L. Reyna, and R. G. Brewer, Phys. Rev. Lett. **61**, 255 (1988).
9. R. Blümel, J. M. Chen, E. Peik, W. Quint, W. Schleich, Y. R. Shen, and H. Walther, Nature **334**, 309 (1988).
10. D. J. Wineland, W. M. Itano, J. C. Bergquist, S. L. Gilbert, J. J. Bollinger, and F. Ascarrunz, in *Non-neutral Plasma Physics*, edited by C. W. Roberson and C. F. Driscoll, A. I. P. Conf. Proc. **175**, (Am. Inst. Phys., New York, 1988), p. 93.
11. P. Toschek et al., these Proceedings.
12. S. L. Gilbert, J. J. Bollinger, and D. J. Wineland, Phys. Rev. Lett. **60**, 2022 (1988).
13. W. M. Itano, J. C. Bergquist, R. G. Hulet, and D. J. Wineland, Phys. Rev. Lett. **59**, 2732 (1987).
14. J. C. Bergquist, D. J. Wineland, W. M. Itano, H. Hemmati, H.-U. Daniel, and G. Leuchs, Phys. Rev. Lett. **55**, 1567 (1985).

15. E. C. Beaty J. Appl. Phys. **61**, 2118 (1987).

16. H. Hemmati, J. C. Bergquist, and W. M. Itano, Opt. Lett. **8**, 73 (1983).

17. W. M. Itano, J. C. Bergquist, and D. J. Wineland, Science **237**, 612 (1987); D. J. Wineland and W. M. Itano, Phys. Today **40** No. 6, 34 (1987).

18. H. G. Dehmelt, Bull. Am. Phys. Soc. **20**, 60 (1975).

19. D. J. Wineland and W. M. Itano, Phys. Lett. **82A**, 75 (1981).

20. R. H. Dicke, Phys. Rev. **89**, 472 (1953).

21. D. J. Wineland and W. M. Itano, Phys. Rev. A **20**, 1521 (1979).

22. J. C. Bergquist, W. M. Itano, and D. J. Wineland, Phys. Rev. A **36**, 428 (1987).

23. W. H. Press, B. P. Flannery, S. A. Teukolsky, and W. T. Vetterling, *Numerical Recipes* (Cambridge Univ. Press, London, 1986).

24. R. F. Wuerker, H. Shelton, and R. V. Langmuir, J. Appl. Phys. **30**, 342 (1959).

25. A. Rahman and J. P. Schiffer, Phys. Rev. Lett. **57**, 1133 (1986); D. H. E. Dubin and T. M. O'Neil, *ibid.* **60**, 511 (1988); J. P. Schiffer, *ibid.* **61**, 1843 (1988).

26. J. J. Thomson, Phil. Mag. **7**, 237 (1904); *The Corpuscular Theory of Matter* (Scribner's Sons, New York, 1907).

27. D. A. Church, J. Appl. Phys. **40**, 3127 (1969).

28. J. P. Schiffer and P. Kienle, Z. Phys. A **321**, 181, (1985); J. P. Schiffer and O. Poulsen. Europhys. Lett. **1**, 55 (1986); D. Habs, in *Lecture Notes in Physics 296*, edited by M. Month and S. Turner (Springer-Verlag, Berlin, 1988), p. 310.

References
Quantum Optics of Single, Trapped Ions

1. W.M. Itano, J.C. Bergquist, R.G. Hulet, and D.J. Wineland, "Radiative decay rates in Hg^+ from observations of quantum jumps in a single ion," Phys. Rev. Lett. 59, 2732-2735 (1987).

2. W.M. Itano, J.C. Bergquist, and D.J. Wineland, "Photon antibunching and sub-Poissonian statistics from quantum jumps in one and two atoms," Phys. Rev. A 38, 559-562 (1988).

3. F. Diedrich, J.C. Bergquist, W.M. Itano, and D.J. Wineland, "Laser cooling to the zero point energy of motion," Phys. Rev. Lett. 62, 403-406 (1989).